Toward an improved comparison of the proton-to-antiproton charge-to-mass ratio

Takashi Higuchi (Univ. of Tokyo, RIKEN)
for the BASE collaboration

Outline

1. Introduction

- Background
- Principle of the measurement

2. Experimental methods

- Basics of the Penning Trap
- Image current detection
- Sideband coupling

3. Review of the 2014 measurement

- Preparation
- Measurement procedure
- Result and limitations

4. Development during 2017 run

Background

- **BASE** (**B**aryon **A**ntibaryon **S**ymmetry **E**xperiment):

  High-precision CPT tests by comparison of the fundamental properties of the proton and the antiproton.

- **Two major targets :**

  Magnetic moment $\mu_{\overline{p},p}$ / Charge-to-mass ratio $(q/m)_{\overline{p},p}$

- **Proton-antiproton charge-to-mass ratio comparison** $(q/m)_{\overline{p}}/(q/m)_p$

  - First performed by the TRAP collaboration in 1990, then in 1995/1999.
    -> Relative precision **90 p.p.t. (1999)** G. Gabrielse *et al.* PRL **82**, 3198 (1999)
  - 2014 BASE : **69 p.p.t.** S.Ulmer *et al.*, *Nature* **524**, 196 (2015)

  → Further improvement is aimed

- This talk:
  review of the 2014 measurement / developments for an improved measurement

Outline

1. **Introduction**
   - Background
   - Principle of the measurement
2. **Experimental methods**
   - Basics of the Penning Trap
   - Image current detection
   - Sideband coupling
3. **Review of the 2014 measurement**
   - Preparation
   - Measurement procedure
   - Result and limitations
4. **Development during 2017 run**

Outline

1. **Introduction**
   - Background
   - Principle of the measurement
2. **Experimental methods**
   - Basics of the Penning Trap
   - Image current detection
   - Sideband coupling
3. **Review of the 2014 measurement**
   - Preparation
   - Measurement procedure
   - Result and limitations
4. **Development during 2017 run**

Principle of the measurement

- Comparison of *q*/*m* by alternate measurements of the cyclotron frequencies of two particles in the same magnetic field.

cyclotron frequency : $\nu_c = \frac{1}{2\pi}\frac{q}{m}B$

$$\frac{\nu_{c,1}}{\nu_{c,2}} = \frac{\cancel{(1/2\pi)B}}{\cancel{(1/2\pi)B}}\frac{(q/m)_1}{(q/m)_2}$$

$$= \frac{(q/m)_1}{(q/m)_2}$$

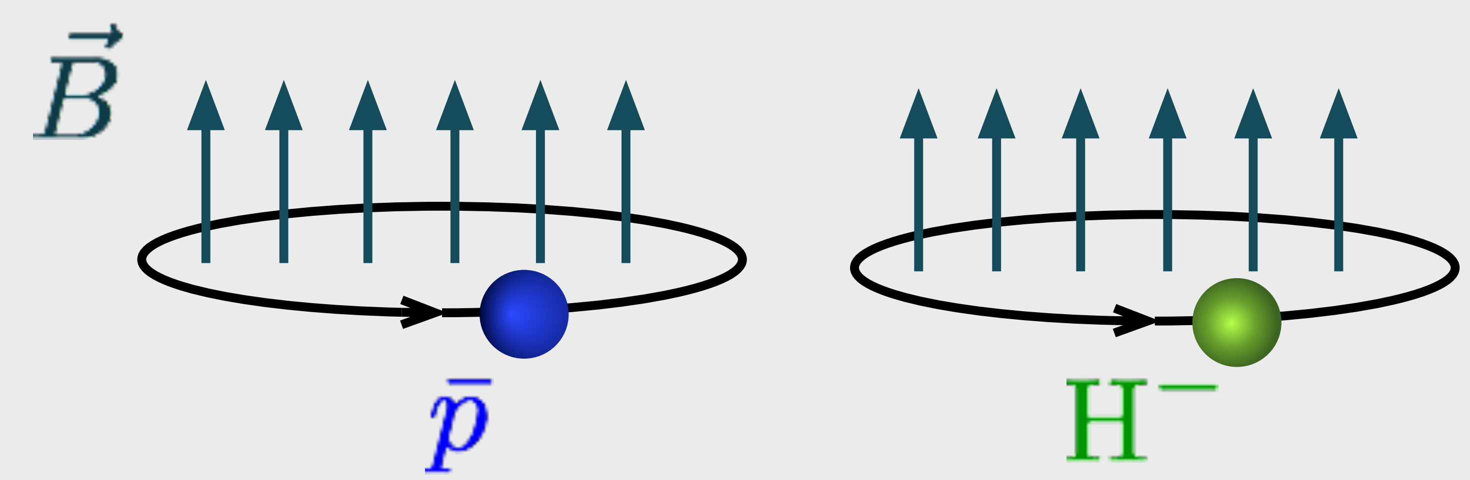

- In this case :

an antiproton $\bar{p}$ and a negative Hydrogen ion H^-

Why H⁻ ion ?

- The H^- ion is used as a proxy of the proton to avoid a systematic effect.
- If a proton and an antiproton are compared, inversion of the electric potential will induce a large difference in the axial positions.
- The measured ratio *R* can be converted to the proton-to-antiproton ratio with enough precision.

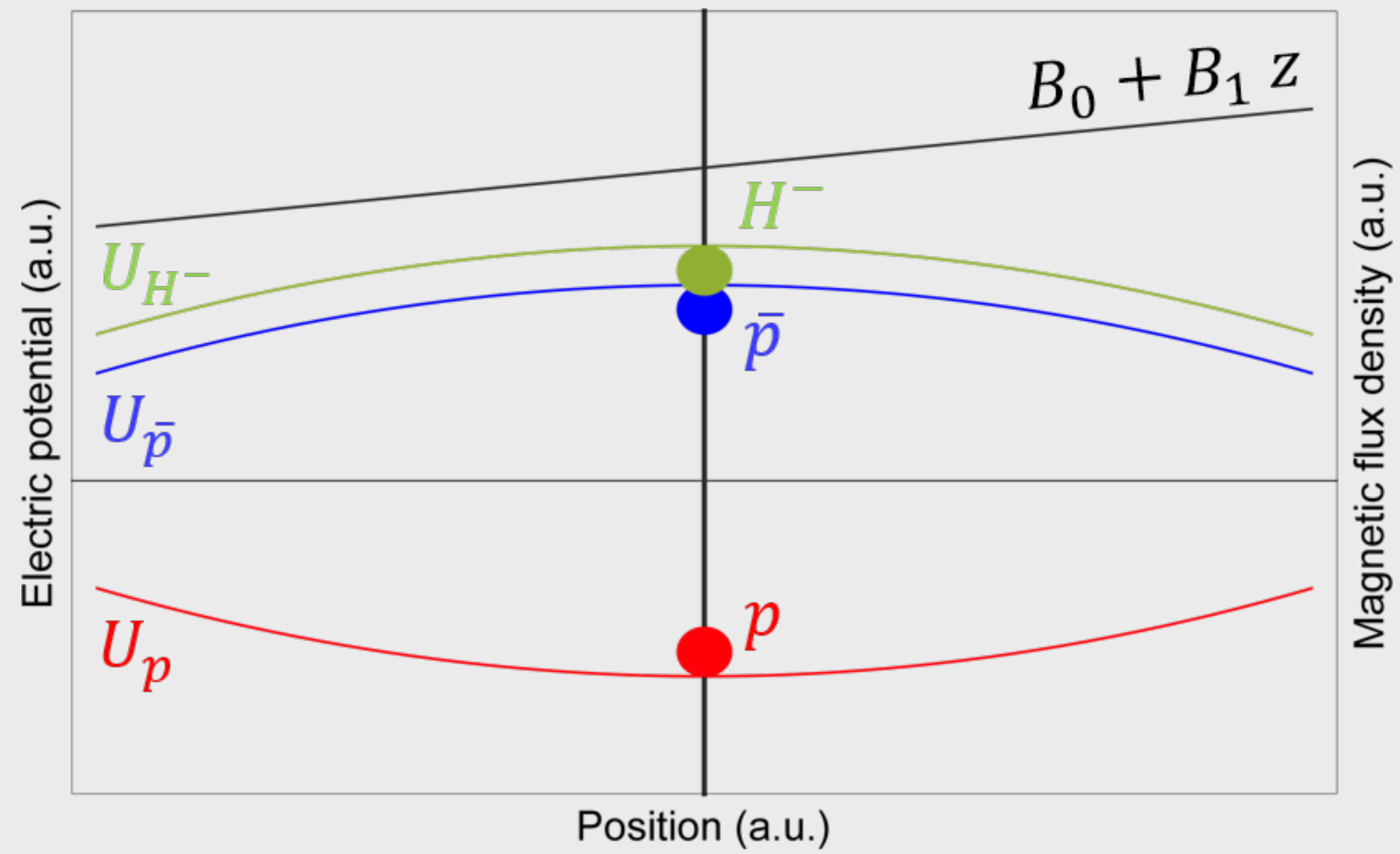

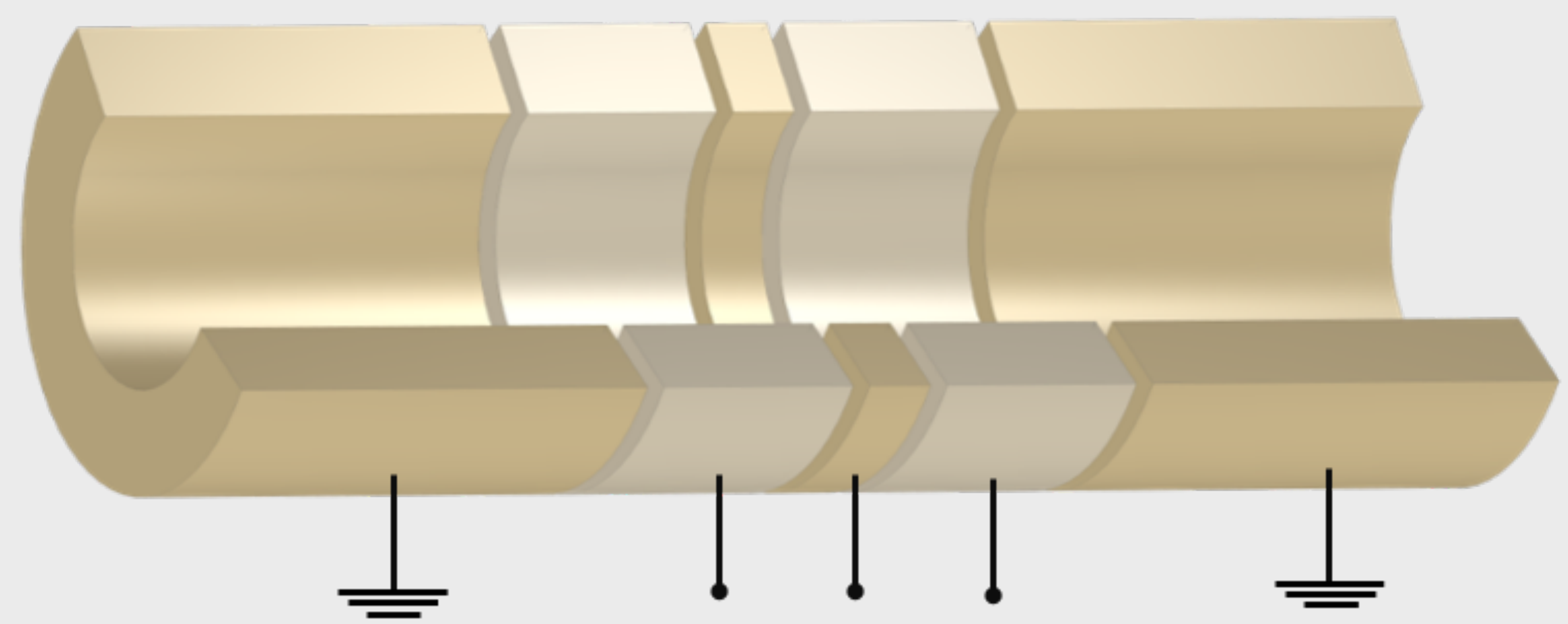

$$R = \frac{\nu_{c,\bar{p}}}{\nu_{c,\mathrm{H^-}}} = \frac{(q/m)_{\bar{p}}}{(q/m)_p} \boxed{\frac{m^*_{\mathrm{H^-}}}{m_p}}$$

known with enough precision

Why H$^-$ ion ?

- The H$^-$ ion is used as a proxy of the proton to avoid a systematic effect.
- If a proton and an antiproton are compared, inversion of the electric potential will induce a large difference in the axial positions.
- The measured ratio *R* can be converted to the proton-to-antiproton ratio with enough precision.

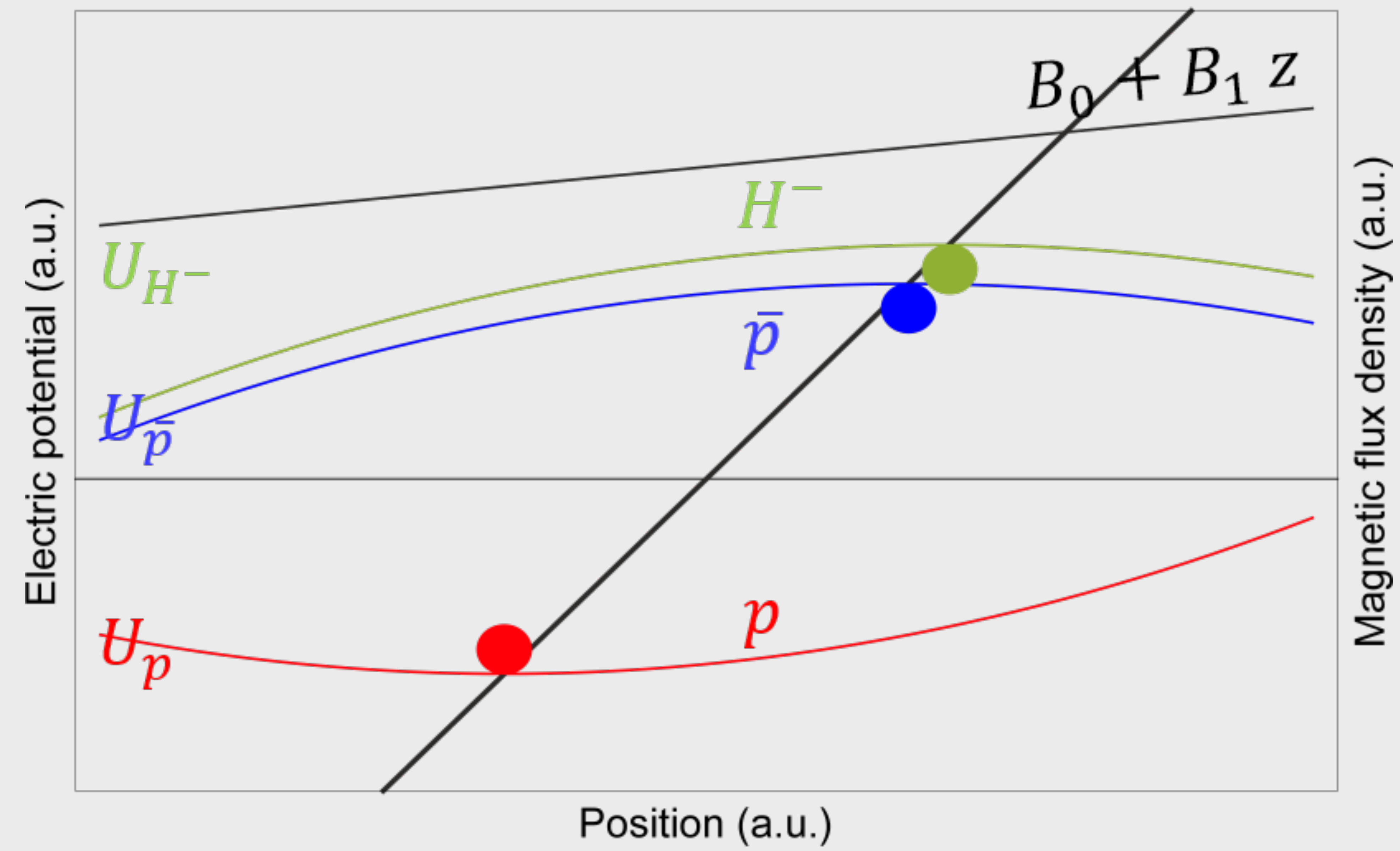

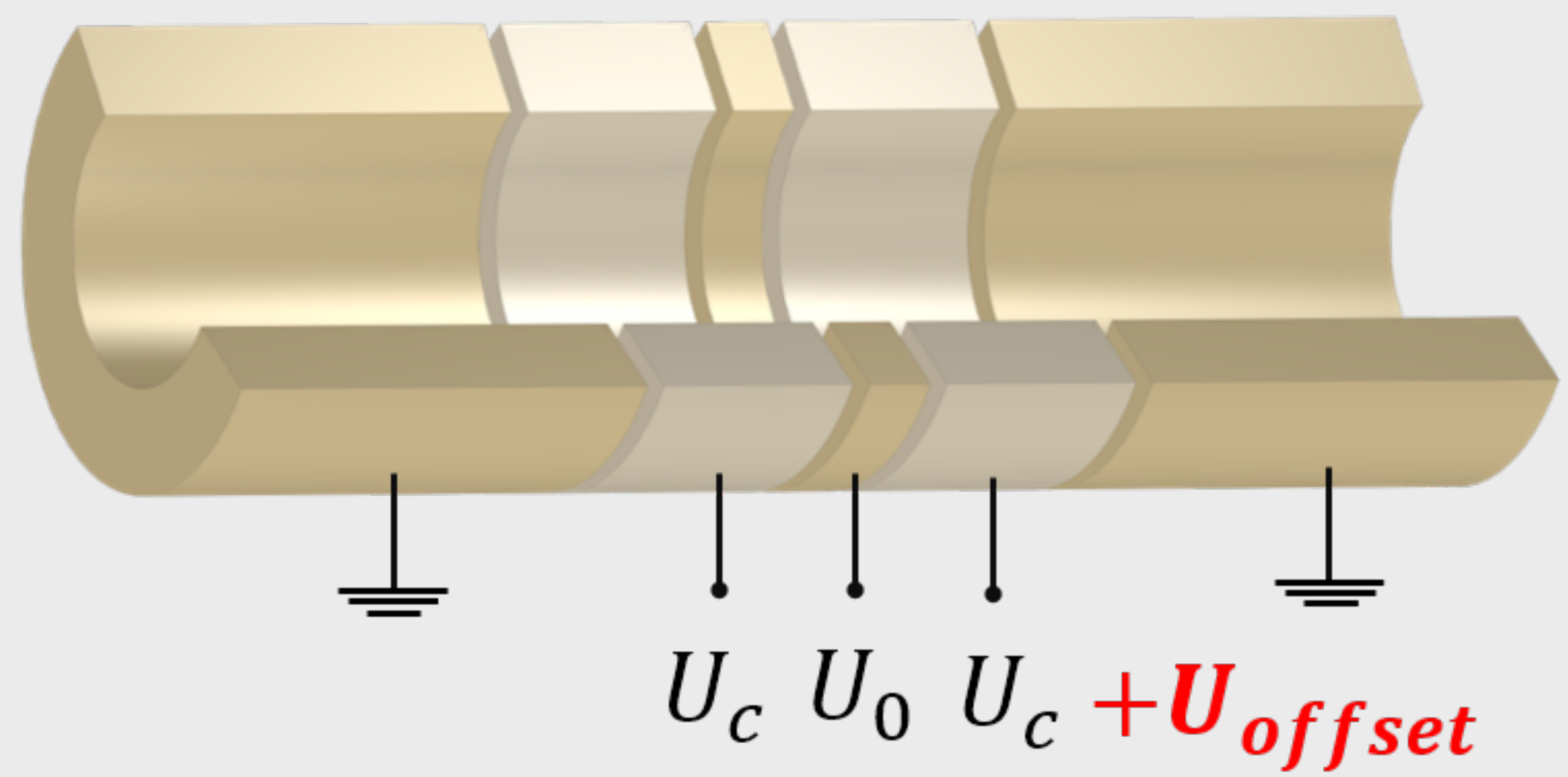

$$R = \frac{\nu_{c,\bar{p}}}{\nu_{c,\mathrm{H}^-}} = \frac{(q/m)_{\bar{p}}}{(q/m)_p} \frac{m^*_{\mathrm{H}^-}}{m_p}$$

known with enough precision

H^- effective mass

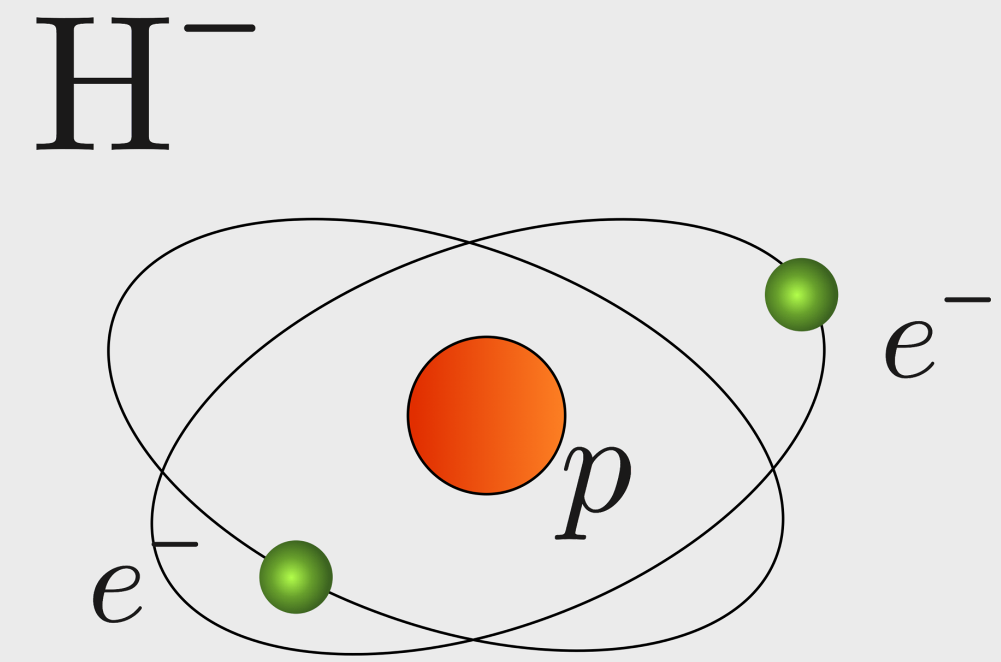

- The mass ratio $m^*_{H^-}/m_p$:

$$\frac{m^*_{H^-}}{m_p} = 1 + 2\frac{m_e}{m_p} - \frac{E_b}{m_p} - \frac{E_a}{m_p} + \frac{\alpha_{pol,H^-}B^2}{m_p}$$

	term	contribution (10^{-12})	uncertainty (10^{-12})
	1	1 000 000 000 000.0	0
electron-proton mass ratio *1)	$2m_e/m_p$	1 089 234 043.0	0.1
binding energy	$-E_b/m_p$	−14 493.0	$< 10^{-3}$
electron affinity	$-E_a/m_p$	−803.8	$< 10^{-2}$
polarization effect *2)	$\alpha_{pol,H^-}B^2/m_p$	7.7	$< 10^{-6}$
total		1 001 089 218 753.9	0.1

*1) updated by F. Heiße, *et al.* Phys.Rev.Lett. **119**, 033001(2017) *2) calculated for *B* in 2017

The effective mass of H^- $m^*_{H^-}$ can be converted to m_p
with enough precision (0.1 p.p.t.).

Outline

1. Introduction
   - Background
   - Principle of the measurement
2. **Experimental methods**
   - **Basics of the Penning Trap**
   - **Image current detection**
   - **Sideband coupling**
3. Review of the 2015 measurement
   - Preparation
   - Measurement procedure
   - Result and limitations
4. Development during 2017 run

Basics of the Penning trap

- Particle confinement by a combination of
  - a magnetic field $\vec{B}$
  - a quadrupolar electrostatic potential $\Phi_e(\rho, z)$
- Three eigenmodes of the particle motion:
  - modified cyclotron motion: $\nu_+ \sim$ 29 MHz
  - axial motion: $\nu_z \sim$ 640 kHz
  - magnetron motion: $\nu_- \sim$ 7 kHz
- Related to the cyclotron frequency by

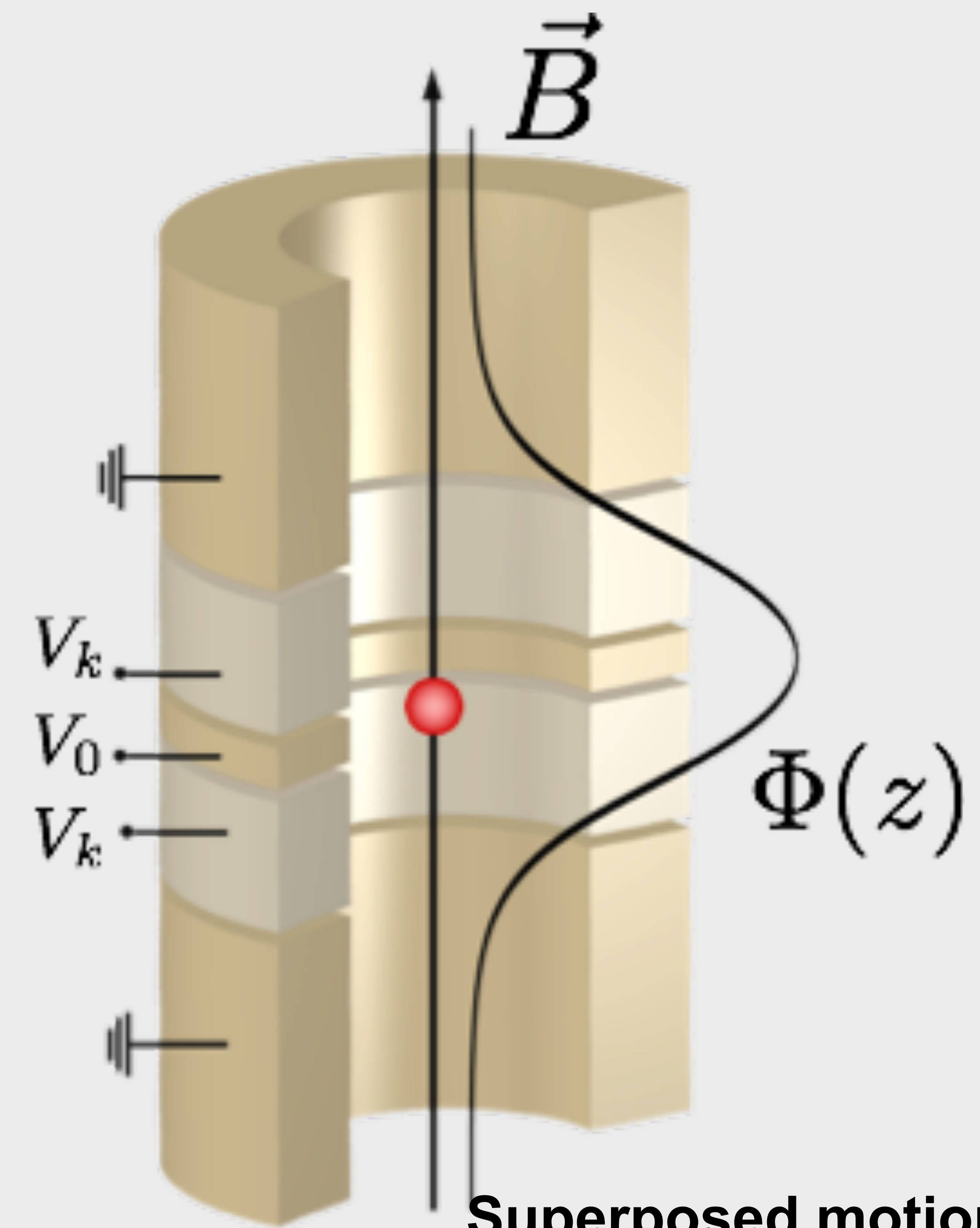

Invariance Theorem

$$\nu_c^2 = \nu_+^2 + \nu_z^2 + \nu_-^2$$

L. S. Brown and G. Gabrielse Rev. Mod, Phys. **58,** 233 (1986)

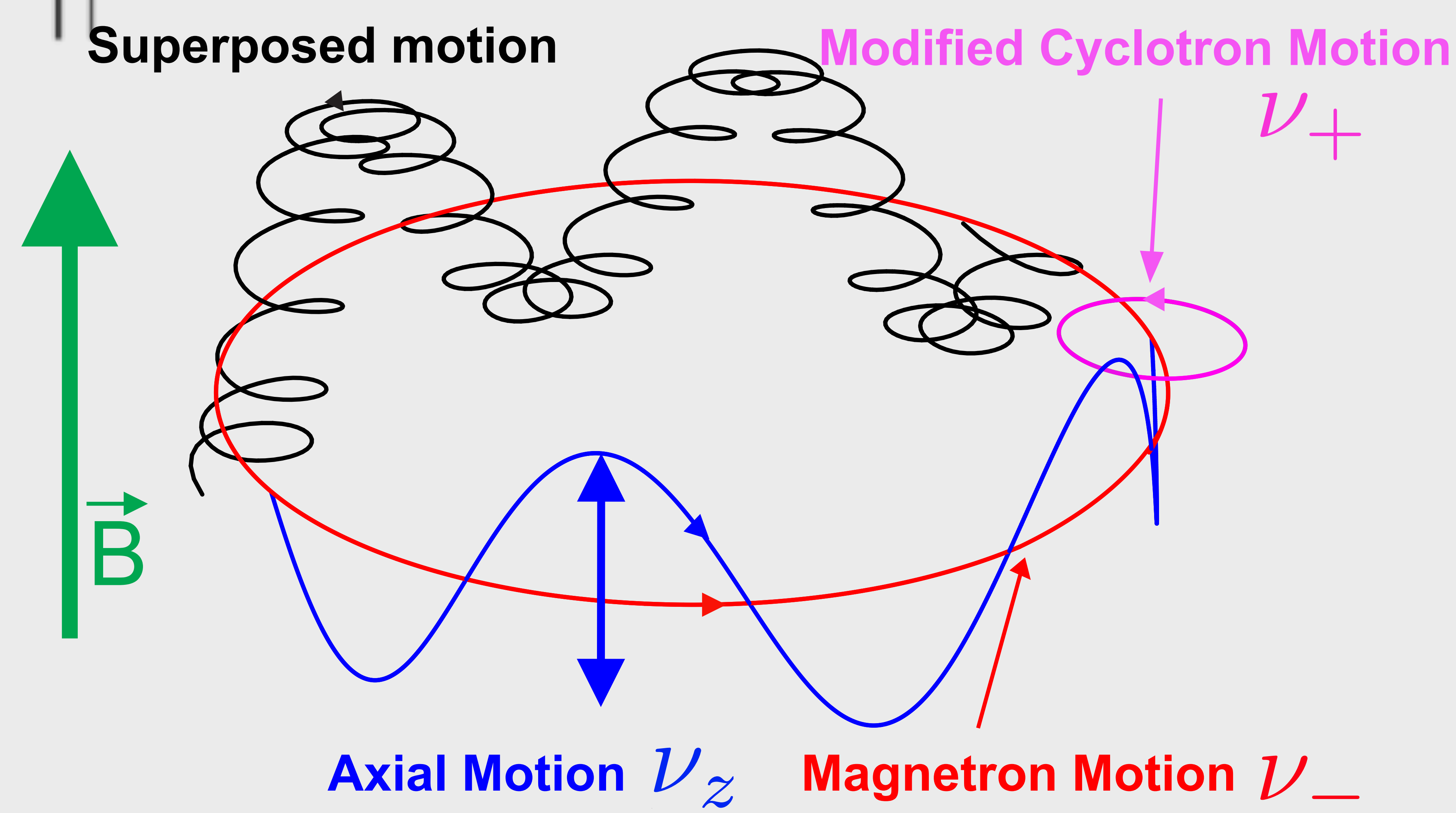

Axial frequency measurement (image current detection)

- The axial motion of the particle is cooled/detected through an interaction with a high-quality superconducting resonator via image currents.
- After reaching the thermal equilibrium with the system, the particle motion shorts a frequency component of the resonator.
  → the axial frequency appears as a dip in the resonance.

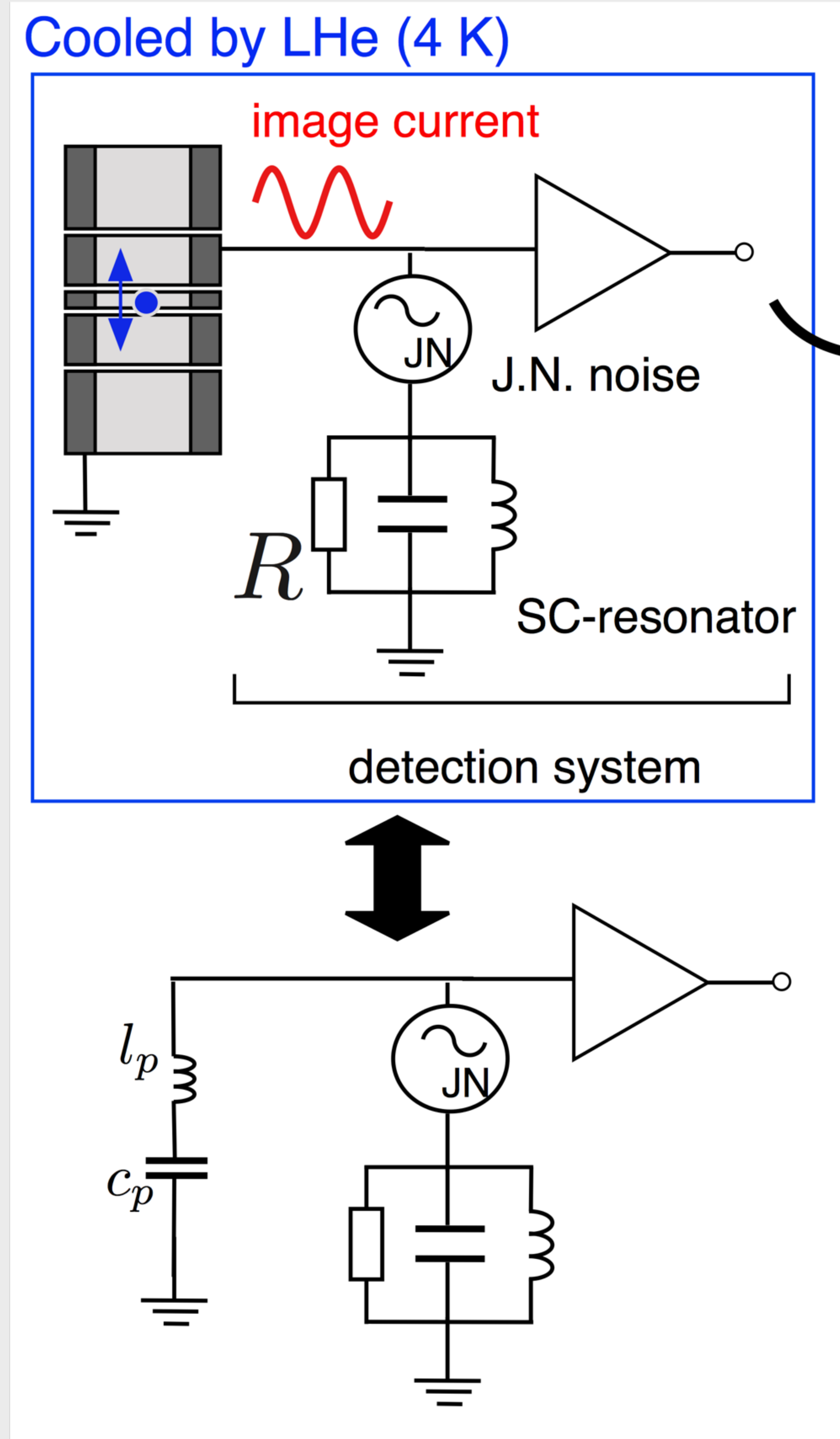

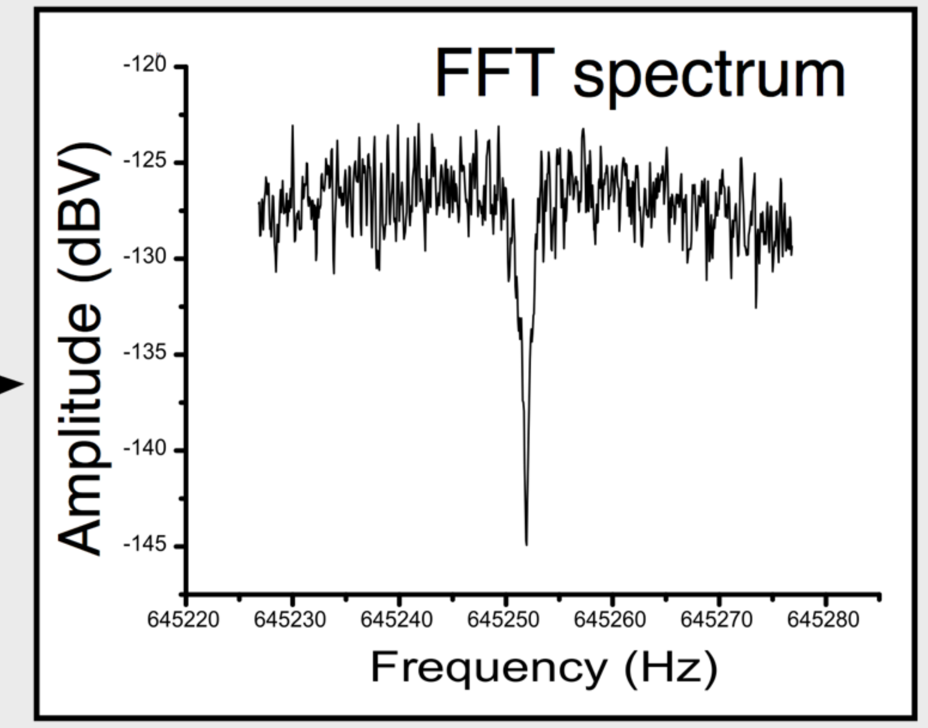

D. J. Wineland and H. G. Dehmelt. *J.Appl.Phys.*, **46,** 920 (1975)

Sideband coupling

- The radial motions can be coupled to the axial motion through a radial excitation at (for the mod. cycl. mode)

$$\nu_{rf} = \nu_+ - \nu_z$$

- The axial component of the resultant coupled motion:

$$z(t) = z_0 \cos\left(\frac{\Omega_0}{2}t\right)\sin(2\pi\nu_z t)$$
$$= \frac{z_0}{2}\left[\sin\left(2\pi\underbrace{\left(\nu_z + \frac{\Omega_0}{4\pi}\right)}_{\nu_l}\right) + \sin\left(2\pi\underbrace{\left(\nu_z - \frac{\Omega_0}{4\pi}\right)}_{\nu_r}\right)\right]$$

Two frequencies which reflect the original frequencies

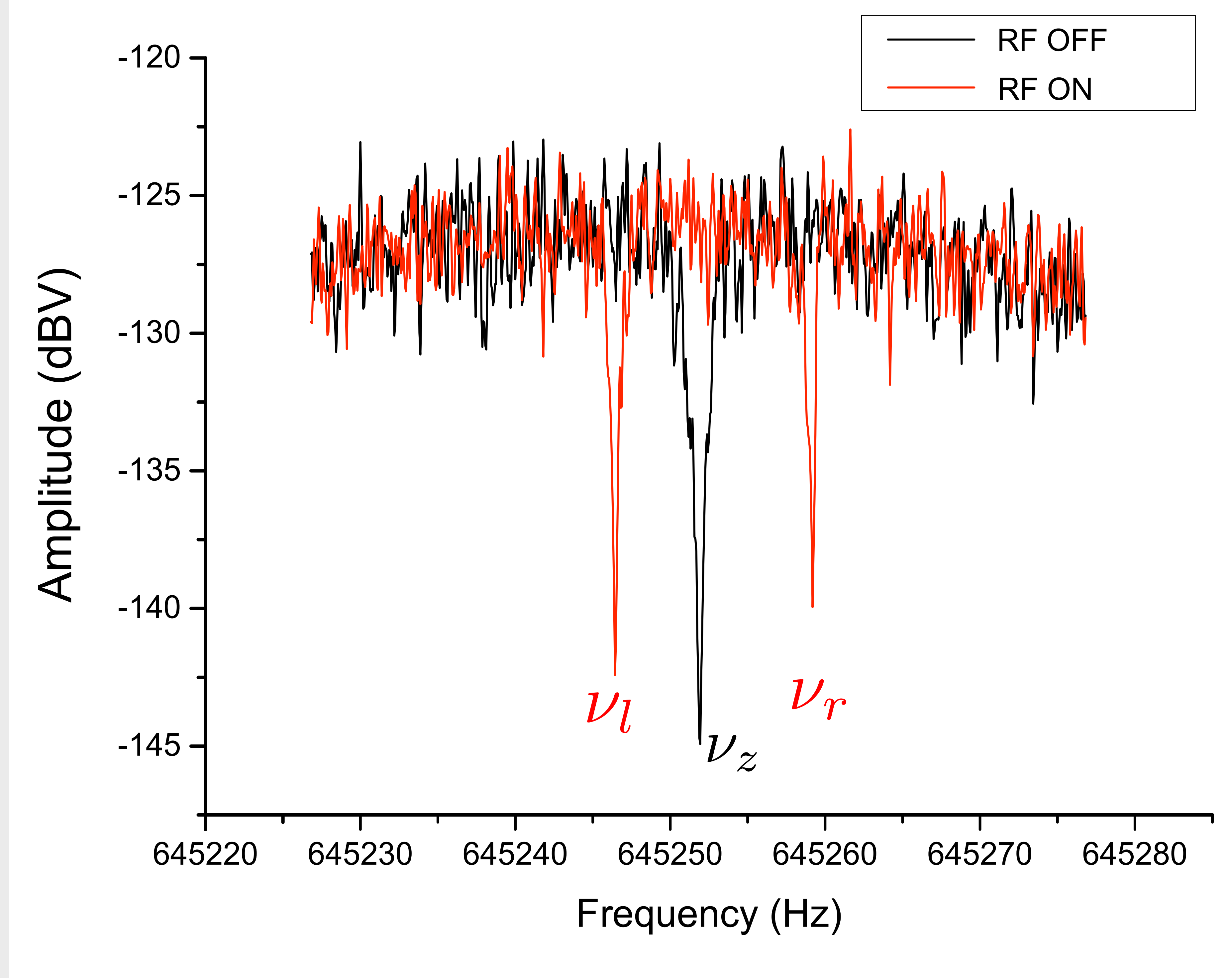

$$\Rightarrow \qquad \nu_+ = \nu_{rf} - \nu_z + (\nu_l + \nu_r)$$

E.A.Cornell *et al.*, *Phys. Rev. A,* **41,** 312 (1990)

Limitation of the sideband coupling method

$$\nu_+ = \nu_{rf} - \nu_z + (\nu_l + \nu_r)$$

single dip   double dip

➡ The stability of the cyclotron frequency is ultimately limited by the axial frequency stability.

➡ The axial frequency fluctuations are well understood

$$\Xi_z^2 = \Xi_V^2 + \Xi_{\mathrm{fit}}^2 + \Xi_{E_+}^2 + \Xi_{\mathrm{temp}}^2$$

white   random-walk

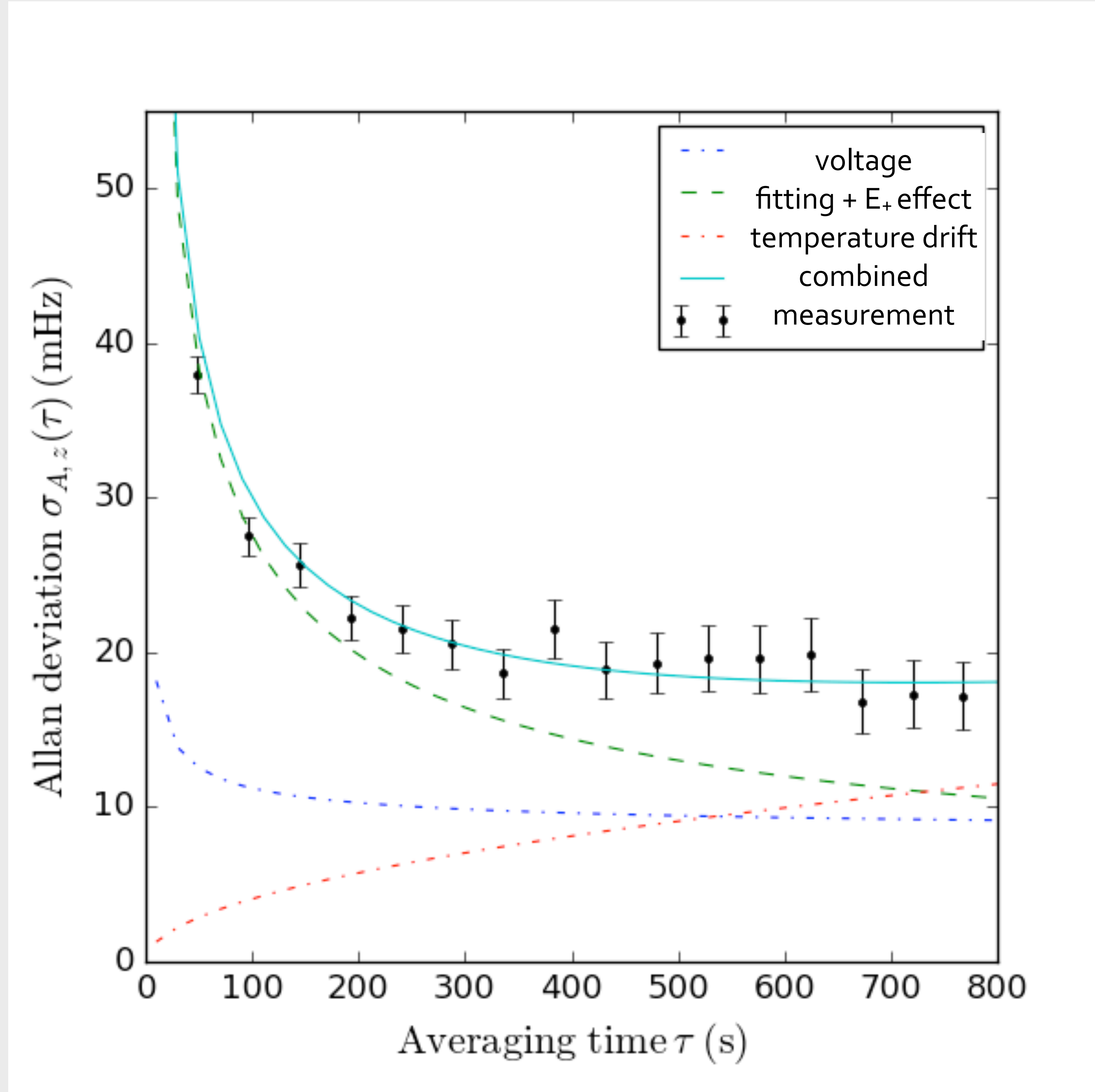

➡ The cyclotron stability limit of the sideband method:

70 mHz (<-> 2.3 p.p.b.)   (for realistic averaging time)

Outline

1. **Introduction**
   - Background
   - Principle of the measurement
2. **Experimental methods**
   - Basics of the Penning Trap
   - Image current detection
   - Sideband coupling
3. **Review of the 2014 measurement**
   - Preparation
   - Measurement procedure
   - Result and limitations
4. **Development during 2017 run**

BASE

Preparation of the measurement

- Antiprotons were provided by the AD, H^- ions were produced by collision of the beam to the degrader (typically ~100 $\overline{p}$, ~30 H^-/AD-shot)
- Removal of contaminant particles by selective excitation
- Extraction of a single $\overline{p}$ and a single H^- from the reservoir

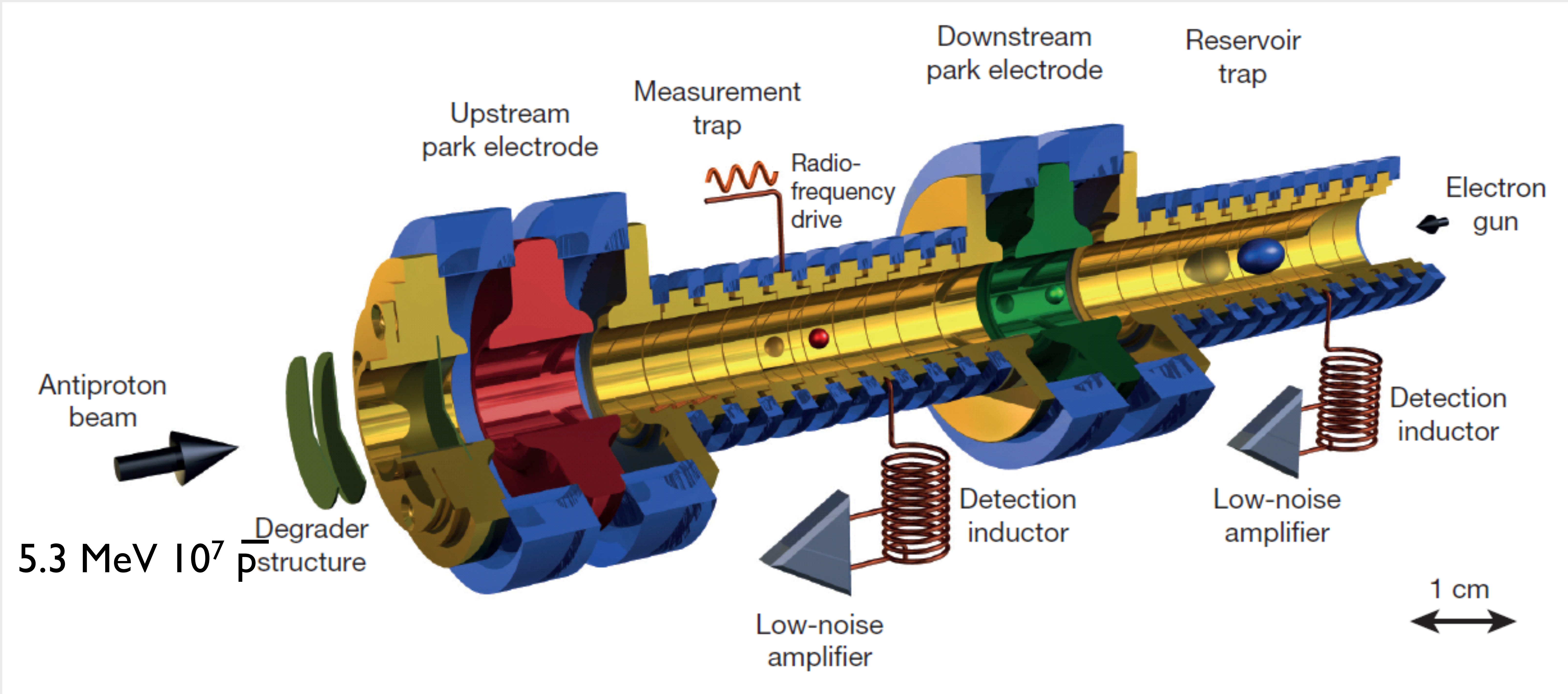

Measurement procedure

- Cyclotron frequency measurement of a single particle while the other was parked on the park electrode.
- Rapid particle exchange enabled a first sampling rate (x60 compared to TRAP1990)
  → enabled 6521 $\bar{p}$ - H^- comparisons in 35 days.
- The measurement sequence was synchronized to the AD operation to minimize magnetic field fluctuations

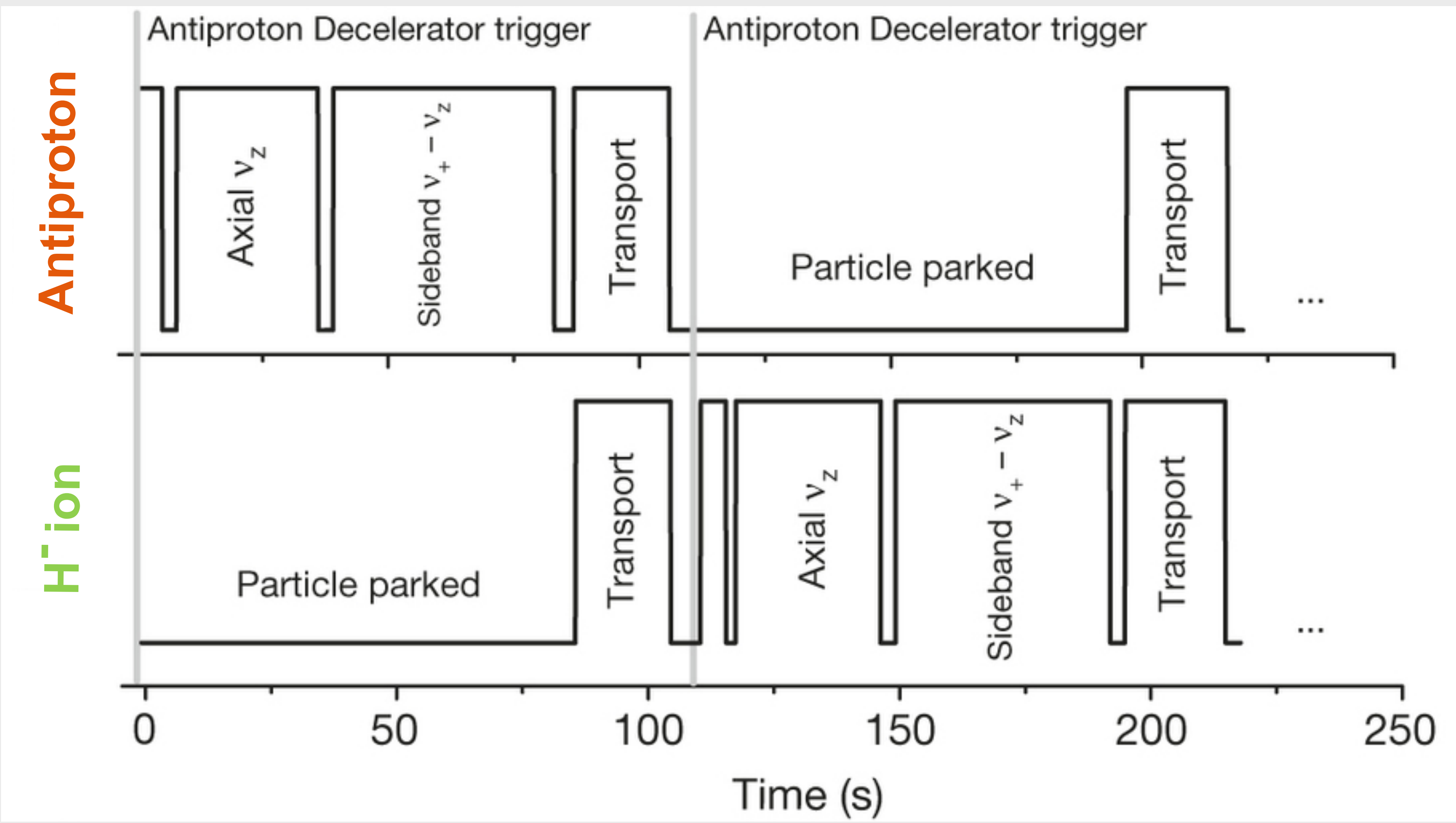

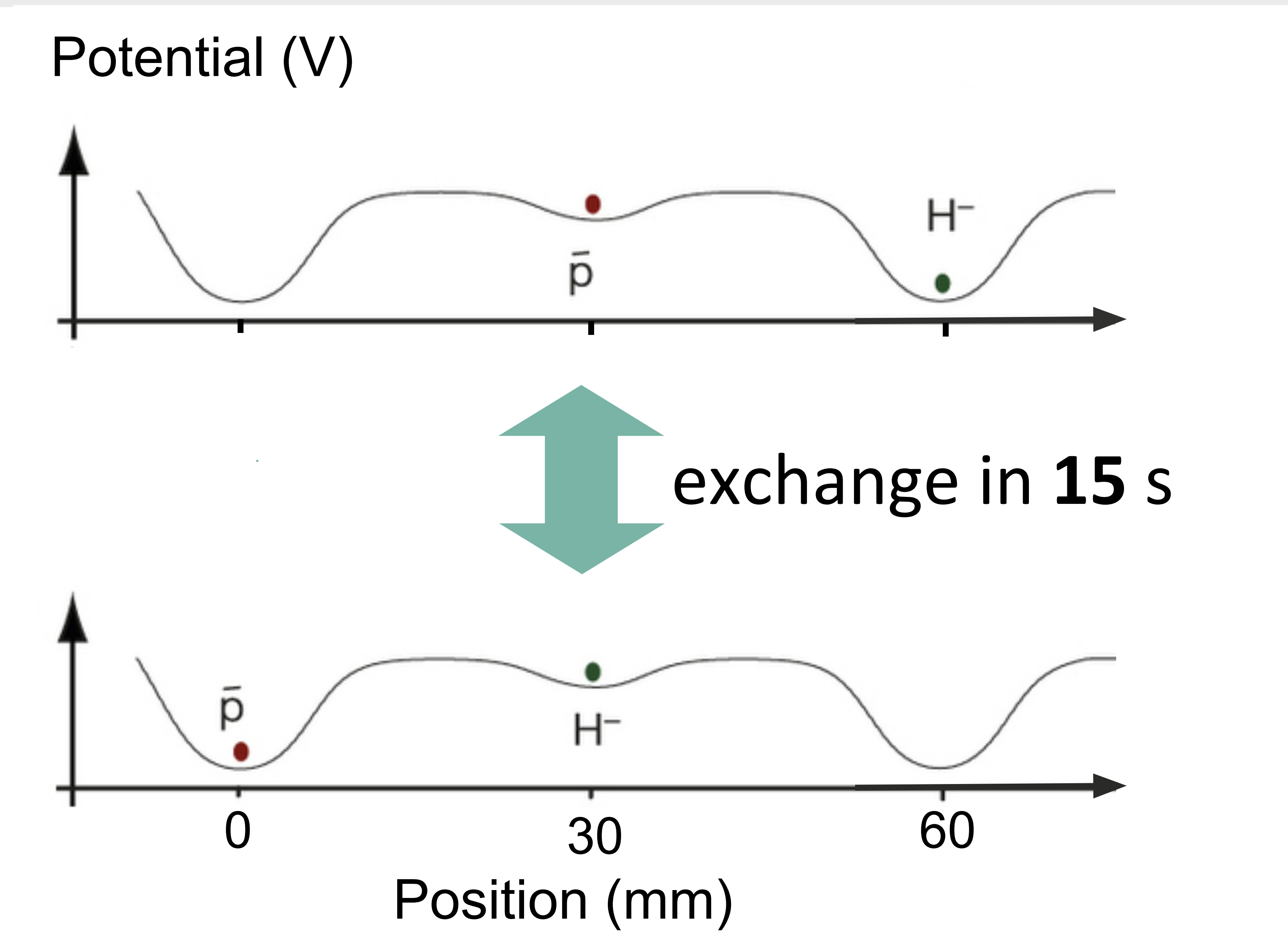

Result of the comparison

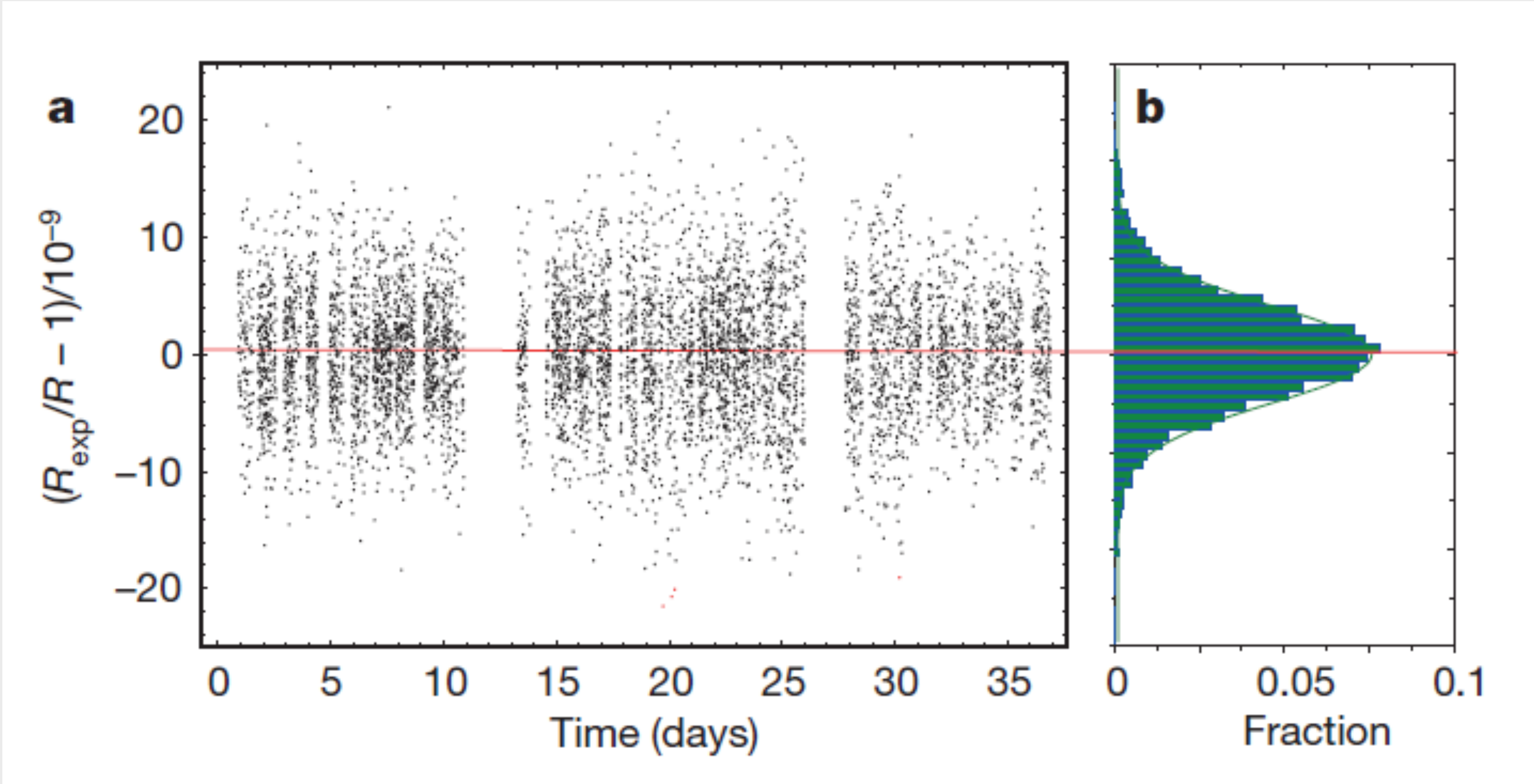

The ratio *R* was determined from 6521 sets of comparison:

$$R_{\mathrm{exp}} = 1.001\,080\,921\,875\,5(64)(26)$$

$$\left|\frac{(q/m)_{\bar{p}}}{(q/m)_p}\right| - 1 = 1(64)(26) \times 10^{-12}$$ **(69 p.p.t.)**

- Consistent with the CPT invariance.
- Exceeding the previous measurement by a factor of 4 in energy resolution.
- Evaluation of a possible sidereal variation
  -> No significant variation in the period of sidereal day down to 720 p.p.t. (95% C.L.)

Major systematic

$$R_{\mathrm{exp}} = 1.001\,080\,921\,875\,5(64)(26)$$

$$\left|\frac{(q/m)_{\bar{p}}}{(q/m)_{p}}\right| - 1 = 1(64)(26) \times 10^{-12}$$

- The cause of the dominant systematic uncertainty:

Adjustment of trapping voltage by 5 mV between $\bar{p}$ and H^-

Axial frequency $\nu_z = \frac{1}{2\pi}\sqrt{\frac{2qC_2}{m}V_0}$

For detection : $\nu_z(V_0) \approx \nu_{\mathrm{res}}$

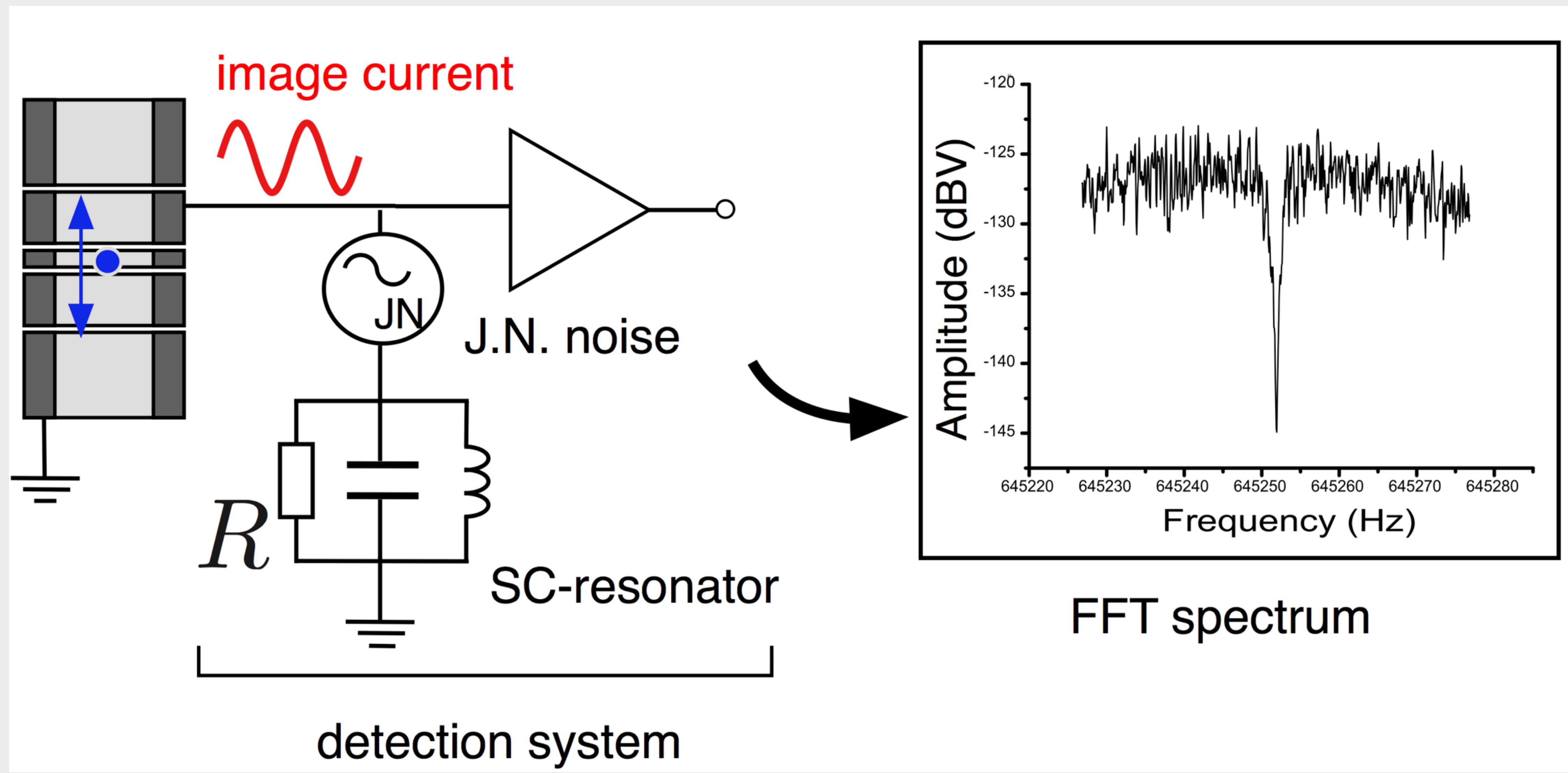

Major systematic

$$R_{\mathrm{exp}} = 1.001\,080\,921\,875\,5(64)(26)$$

$$\left|\frac{(q/m)_{\bar{p}}}{(q/m)_p}\right| - 1 = 1(64)(26) \times 10^{-12}$$

- The cause of the dominant systematic uncertainty:

  Adjustment of trapping voltage by 5 mV between $\bar{p}/H^-$

➡ Shift of the axial position: $\Delta z \sim 30$ nm
Magnetic gradient : $B_1 = 7.58\,(42)$ mT/m
→ shifts the magnetic field experienced by the particles by **0.23 nT**

➡ Corrected by estimating the positions of the particles by potential calculation:
Correction of the ratio: ΔR = **-114(26) p.p.t.** (uncertainty from the ΔB_1)

All the other factors (image charge, a tile of the apparatus etc.) contribute on sub-p.p.t. orders.

Upgrades for an improved measurement

- <u>For systematics</u>: a tunable axial detection system
  - The resonant frequency can be tuned by use of a diode as a variable capacitor.

    → Tune the resonance frequency of the detector instead of the trapping voltage

    → **Removes the the major systematic completely**

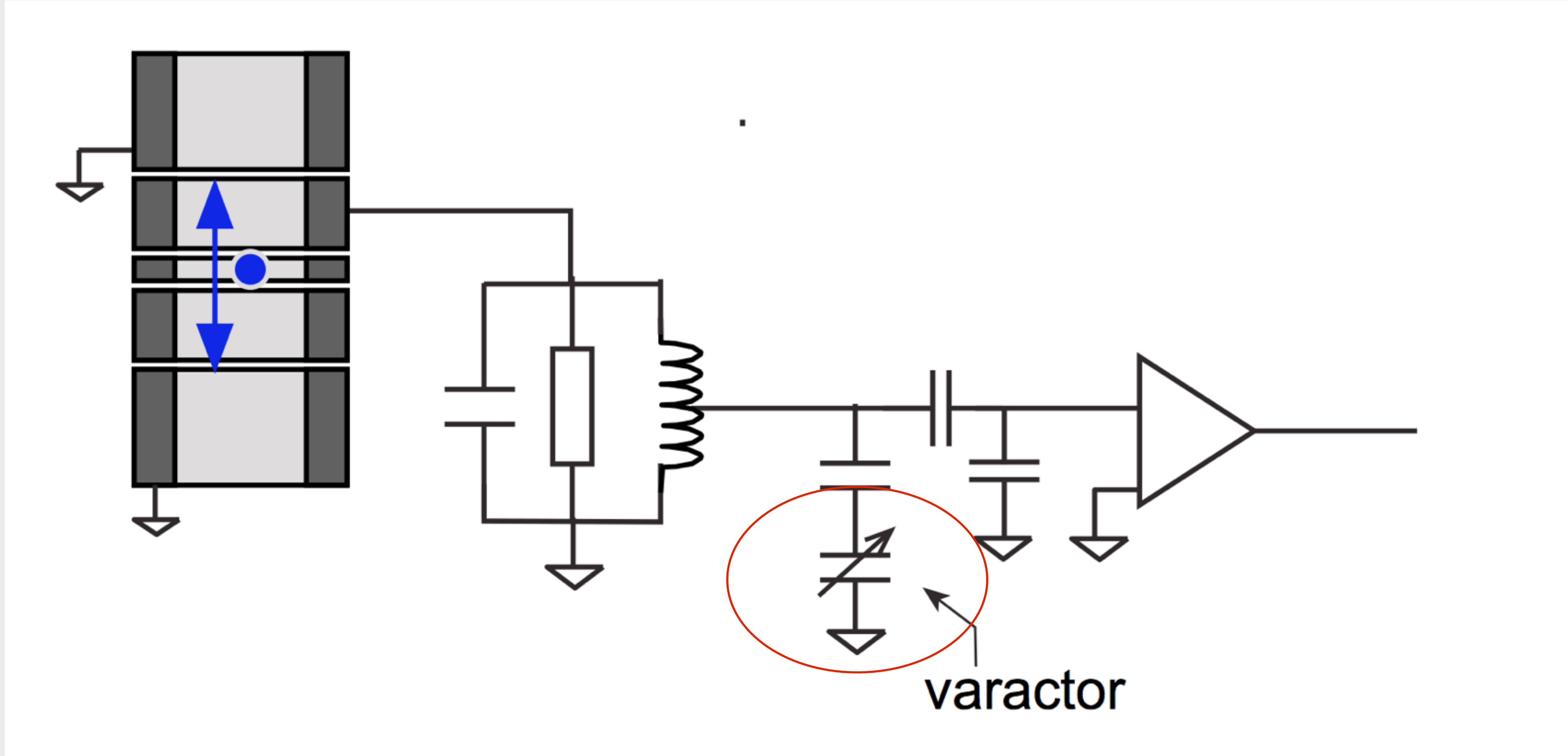

G. Gabrielse and J. Tan, Jour. Appl. Phys. **63**, 5143

- <u>For statistics:</u> an improved magnetic shielding
  - Based on a principle of the self-shielding solenoid
  - Multilayer shielding coil system has been installed

Upgrades for an improved measurement

- <u>For systematics</u>: a tunable axial detection system

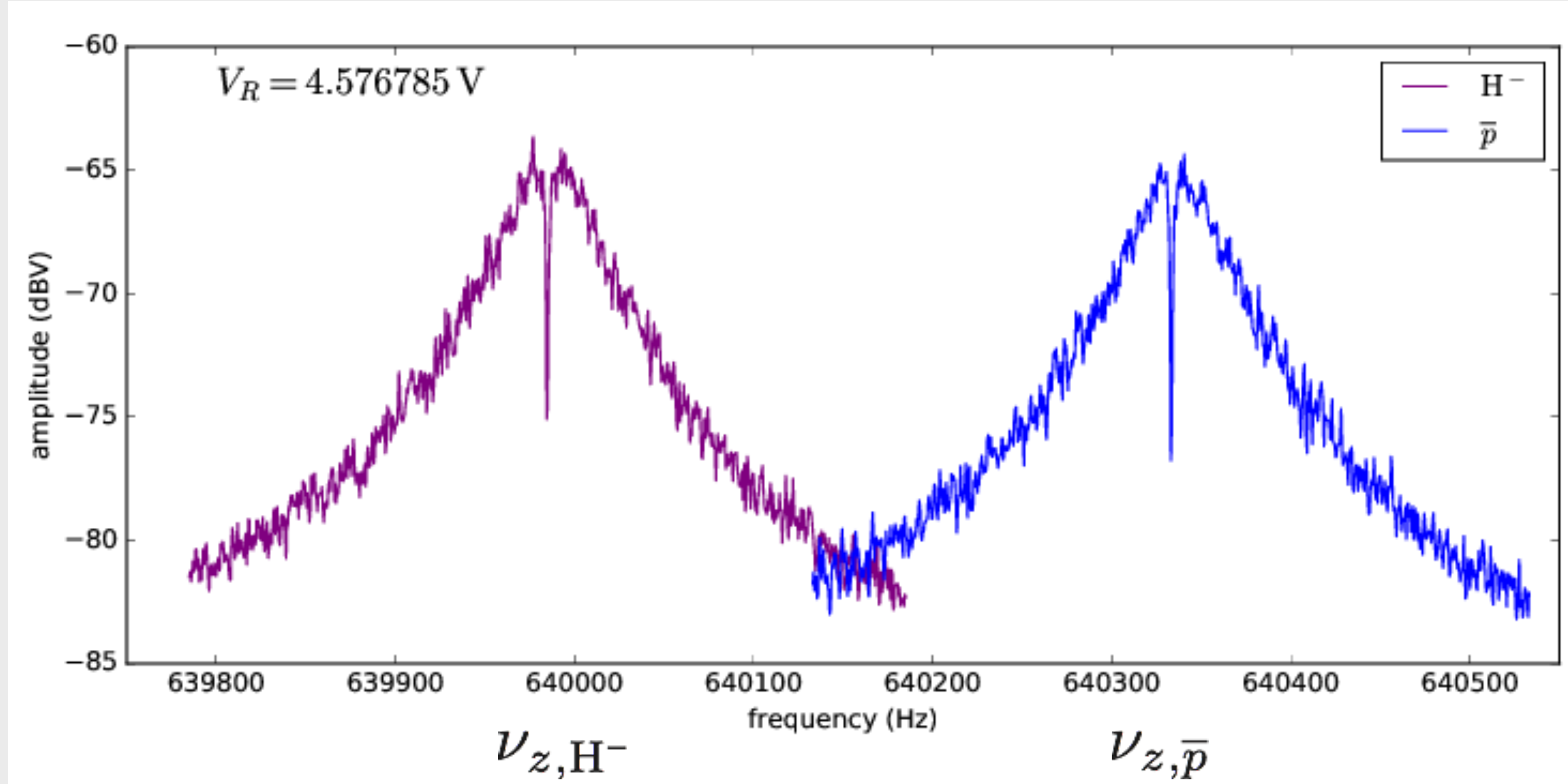

- <u>For statistics:</u> an improved magnetic shielding

Shielding factor: ~10 (2014) -> 95 (2) (2017)

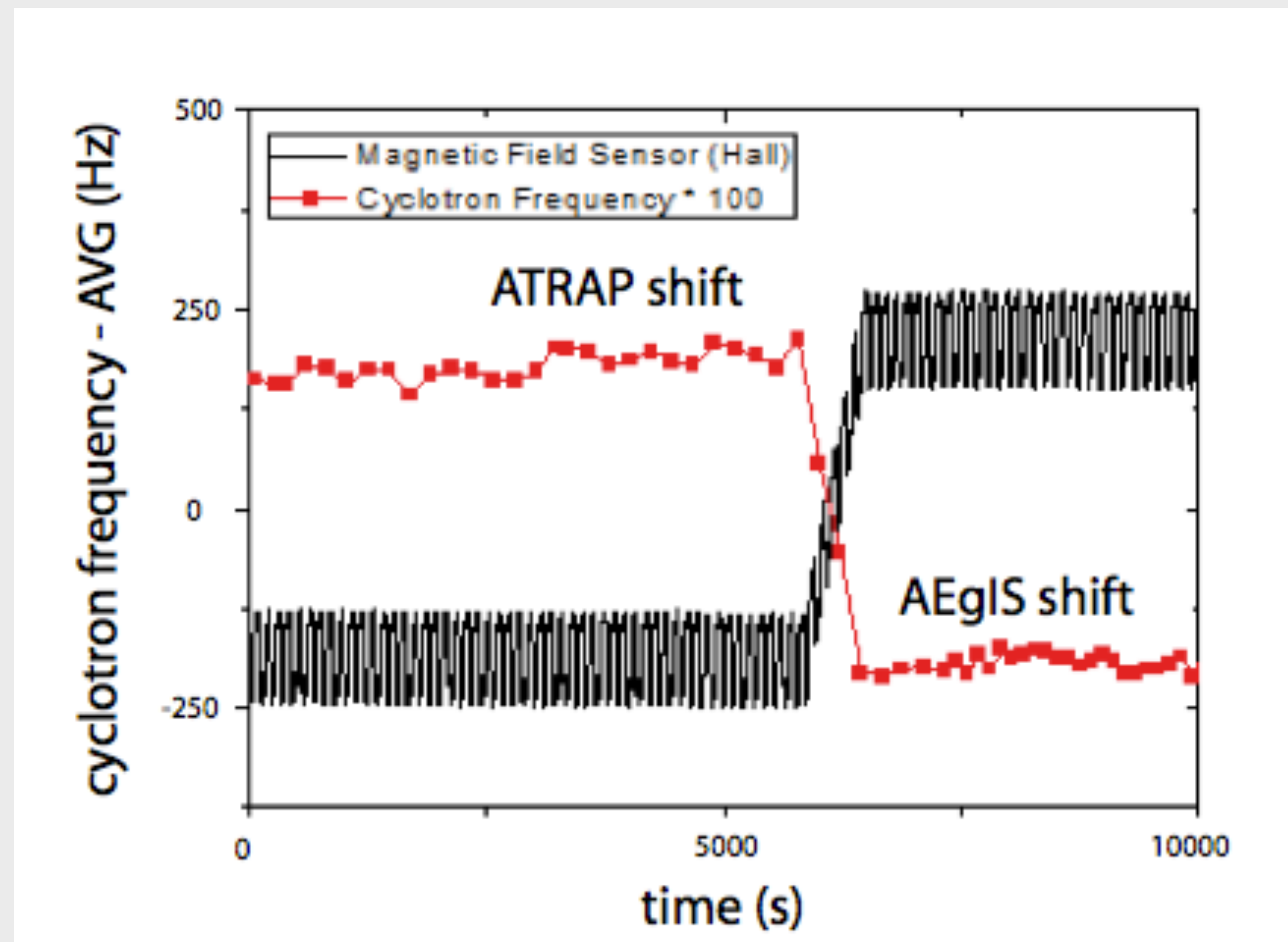

Outline

1. Introduction
    - Background
    - Principle of the measurement
2. Experimental methods
    - Basics of the Penning Trap
    - Image current detection
    - Sideband coupling
3. Review of the 2014 measurement
    - Preparation
    - Measurement procedure
    - Result and limitations
4. **Development during 2017 run**

Development of the frequency stability

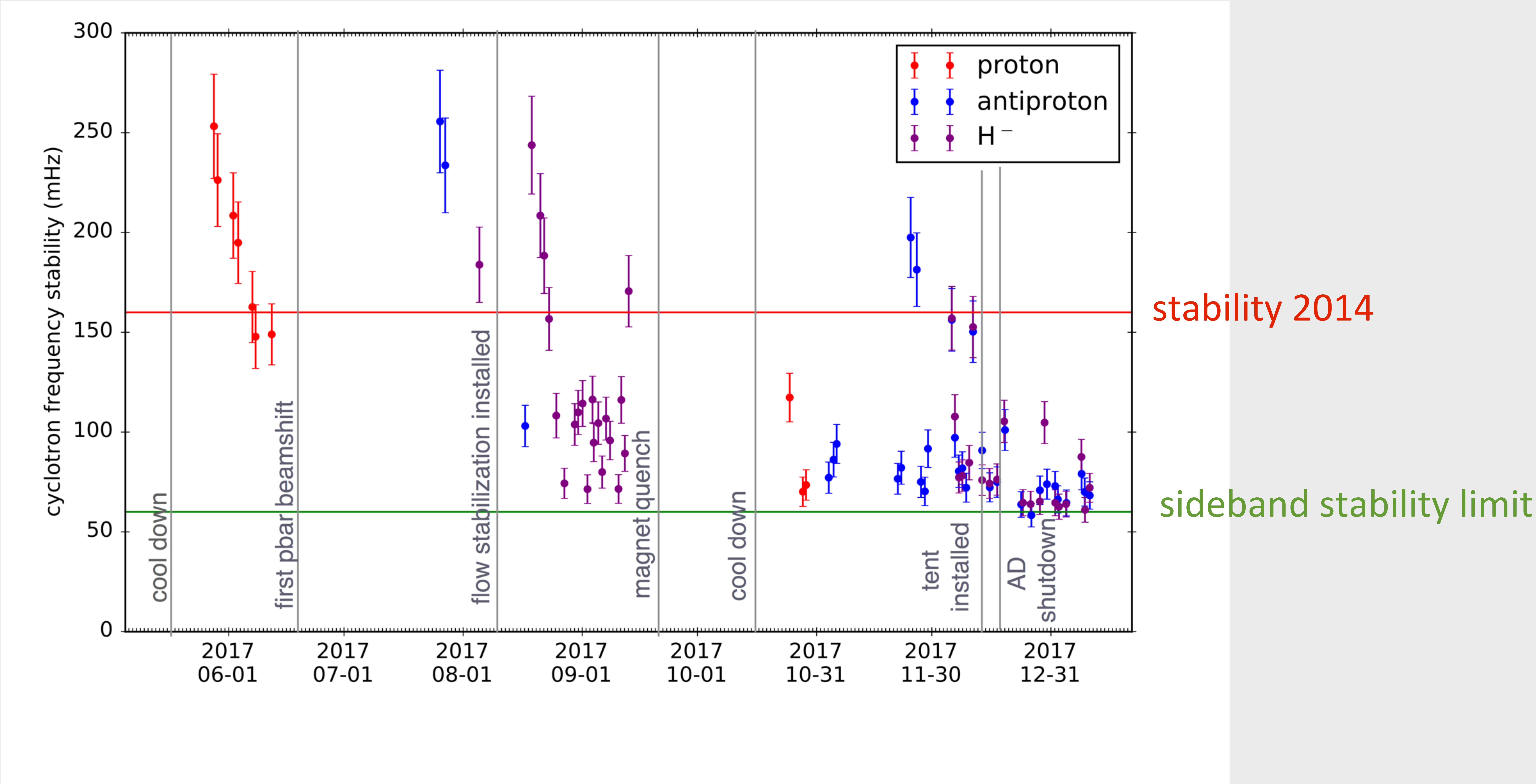

Starting from > 200 mHz, finally reached to ~ 70 mHz, close to the limit of the sideband method (60 mHz)

Development of the frequency stability

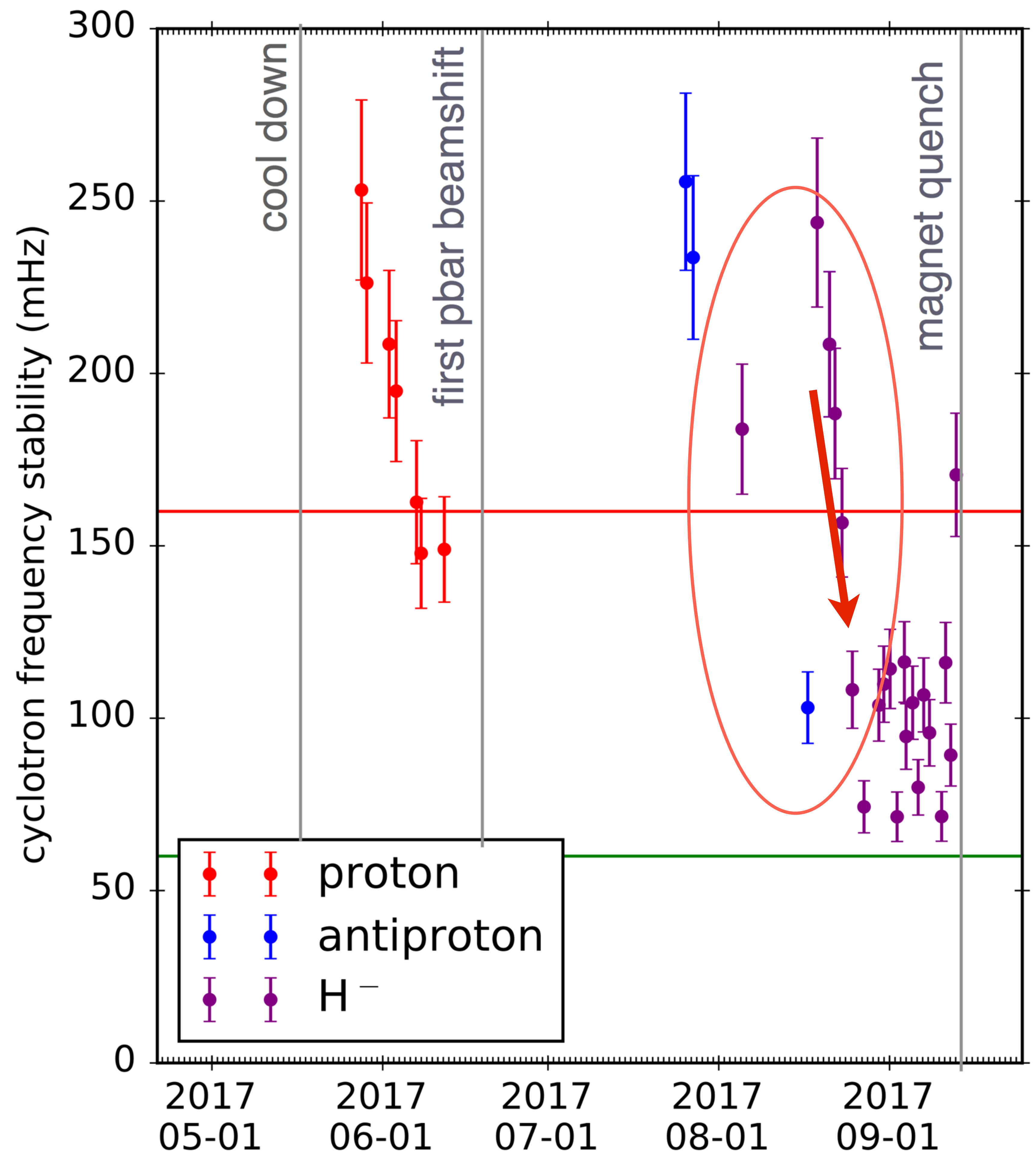

Stability < 100 mHz

Thermal insulation

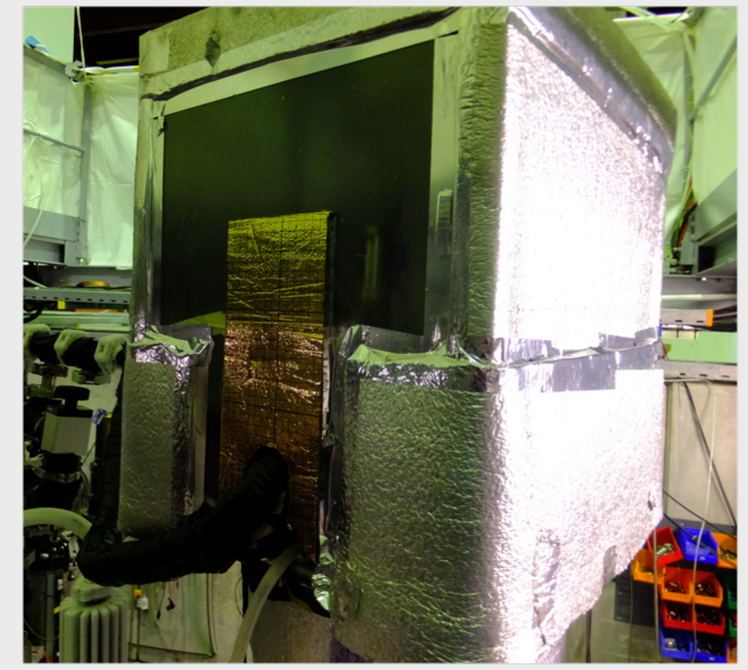

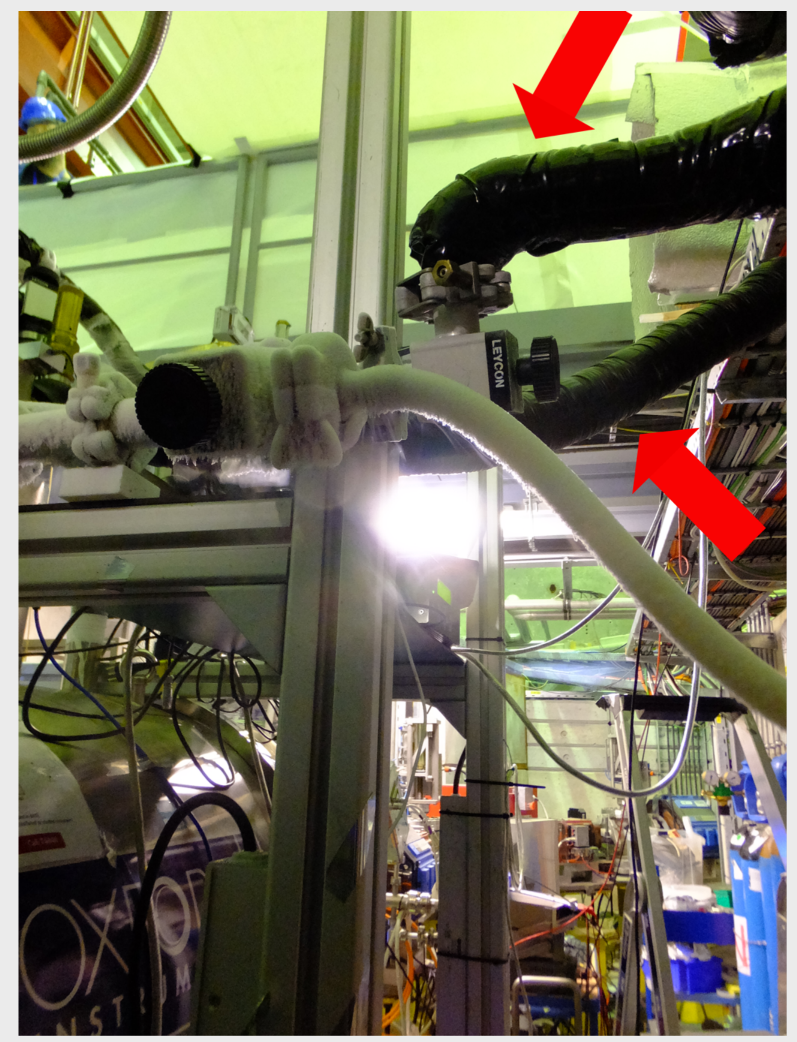

Development of frequency stability

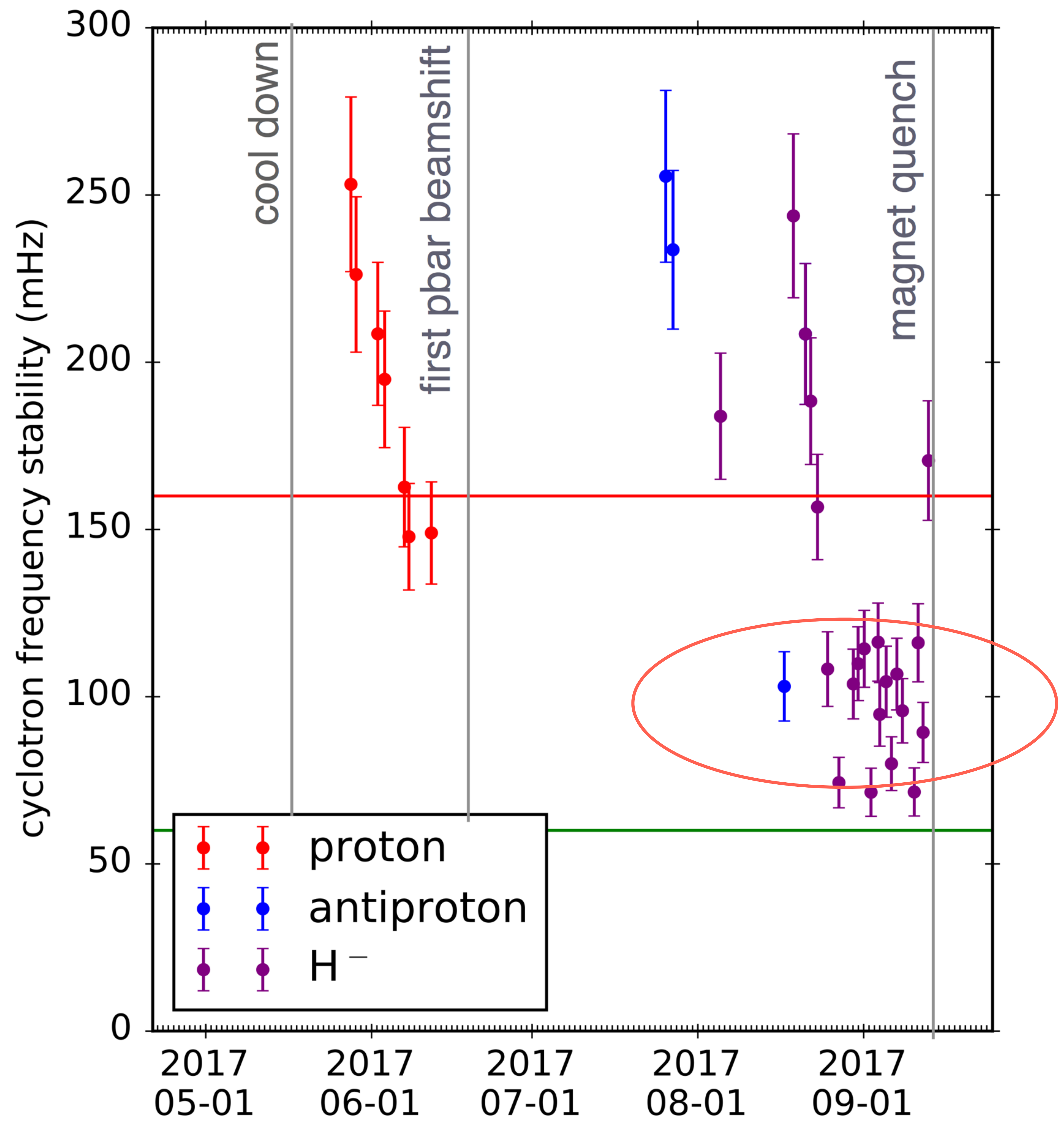

Stability ~ 77 mHz

Flow stabilization

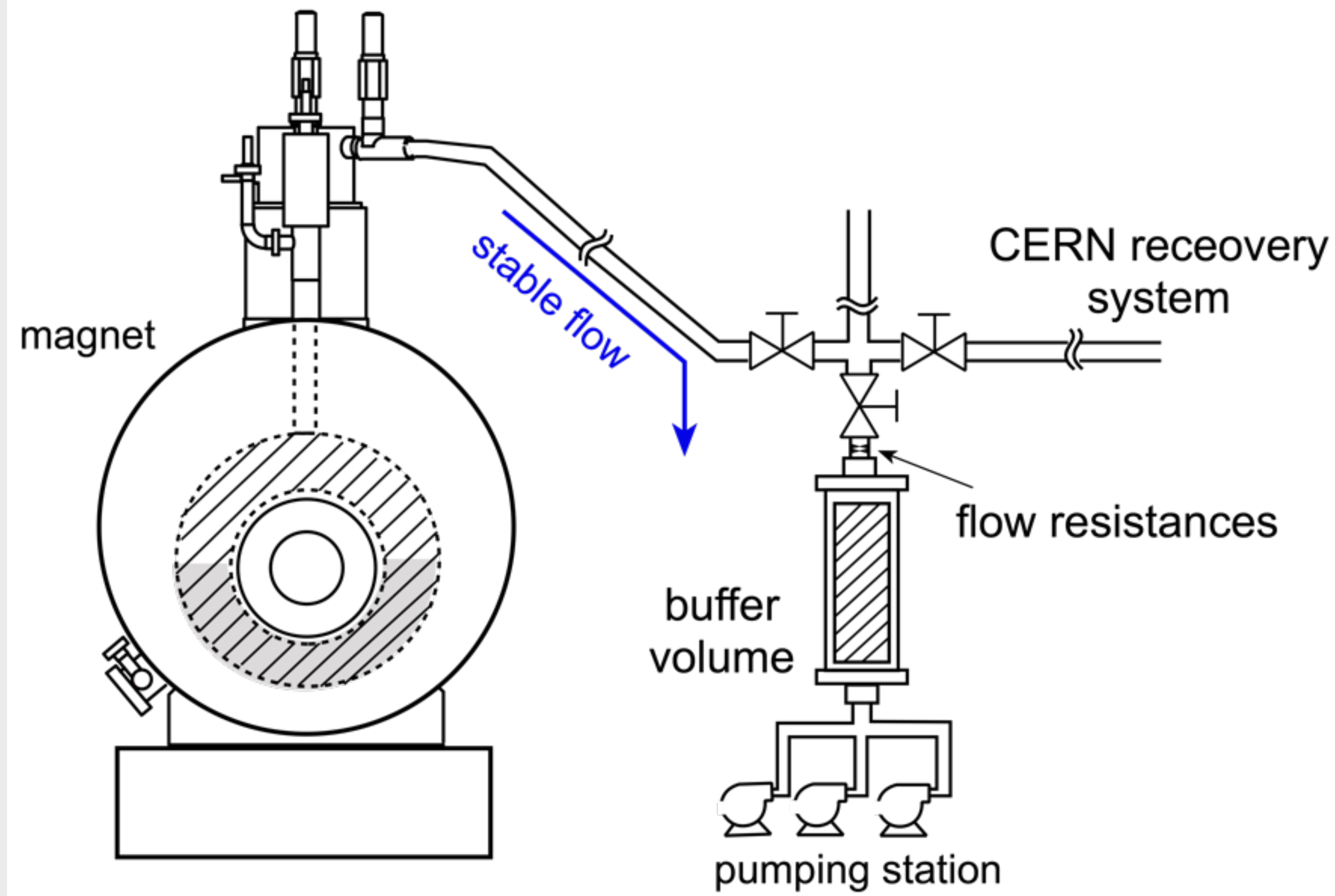

Development of frequency stability

Installation of a tent

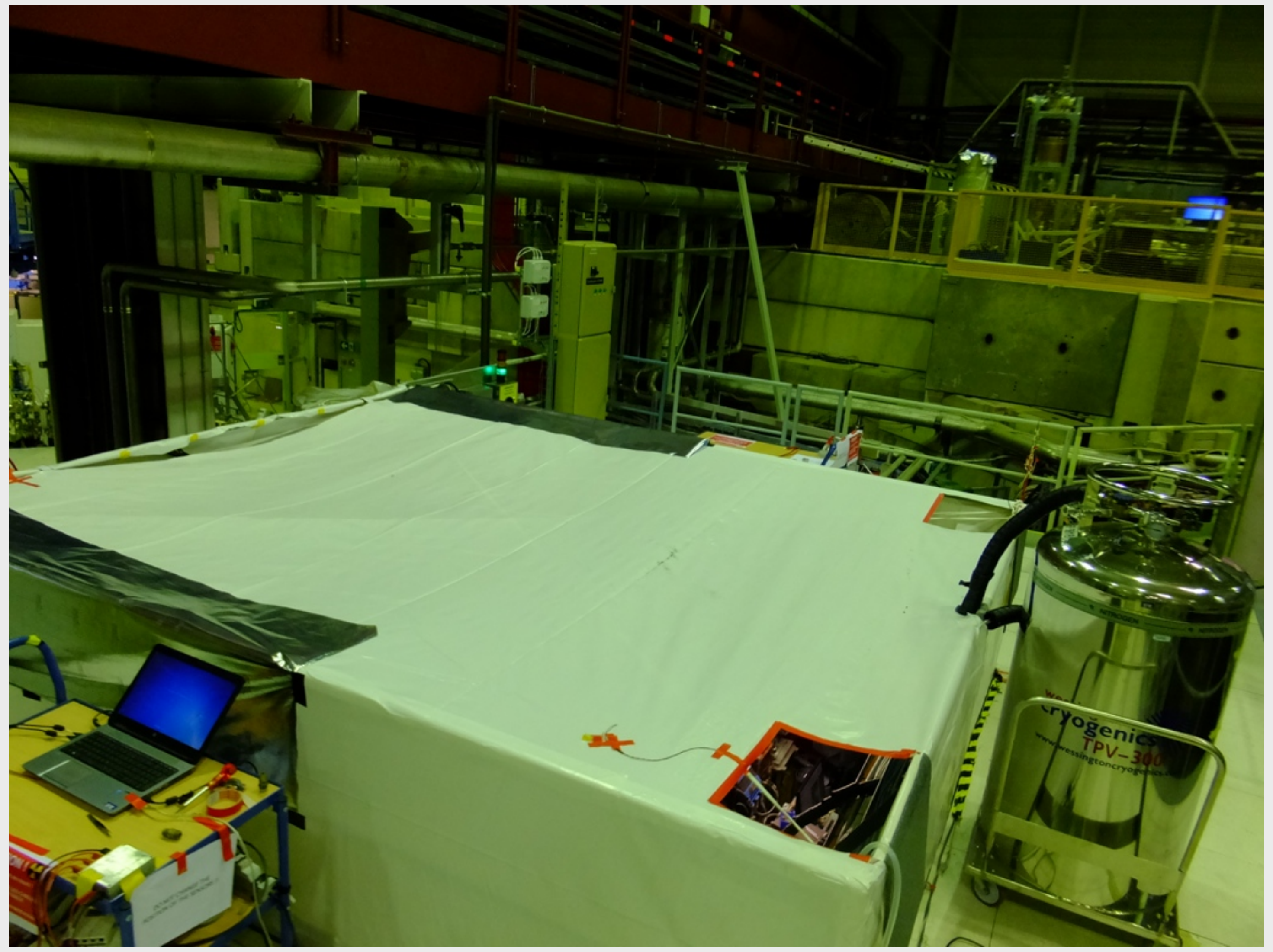

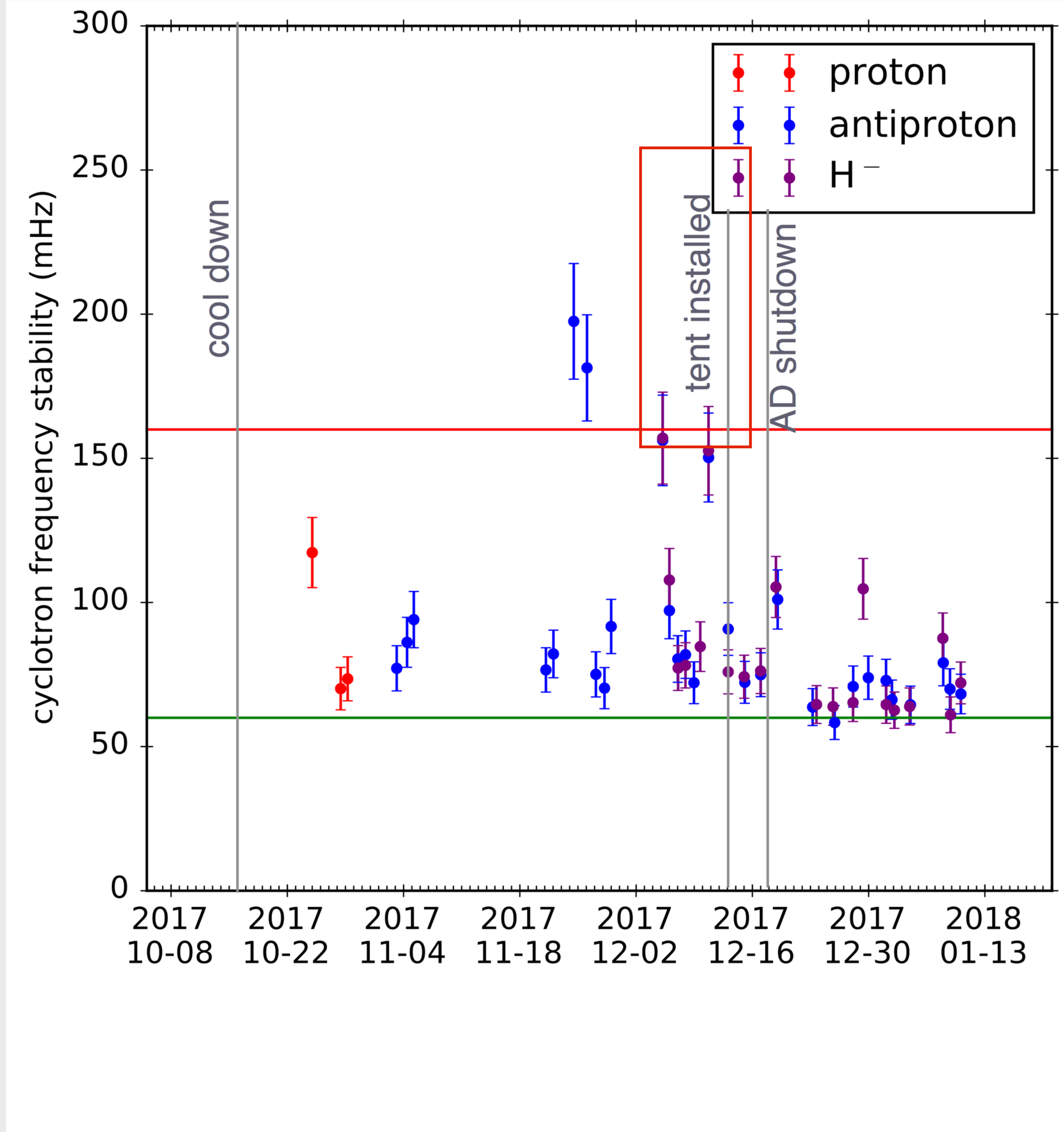

Suppression of temperature fluctuation from the AD air conditioning

➡ Constantly reaching stability < 100 mHz

Development of frequency stability

- After all ...

BASE Zone November 2016

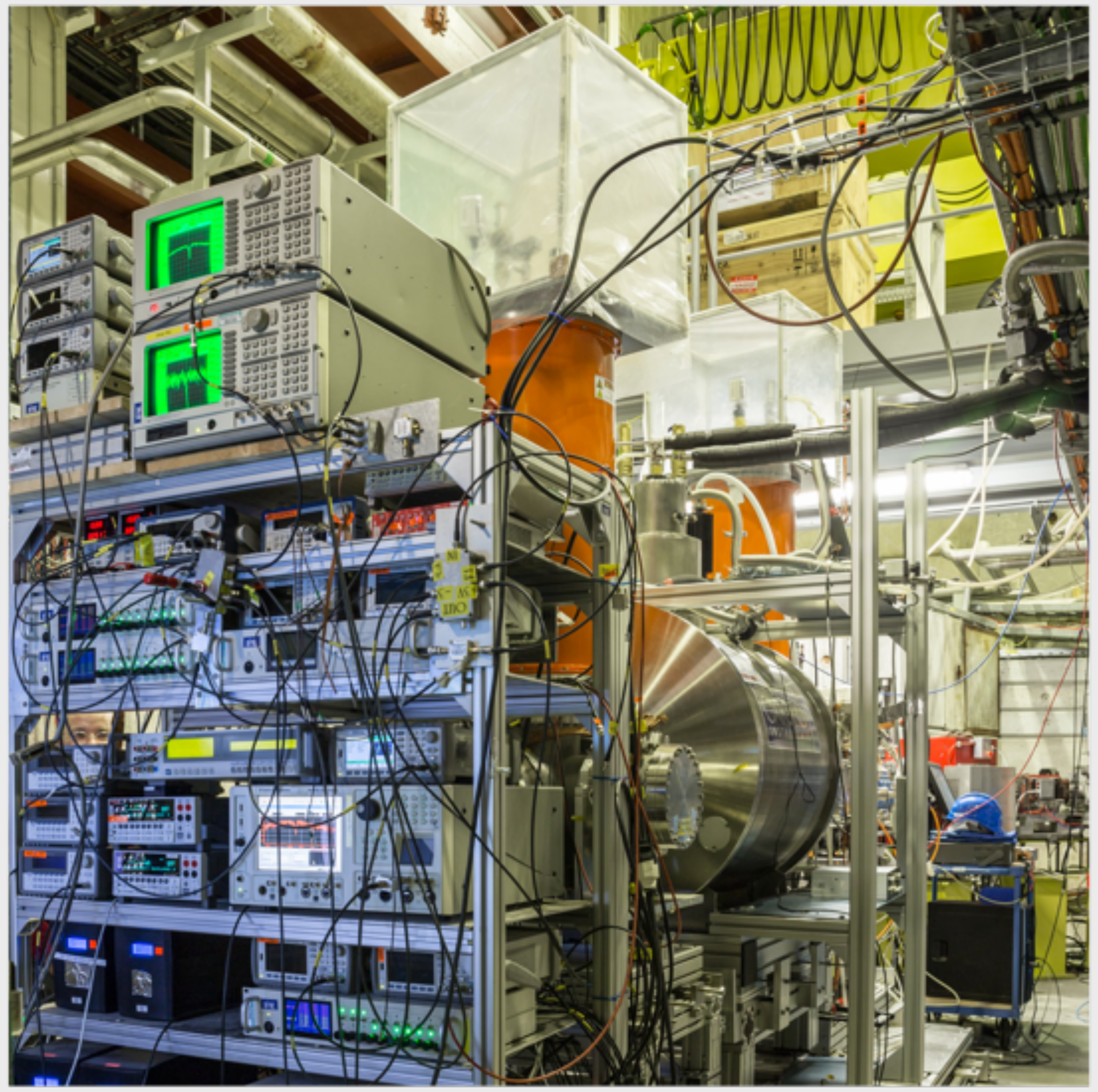

BASE Zone February 2018

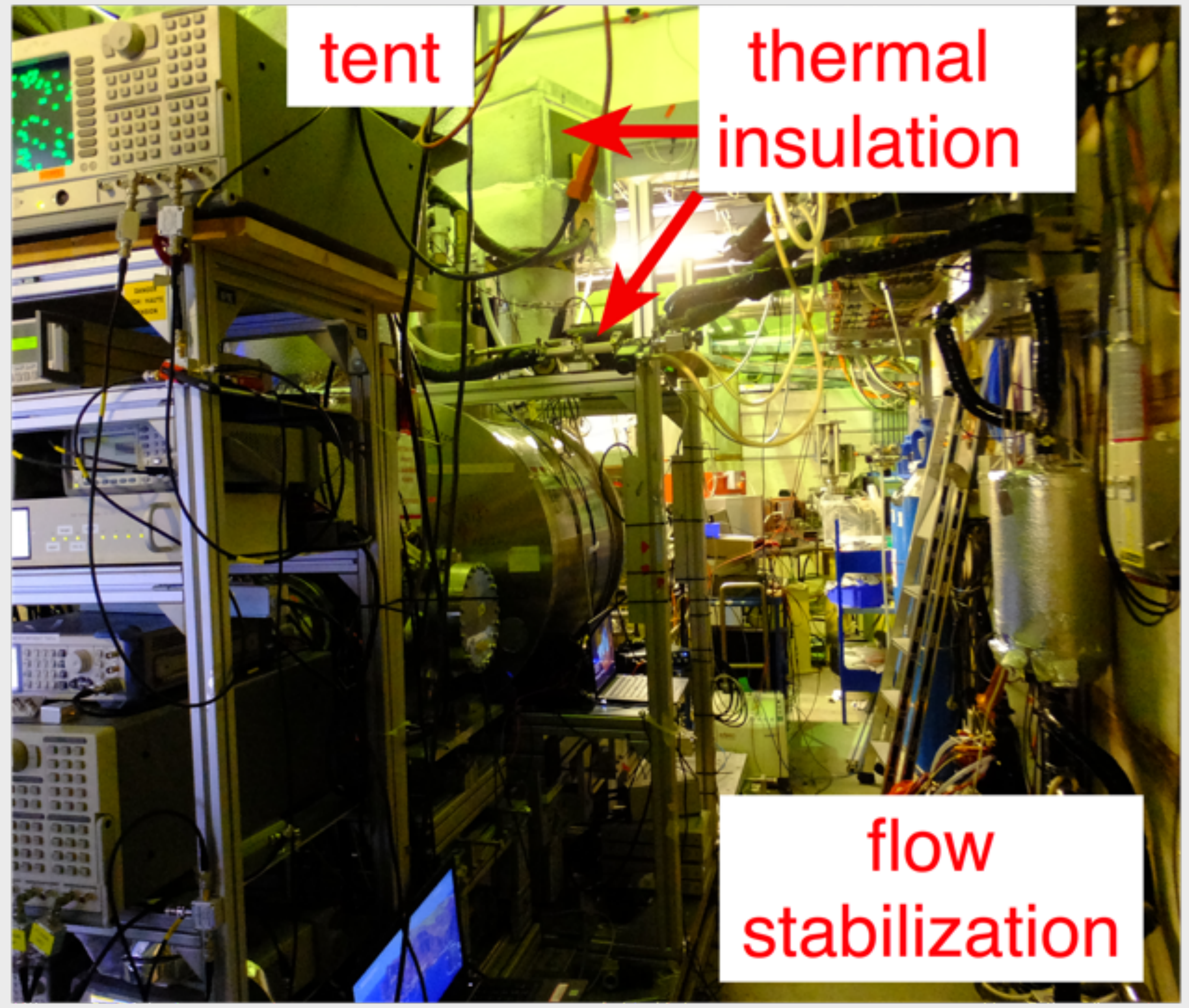

Development of frequency stability

- After all …

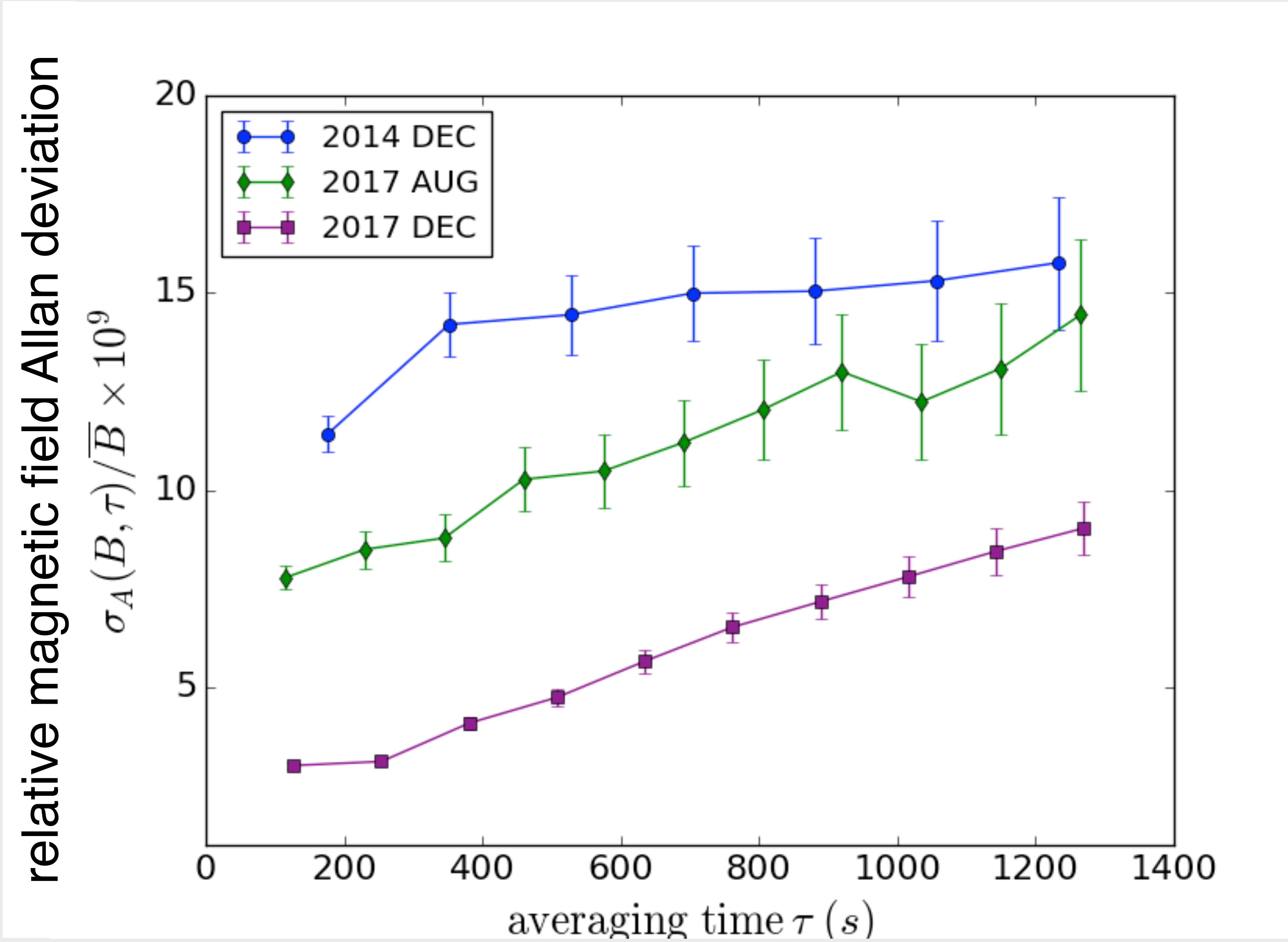

A factor > 3 improvement from 2014

➡ **Improved measurement is possible !**

Summary

- In 2014, we compared the q/m ratio between the proton and the antiproton with a relative precision of 69 p.p.t.. We aim to improve the precision further.
- The improved measurement anticipated by
  - Upgrade which removes the source of the major systematic uncertainty
  - Improvement of the cyclotron frequency stability by a factor > 3

Thank you !

The BASE collaboration

T. Higuchi, J. Harrington, M. Borchert, J. Morgner,
S. Sellner, C. Smorra, A. Mooser, G. Schneider, N. Schön, M. Wiesinger,
K. Blaum, Y. Matsuda, C. Ospelkaus, W. Quint, J. Walz, Y. Yamazaki
and S. Ulmer

Cyclotron excitation

Cyclotron excitation

- With the cyclotron detector,
- The excited peak observable for $E_+ > 1.5$ eV -> $\rho_+ > 80$um (for SB: 10 um)
- Much characterization of the trap required

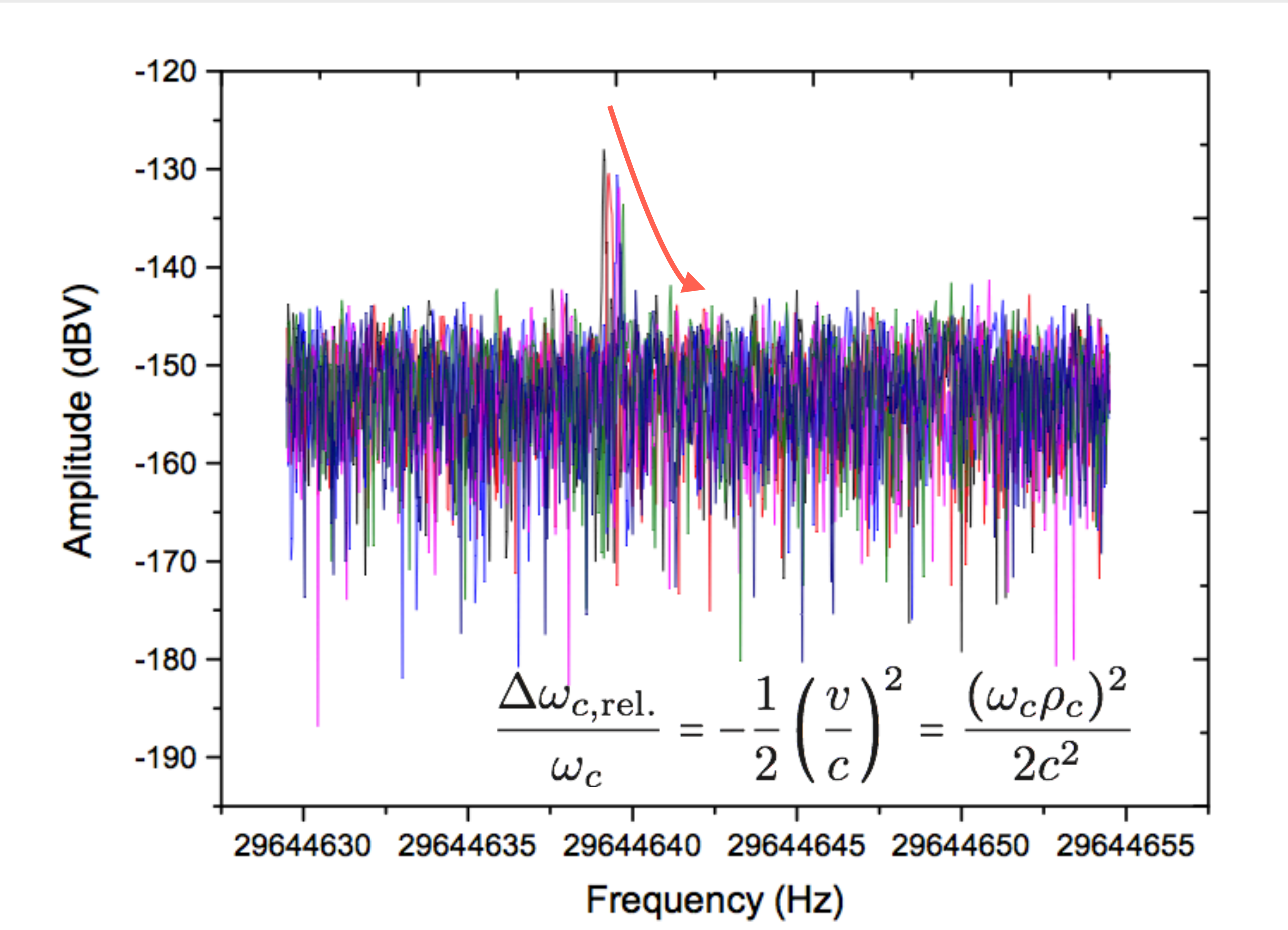

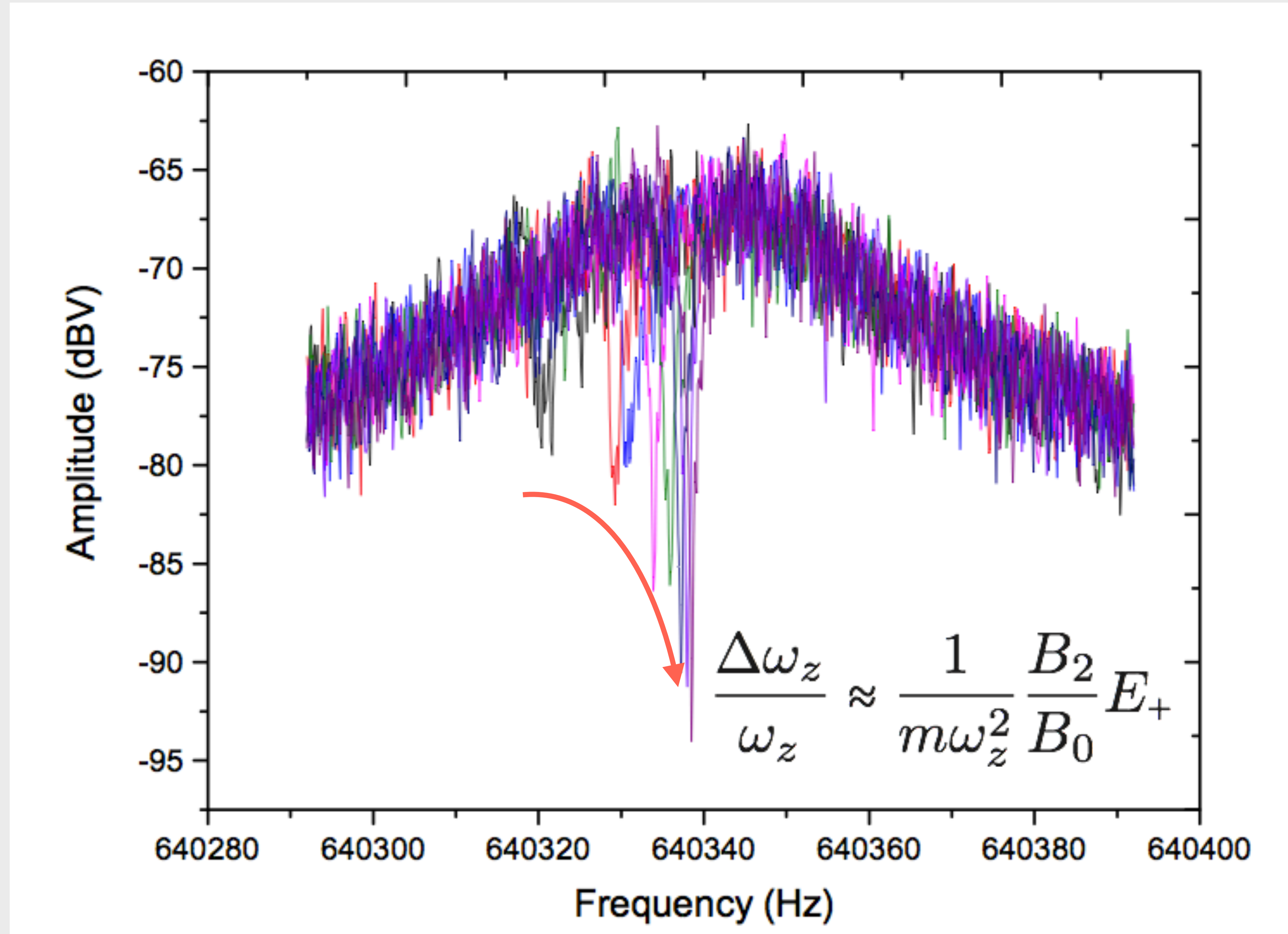

$B_2 = -0.27$ T/m^2

q/m comparison data analysis

Details of data analysis

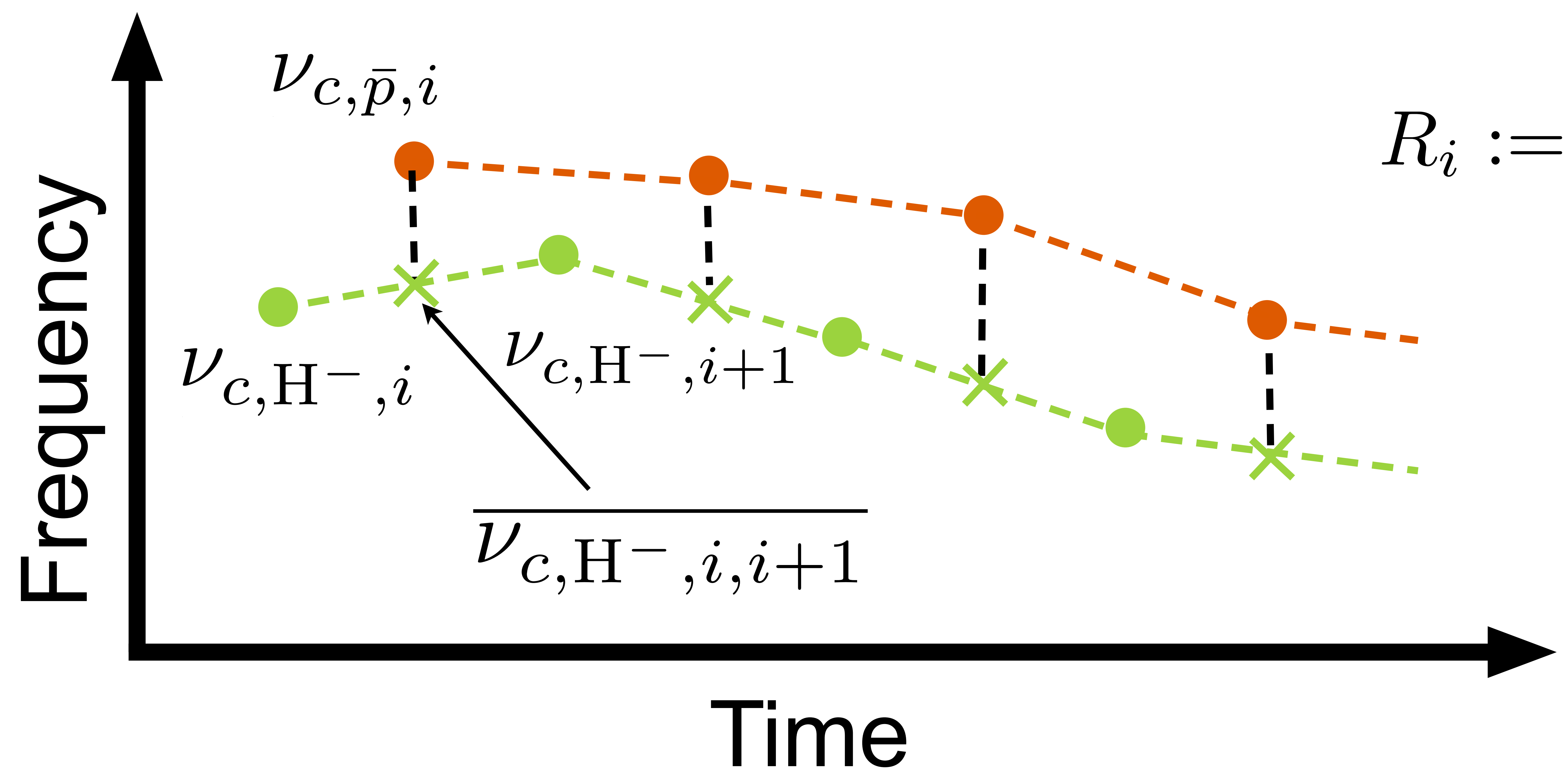

$$R_i := \frac{\nu_{c,\bar{p},i}}{\overline{\nu_{c,\mathrm{H}^-,i,i+1}}}$$

One set of data is interpolated to determine the ratio between the measurements at the same time.
(The reciprocal ratio $\overline{\nu_{c,\bar{p},i,i+1}}/\nu_{c,\mathrm{H}^-,i}$ was also evaluated.)

Details of data analysis

- Systematic shifts due to a drift of the magnetic field

  $1/B_0 \times(\Delta B/\Delta t) = -5\ (1) \times 10^{-9}$/hour

  is cancelled by evaluating interpolation of alternative measurement.
- The uncertainty of the mean of *R* is estimated by correlational matrix.
- The data evaluation is carefully justified by
  - Gaussian distribution of the sample of ratio *R.*
  - Evaluating the ratio between identical particles ($\bar{p}$-to-$\bar{p}$, H^- -to-H^-).

$$R_{\mathrm{exp,id}} - 1 = -3(79) \times 10^{-12}$$

  - Comparison to a simulation based on a modeled characteristic of magnetic field fluctuations.

Systematic corrections of the ratio *R*

- Dominant factor : Adjustment of trapping potential by 5mV is needed between the antiproton and the H- ion.

  -> leading to a shift of position (~30 nm) due to a slight asymmetry of the trap. A magnetic field gradient (B_1 = 7.58 (42) mT/m)change shifts the cyclotron frequency of the H- ion.

  Correction of $\Delta R/R$: -114(26) p.p.t

- Sub-p.p.t corrections :

  Image charge shift : 0.047(4) p.p.t

  Relativistic shift : -0.024(2) p.p.t

  A tilt of the apparatus, voltage drift during the measurement etc.

Voltage offset from a voltage divider

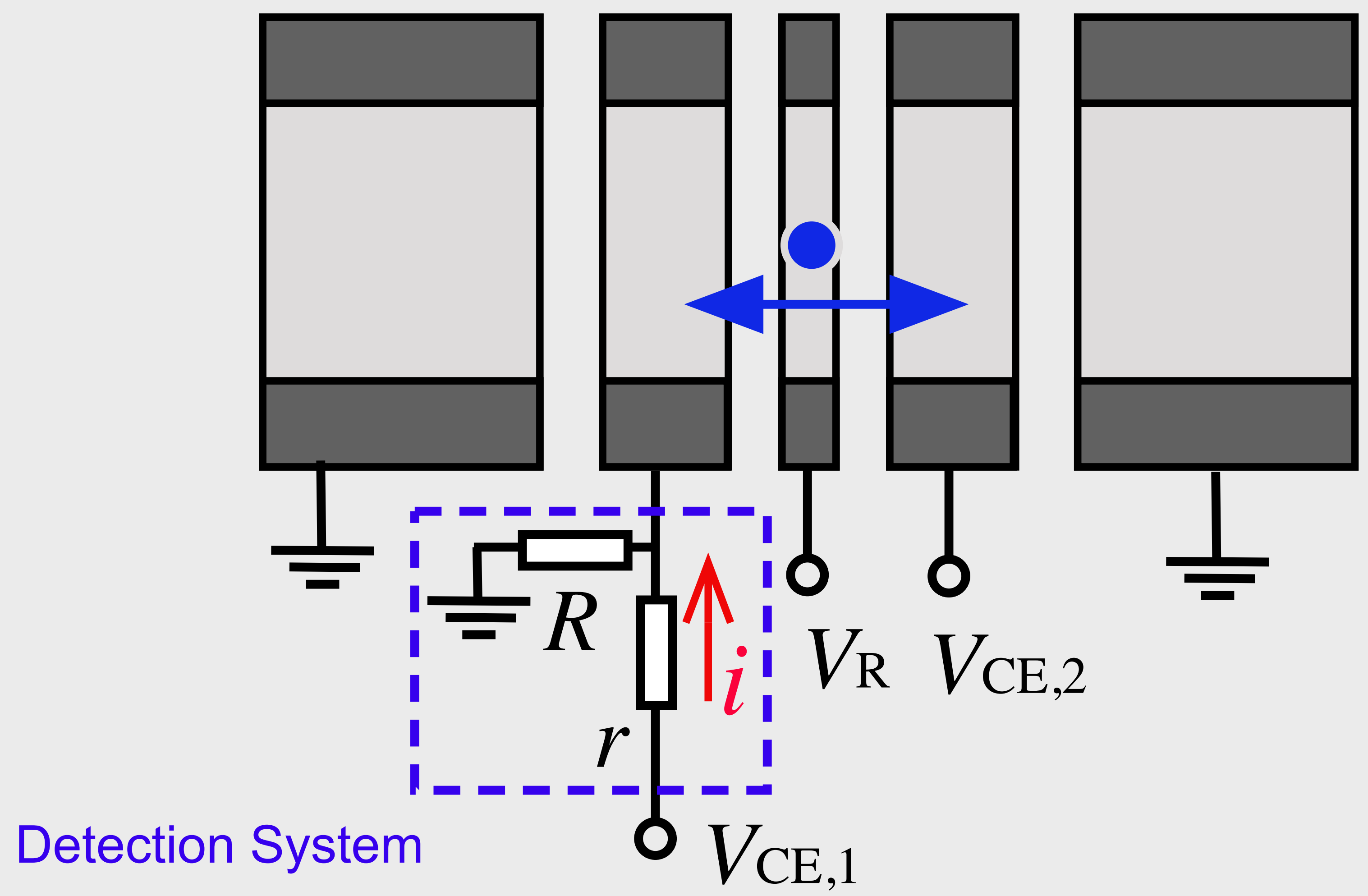

The effective resistive component *r* induces a voltage drop due to the leakage current *i*.

The voltage offset ΔV_{CE} differs between $\bar{p}$ and H^- by 5.003 mV × 1.5/100 = 75 uV
→ Produces a shift of potential minimum by 30 nm

$$\Delta V_{CE,1} = i \times r$$
$$= \boxed{\frac{r}{r+R}} \times V_{CE,1}$$

~ 1.5 (2) %

$$V_{CE,1} \rightarrow V_{CE,1} - \Delta V_{CE,1}$$

Trap optimization

- The electric trapping potential is calculated by solving a Laplace equation. The offsets of the parameters are calibrated by systematic measurements.

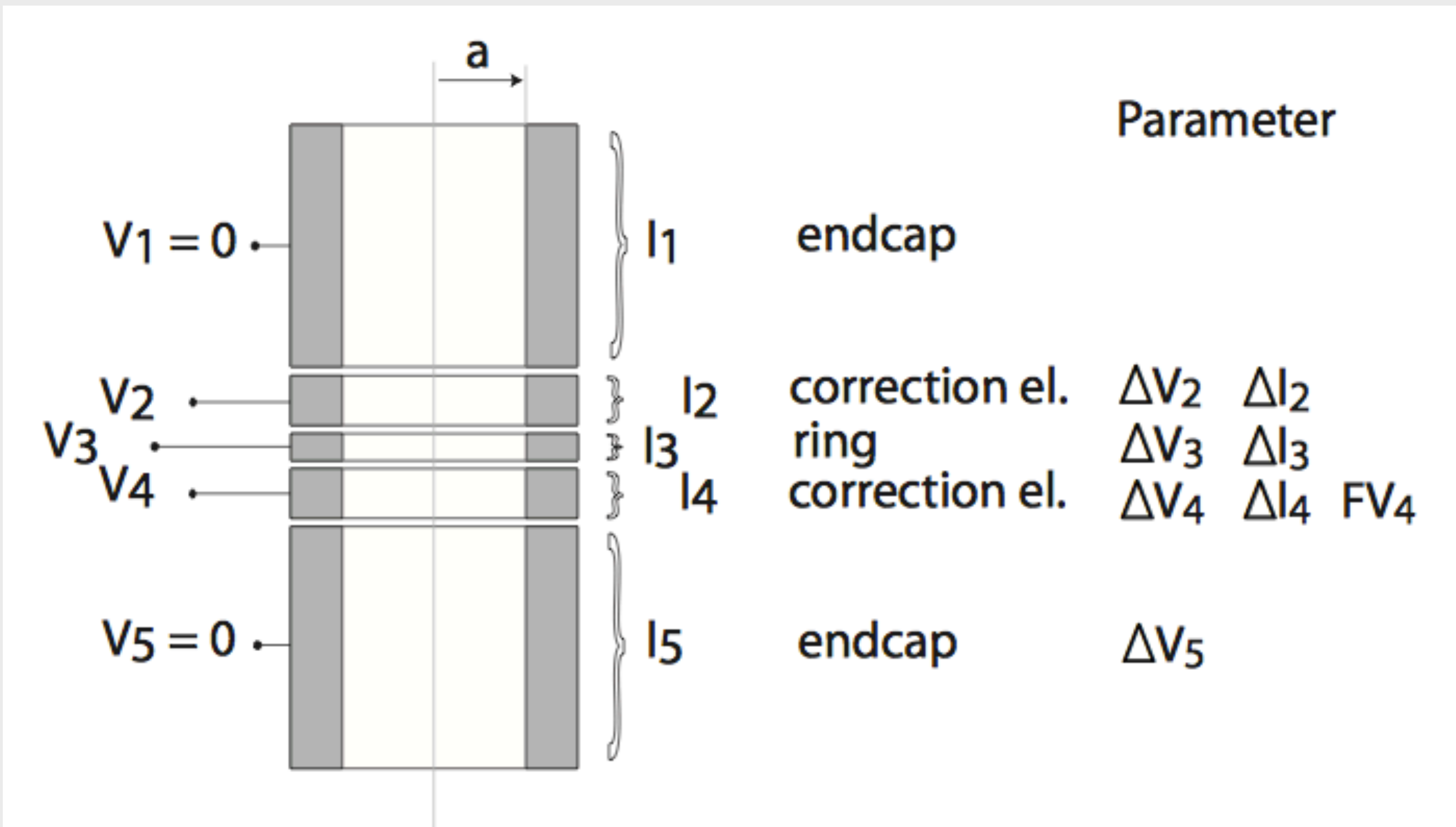

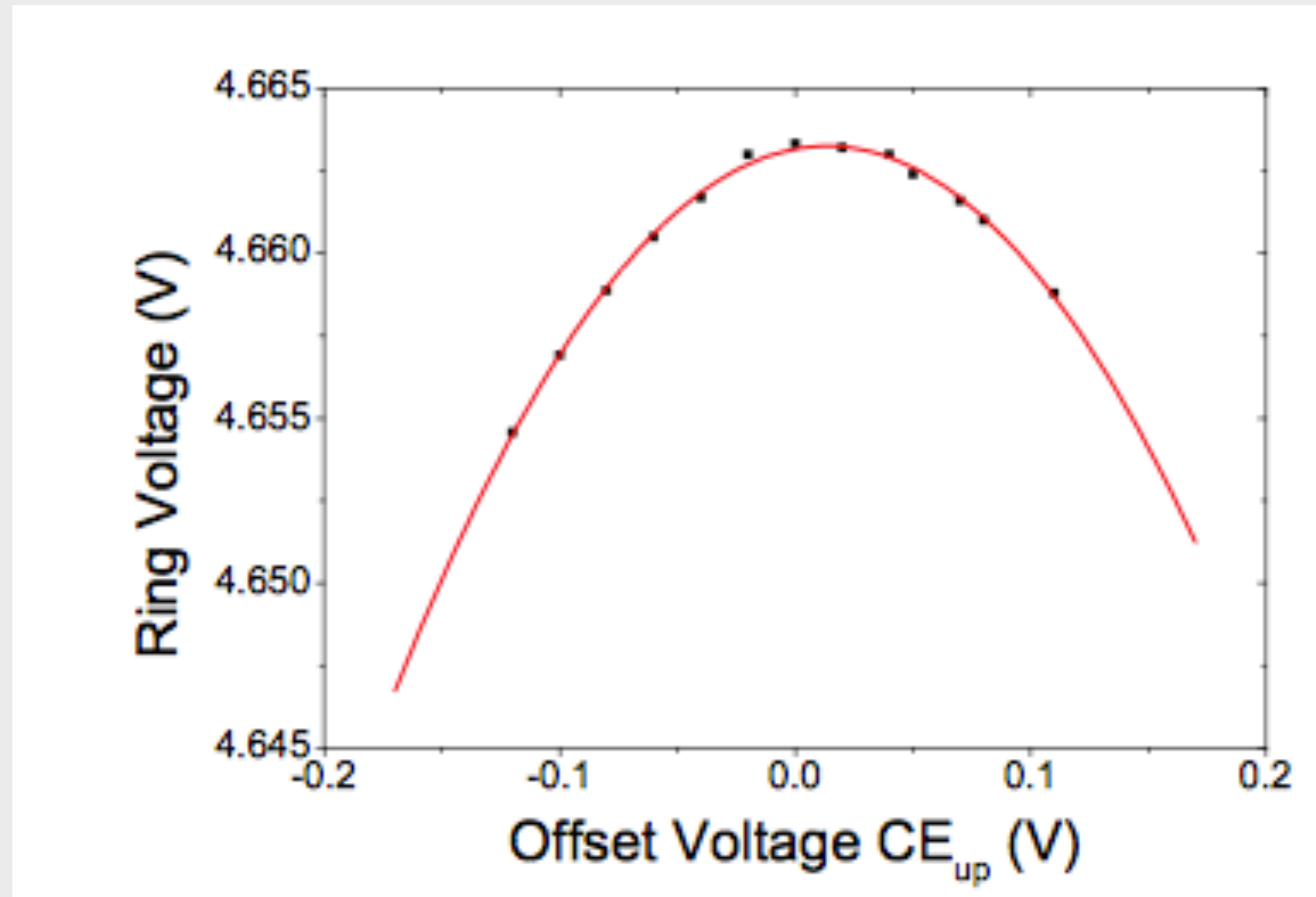

- A position of the particle is determined by calculating the potential minimum.

Sub-p.p.t. contributions

Effect	Shift (p.p.t.)	Uncertainty (p.p.t.)
Magnetic gradient shift	-0.002	0.0002
Magnetic bottle shift	0.009	0.012
Image charge shift	0.047	0.004
Image current shift	<| 0.001 |	<| 0.001 |
Relativistic shift	-0.024	0.002
Voltage drift	0.015	0.003
Tilt of apparatus	-0.027	0.007
Rb-clock	–	3

Magnetic field fluctuations due to the AD

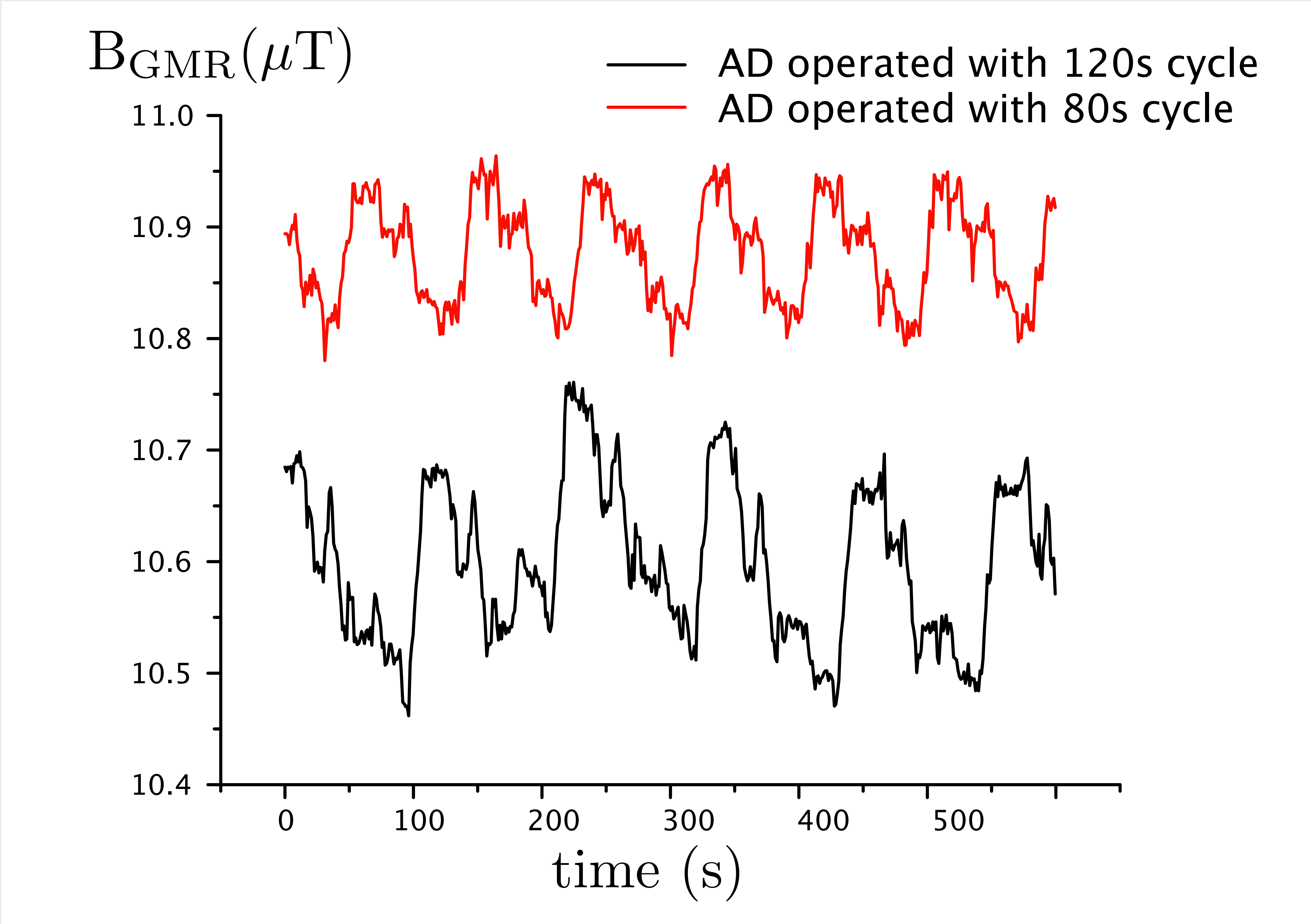

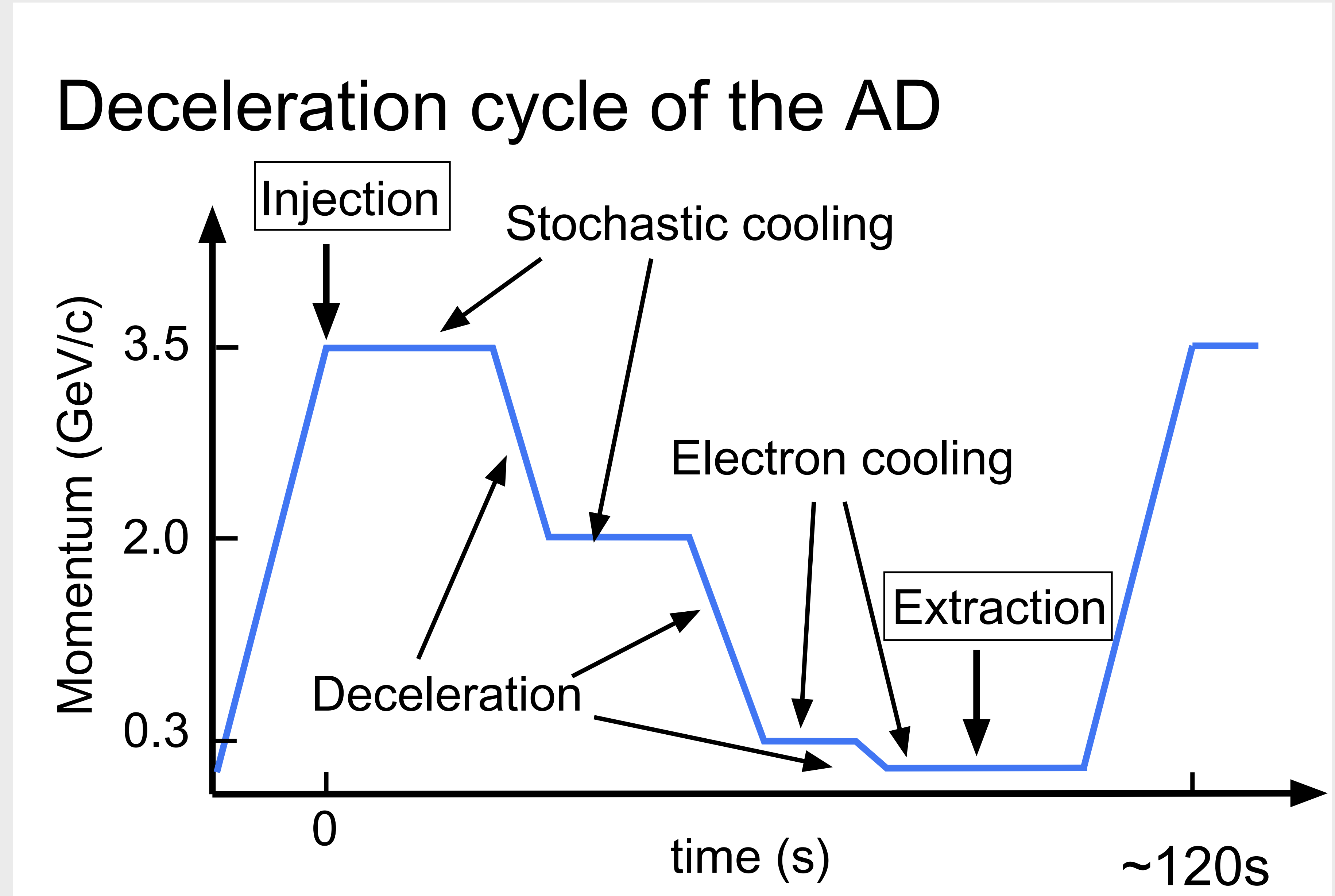

Ambient magnetic field fluctuations synchronized to the AD deceleration cycle. (100-300 nT amplitude)

Triggered measurement scheme

Allan deviation of the cyclotron frequency:

- White-noise component
- Random-walk component
- **Oscillatory component**

A beat between the measurement cycle and the AD cycle.
→ strongly suppressed by using the triggered measurement sequence.

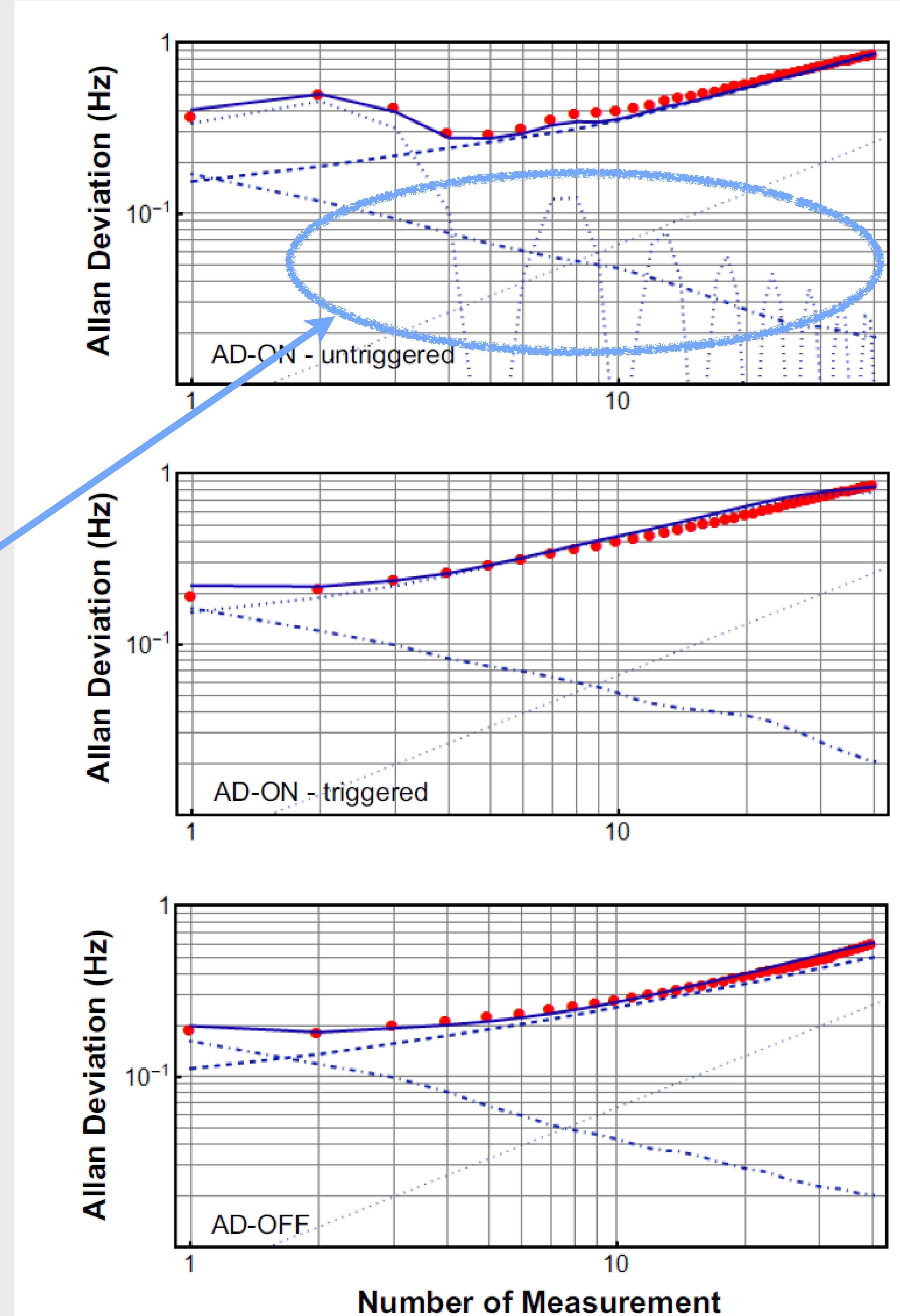

Limit of sidereal variations

- The high data-sampling rate allowed us to test the Lorentz invariance by searching sidereal variations, possibly be mediated by cosmological background fields
- Dataset of $R_{exp,i}$ was processed using a lock-in method.

Method:

- Evaluate $$A_{\text{lock-in}}(T) = \sum_i R_{\text{exp}}(t_i) \times \sin(t_i/T)$$
- The background level is estimated from simulation assuming white noise.
- The statistical significance is estimated by comparison with a simulation assuming a possible oscillating term.

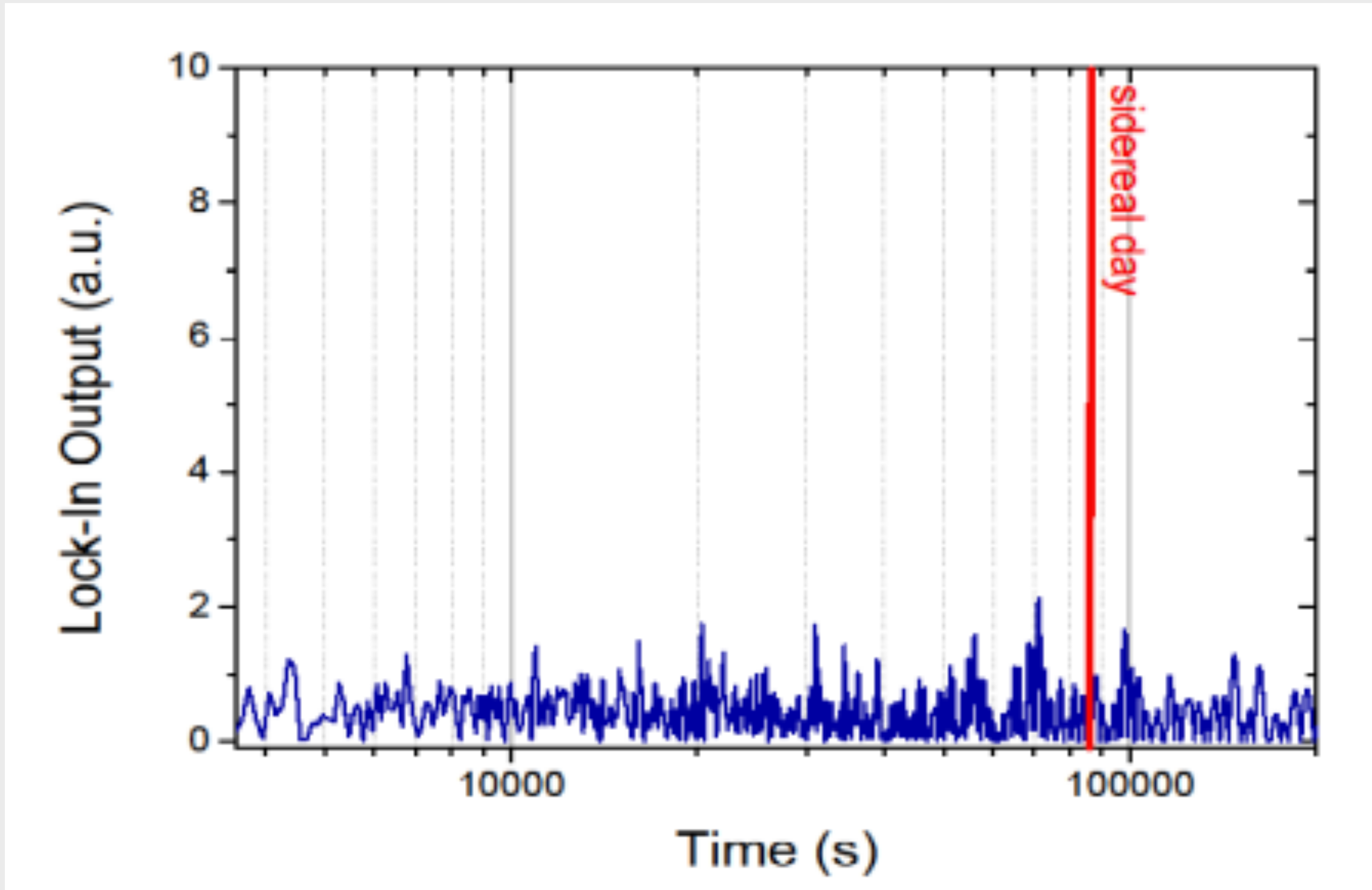

➡ No peak at the sidereal day (= 86164.1s) period.

➡ The possible amplitude of sidereal variation in R_{exp} < 720 p.p.t. at 95% C.L.

Allan deviation

Allan deviation $\sqrt{\sigma_A^2(\tau)}$

$$\sigma_A^2(\tau) = \frac{1}{2(M-1)} \sum_{i=1}^{M-1} (y_{i+1} - y_i)^2$$

y_i : i th data averaged over τ

Measurement-measurement deviation as a function of an averaging time.
→Gives information of noise characteristics.

White noise

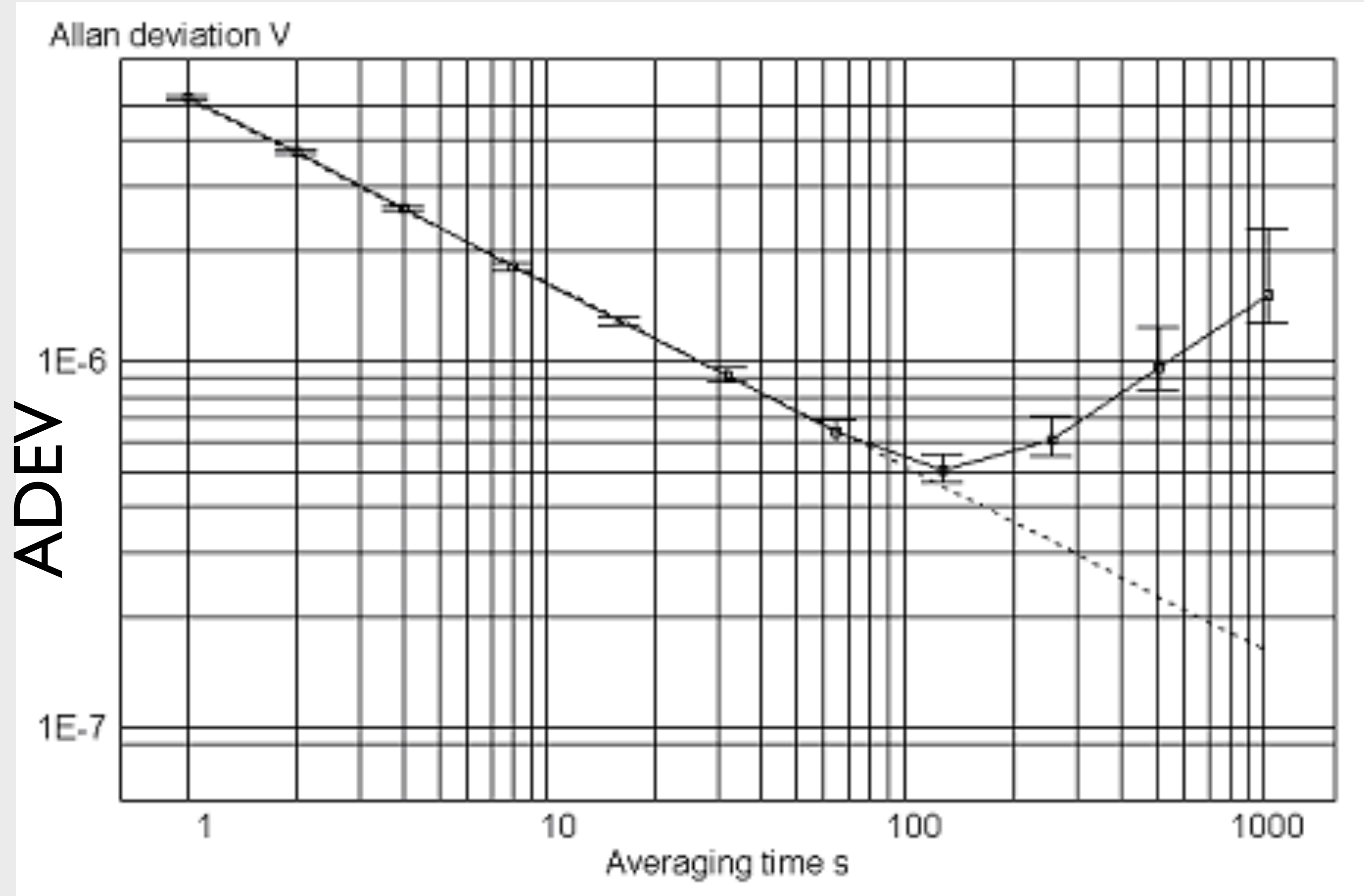

Oscillating noise

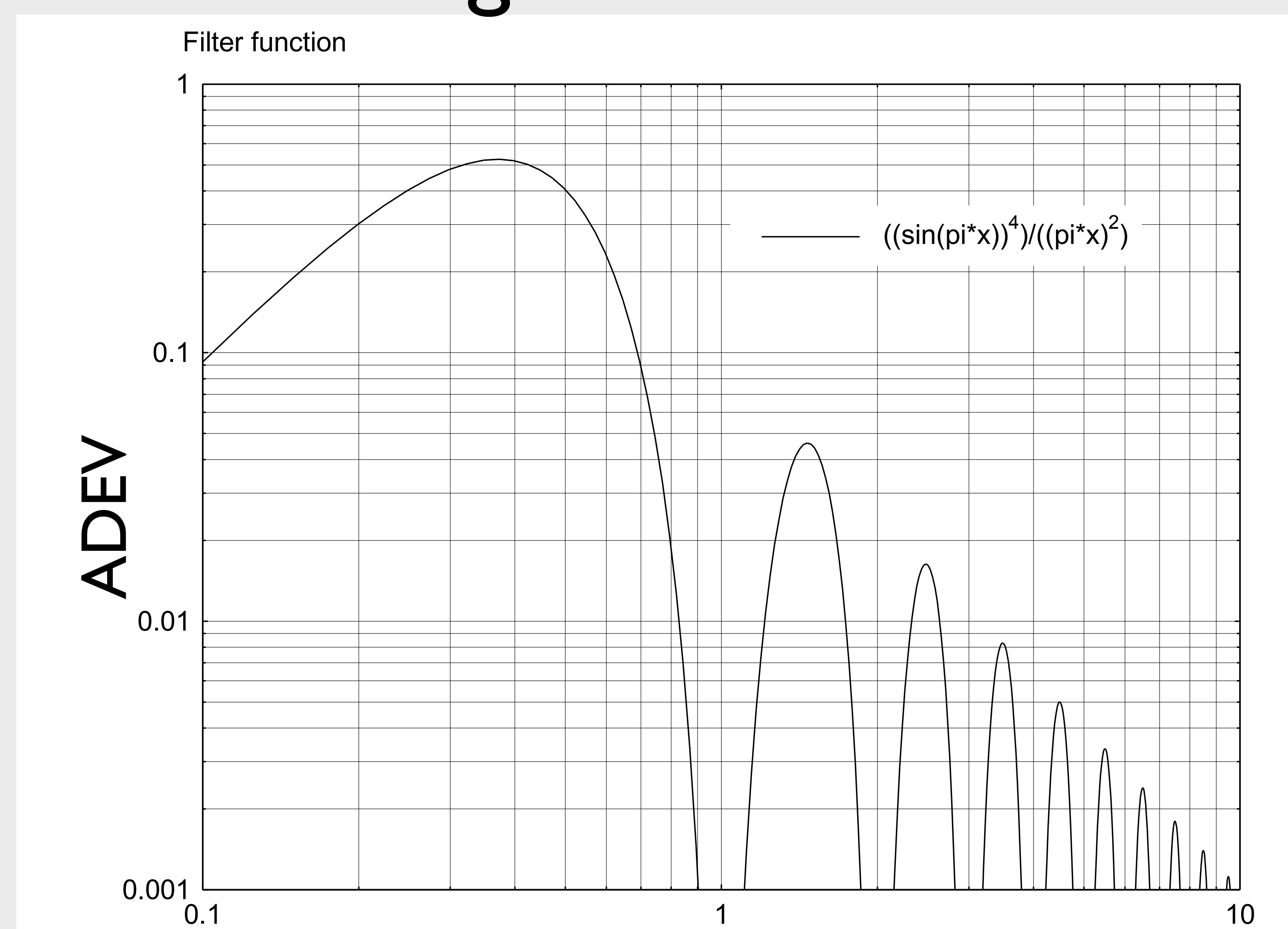

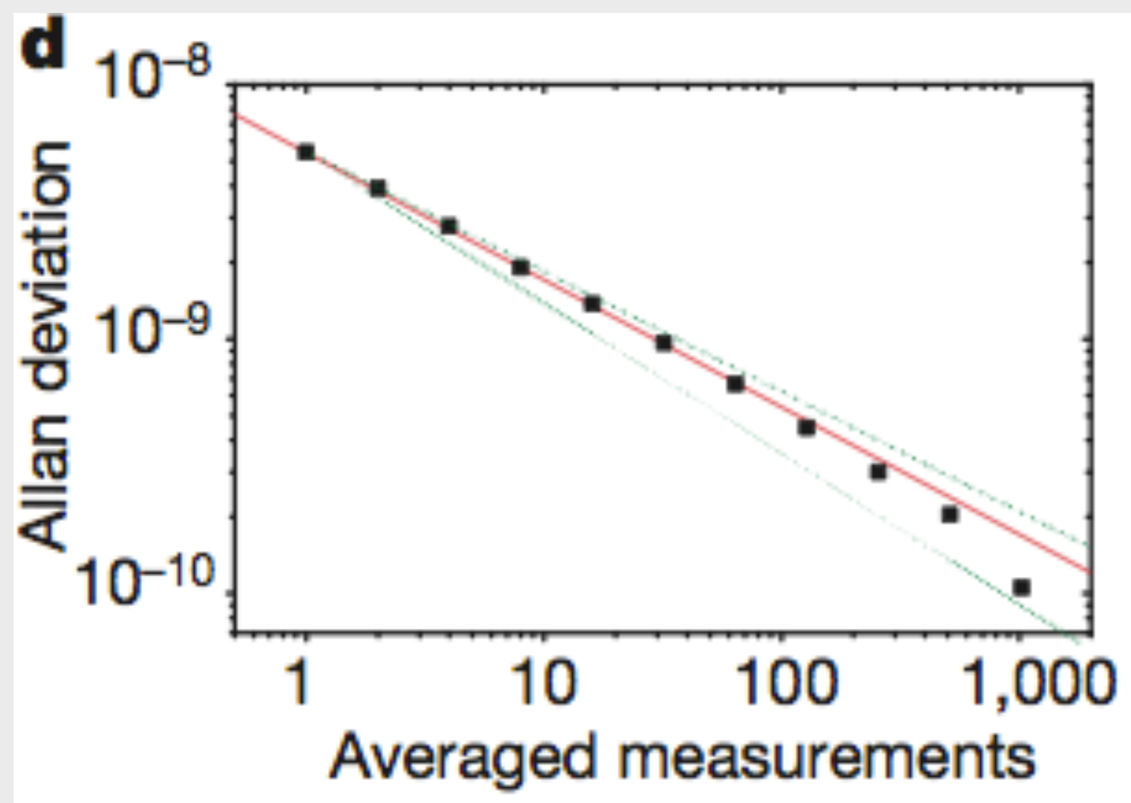

The frequency ratio *R* : white noise

Penning trap basics

Image current detection

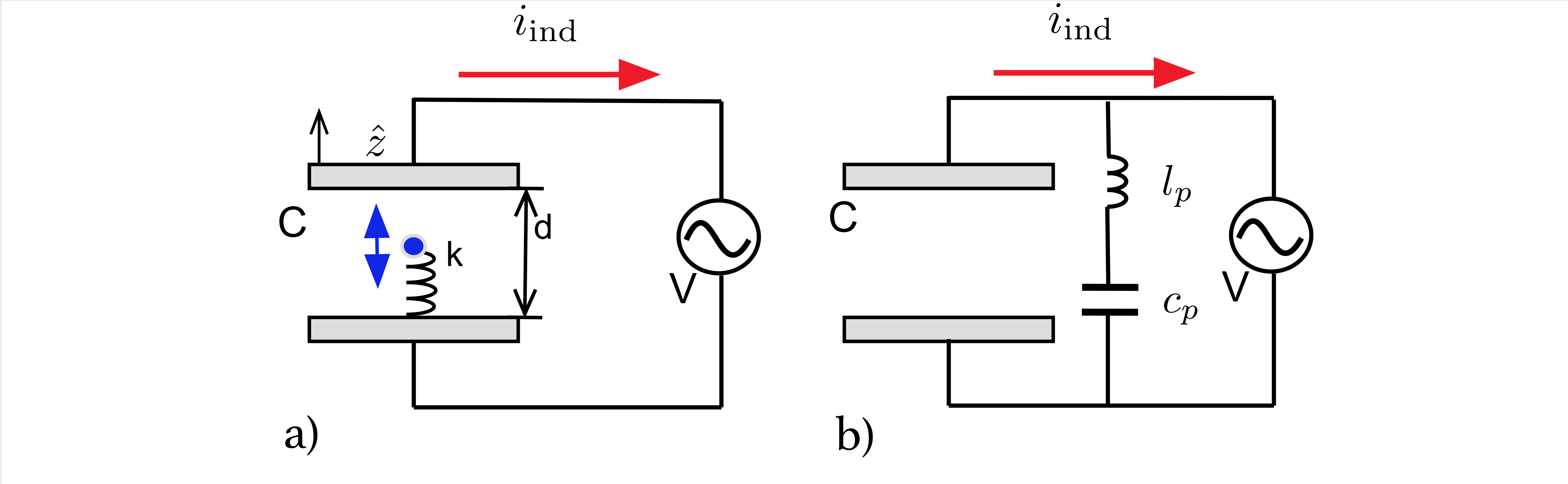

$$m\ddot{z} = -kz + \frac{qV}{d} \quad \Leftrightarrow \quad l_p \frac{di_{\text{ind}}}{dt} + \frac{1}{c_p}\int i_{\text{ind}} = V$$

$$\left(\; i_{\text{ind}} = \frac{q\dot{z}}{d} \qquad l_p = \frac{md^2}{q^2},\, c_p = \frac{1}{(2\pi\nu_z)^2 l_p} \; \right)$$

An image current induced by an oscillating partiocle is equivalently expressed as a inductive component of the particle.

D. J. Wineland and H. G. Dehmelt. *J.Appl.Phys.*, **46,** 920 (1975)

Image current detection

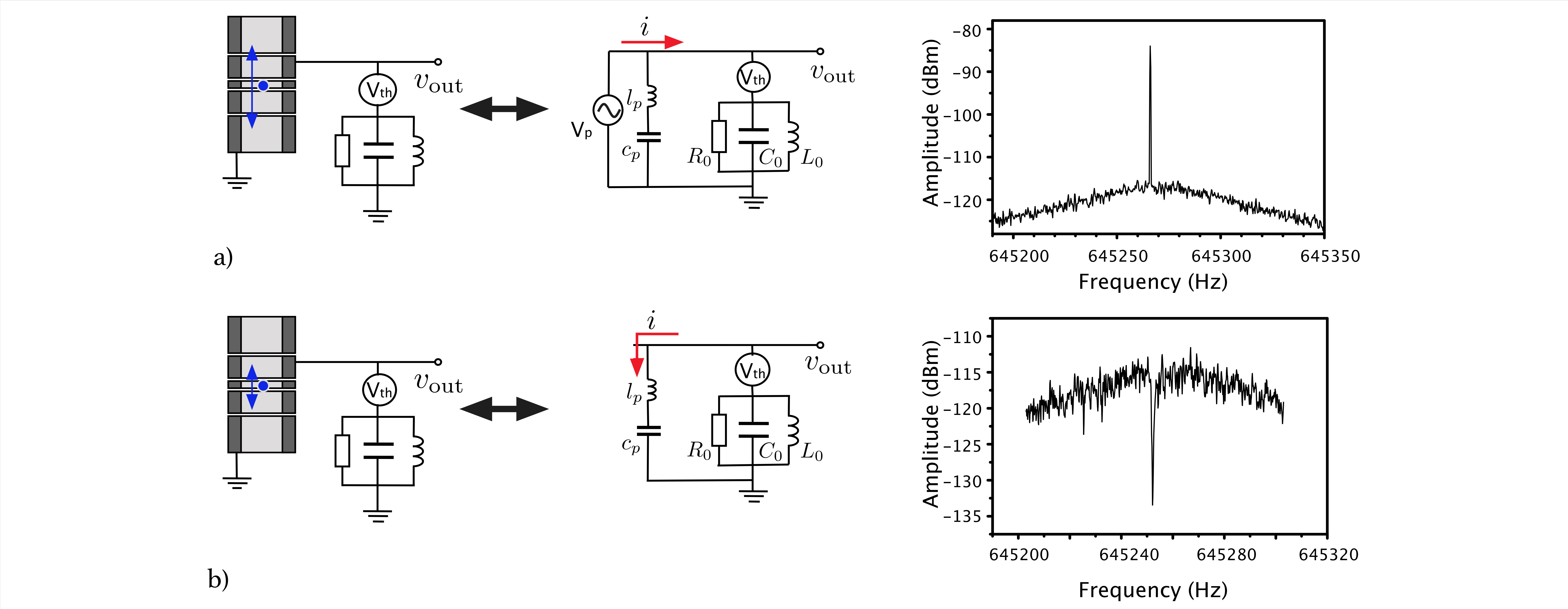

When a particle is excited, the frequency of the particle appears as a peak. When it is cooled though interaction with the resonator, it shorts a frequency component of the thermal noise to the ground.

D. J. Wineland and H. G. Dehmelt. *J.Appl.Phys.*, **46,** 920 (1975)

Counting a number of particles

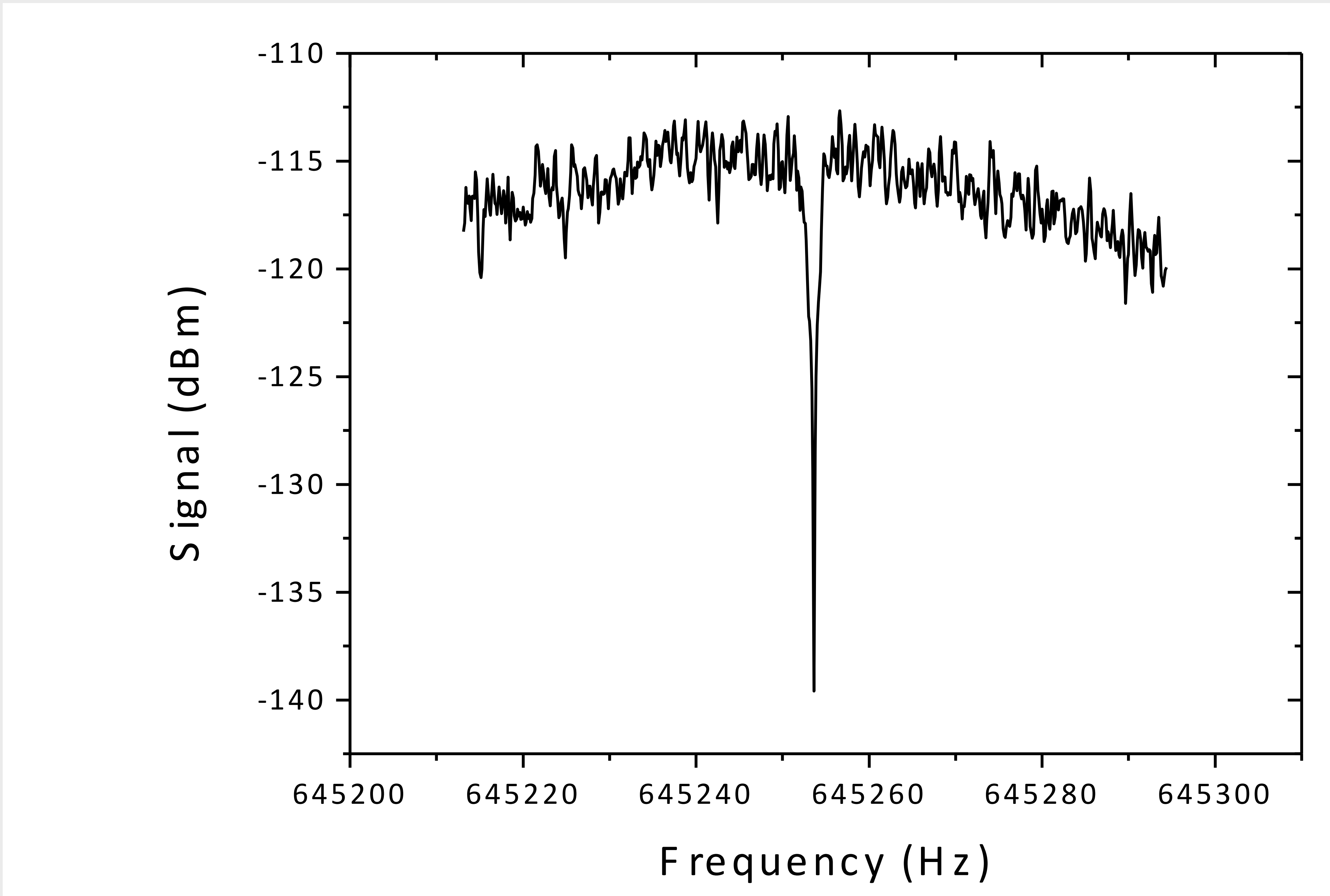

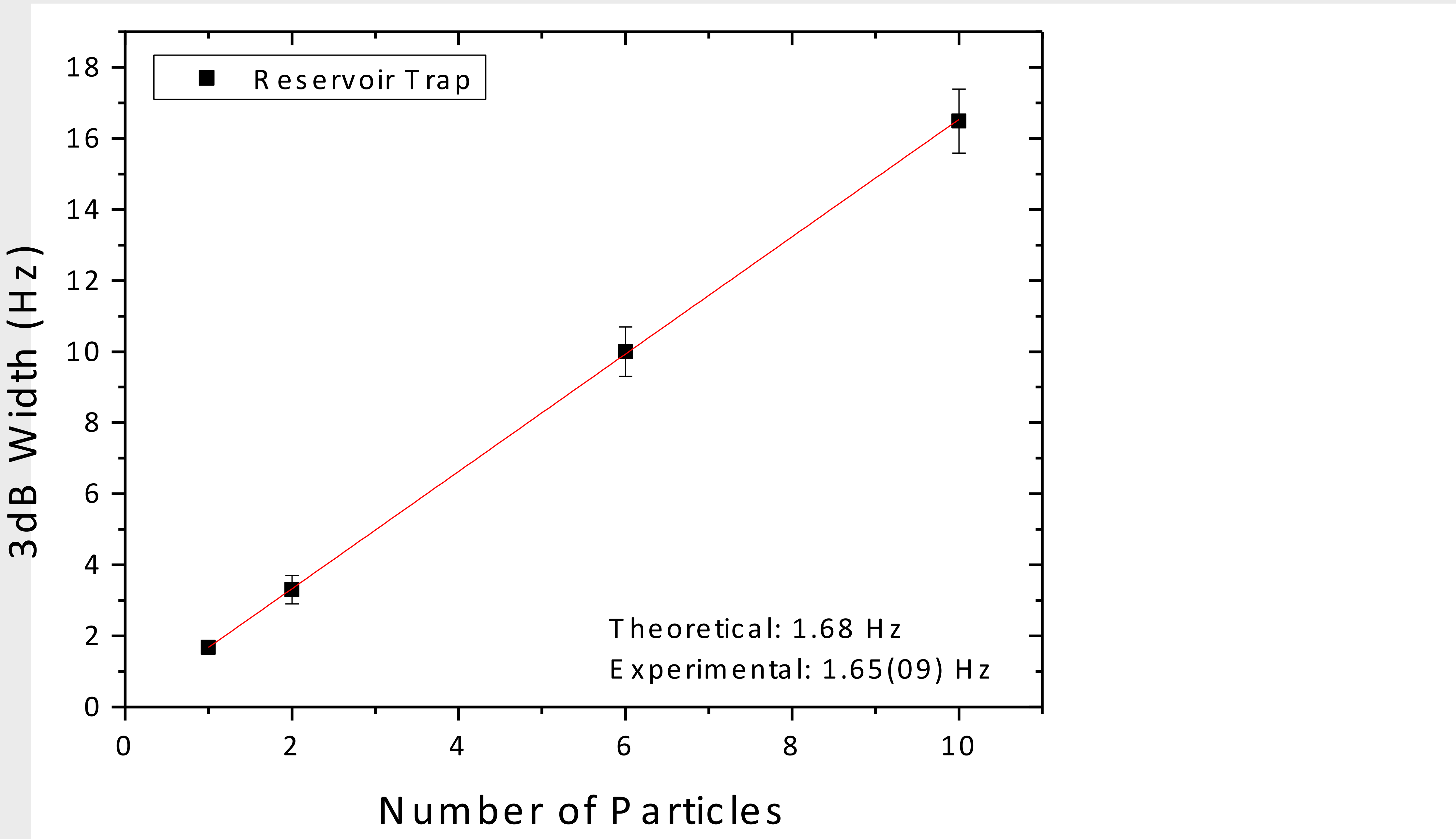

Dip width of n - particle:

$$\Delta\nu_{z,n} = \frac{n}{2\pi}\frac{q^2 R_0}{mD^2} \qquad \tau = \frac{mD^2}{q^2 R_0}$$

(R_0 : From the quality of the resonator $R_0 = 2\pi\nu_{res}LQ$

$\Rightarrow$ $n \propto \Delta\nu_z$

D. J. Wineland and H. G. Dehmelt. *J.Appl.Phys.*, **46,** 920 (1975)

Sideband coupling

- The radial motions are coupled to the axial motion through a radial excitation.

$$\nu_{rf} = \nu_+ - \nu_z,\ \nu_z + \nu_-$$

- The axial component of the coupled motion has two frequency components reflect the original frequencies:

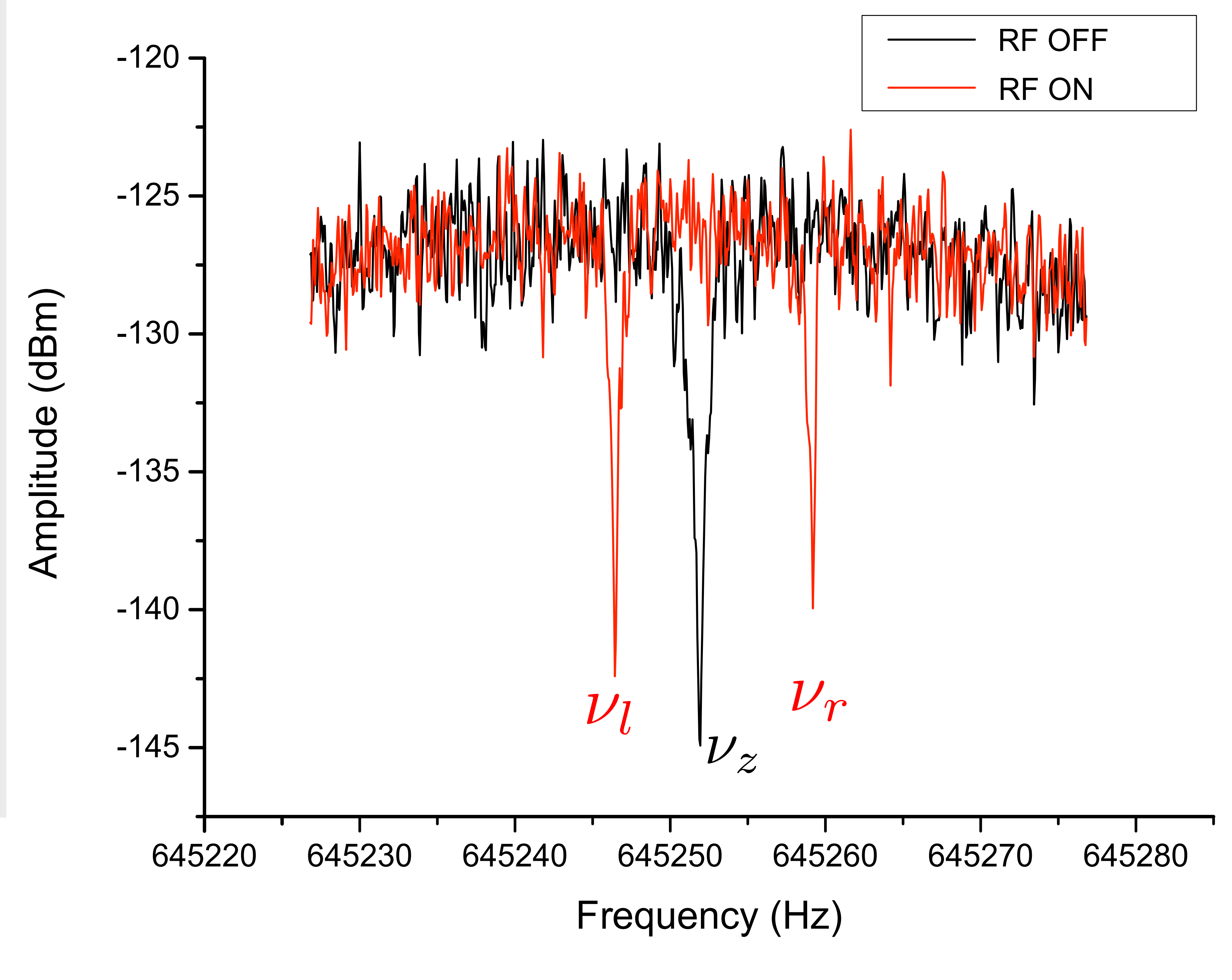

$$z(t) = z_0 \cos\left(\frac{\Omega_0}{2}t\right)\sin(2\pi\nu_z t)$$

$$= \frac{z_0}{2}\left[\sin\left(2\pi\left(\nu_z + \frac{\Omega_0}{4\pi}\right)\right) + \sin\left(2\pi\left(\nu_z - \frac{\Omega_0}{4\pi}\right)\right)\right]$$

$\underbrace{\nu_z + \frac{\Omega_0}{4\pi}}_{\nu_l}$, $\underbrace{\nu_z - \frac{\Omega_0}{4\pi}}_{\nu_r}$

$$\Rightarrow \quad \nu_+ = \nu_{rf} - \nu_z + (\nu_l + \nu_r) \quad \text{(axial-cyclotron coupling)}$$

$$\nu_- = \nu_z - \nu_{rf} - (\nu_l + \nu_r) \quad \text{(axial-magnetron coupling)}$$

E.A.Cornell *et al.*, *Phys.Rev.A*, **41,** 312 (1990)

Sideband coupling (detuned)

When the coupling frequency is detuned :

$$\delta_{\pm} = \nu_{rf} \mp (\nu_{\pm} - \nu_z)$$

$$\nu_{l,r} = \nu_z - \frac{\delta}{2} \pm \sqrt{\frac{\Omega_0^2}{4\pi^2} + \delta^2}$$

$$\left(\Omega_0 := \frac{qE_0}{4\pi m\sqrt{\nu_{\pm}\nu_z}} \text{ tuned-Rabi frequency}\right)$$

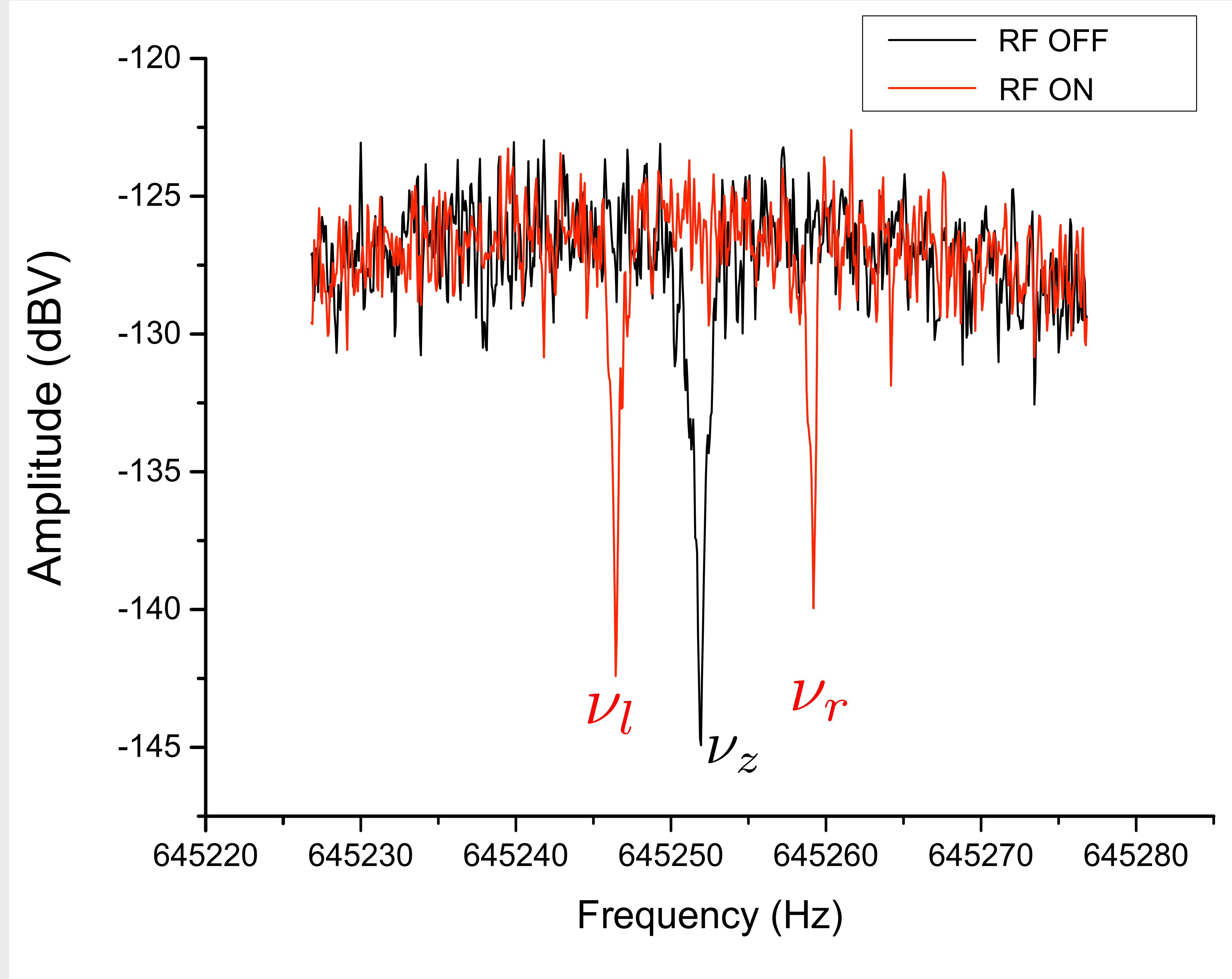

The detuning is cancelled

$$\Rightarrow \begin{aligned} \nu_+ &= \nu_{rf} - \nu_z + (\nu_l + \nu_r) && \text{(axial-cyclotron coupling)} \\ \nu_- &= \nu_z - \nu_{rf} - (\nu_l + \nu_r) && \text{(axial-magnetron coupling)} \end{aligned}$$

E.A.Cornell *et al.*, *Phys.Rev.A,* **41,** 312 (1990)

Effects of trap imperfections

Energy of eigenmodes of a particle couple to trap imperfection
-> shifts the eigenfrequencies

Electric potential (ideally harmonic):

$$\Phi_e(z) = V_0 \sum_{j=0}^{n} C_j z^j$$

$$\frac{\Delta\omega_+}{\omega_+} = \frac{1}{qV_0}\frac{C_4}{C_2^2}\left(-\frac{3}{4}\left(\frac{\omega_z}{\omega_+}\right)^4 E_+ + \frac{3}{2}\left(\frac{\omega_z}{\omega_+}\right)^2 E_z - 3\left(\frac{\omega_z}{\omega_+}\right)^2 |E_-|\right),$$

$$\frac{\Delta\omega_z}{\omega_z} = \frac{1}{qV_0}\frac{C_4}{C_2^2}\left(-\frac{3}{2}\left(\frac{\omega_z}{\omega_+}\right)^2 E_+ + \frac{3}{4}E_z - 3|E_-|\right),$$

$$\frac{\Delta\omega_-}{\omega_-} = \frac{1}{qV_0}\frac{C_4}{C_2^2}\left(-3\left(\frac{\omega_z}{\omega_+}\right)^2 E_+ + 3E_z - 3|E_-|\right),$$

L.S. Brown and G.Gabrielse, *Rev.Mod. Phys.* **58**, 233 (1986)

Effects of trap imperfections

Energy of eigenmodes of a particle couple to trap imperfection
-> shifts the eigenfrequencies

Magnetic field :

$$\vec{B}(\rho, z) = B_0 \vec{e_z} + B_2 \left(\left(z^2 - \frac{\rho^2}{2} \right) \vec{e_z} - \rho z \vec{e_\rho} \right)$$

$$\frac{\Delta\omega_c}{\omega_c} = -\frac{1}{m\omega_z^2} \left(\frac{B_1}{B_0} \right)^2 E_+$$

$$\frac{\Delta\omega_+}{\omega_+} = \frac{1}{m\omega_z^2} \frac{B_2}{B_0} \left(-\left(\frac{\omega_z}{\omega_+} \right)^2 E_+ + E_z - 2|E_-| \right),$$

$$\frac{\Delta\omega_z}{\omega_z} = \frac{1}{m\omega_z^2} \frac{B_2}{B_0} \left(E_+ + |E_-| \right),$$

$$\frac{\Delta\omega_-}{\omega_-} = \frac{1}{m\omega_z^2} \frac{B_2}{B_0} \left(2E_+ - E_z + 2|E_-| \right).$$

L.S. Brown and G.Gabrielse, *Rev.Mod. Phys.* **58**, 233 (1986)

Apparatus

Trap stack of BASE/CERN

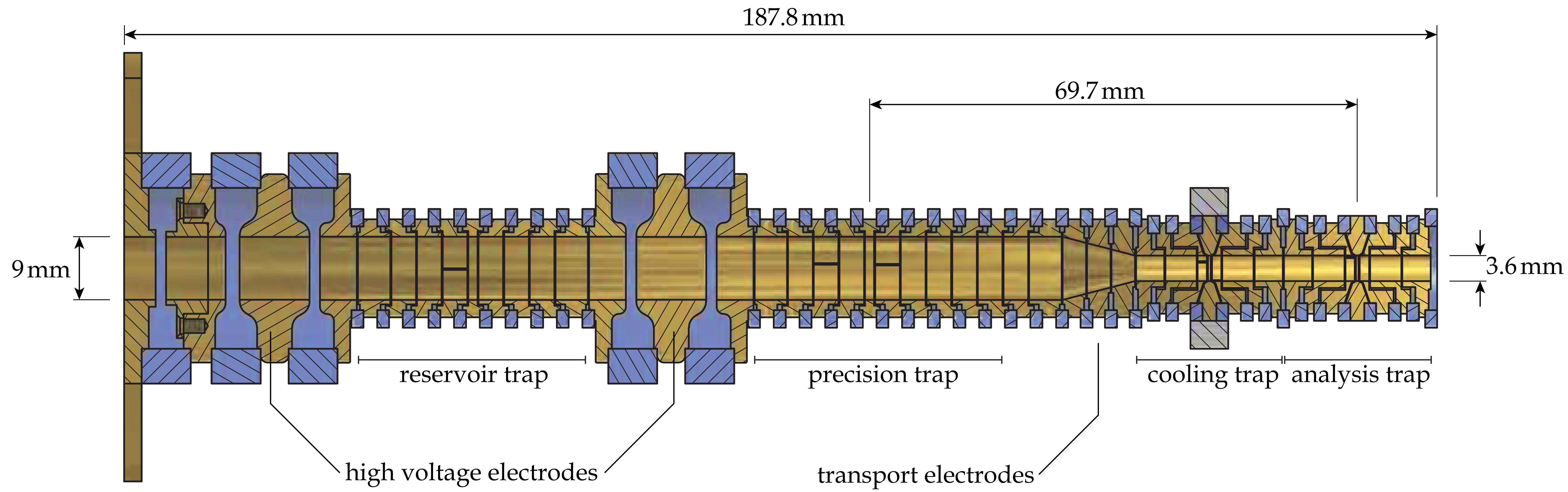

- Four Penning Traps: PT and AT + Reservoir Trap ad Cooling Trap
- Reservoir Trap: serves as an antiproton reservoir
- Adiabatic transport, no heating with resolution of 4mK

Degrader / Reservoir Trap

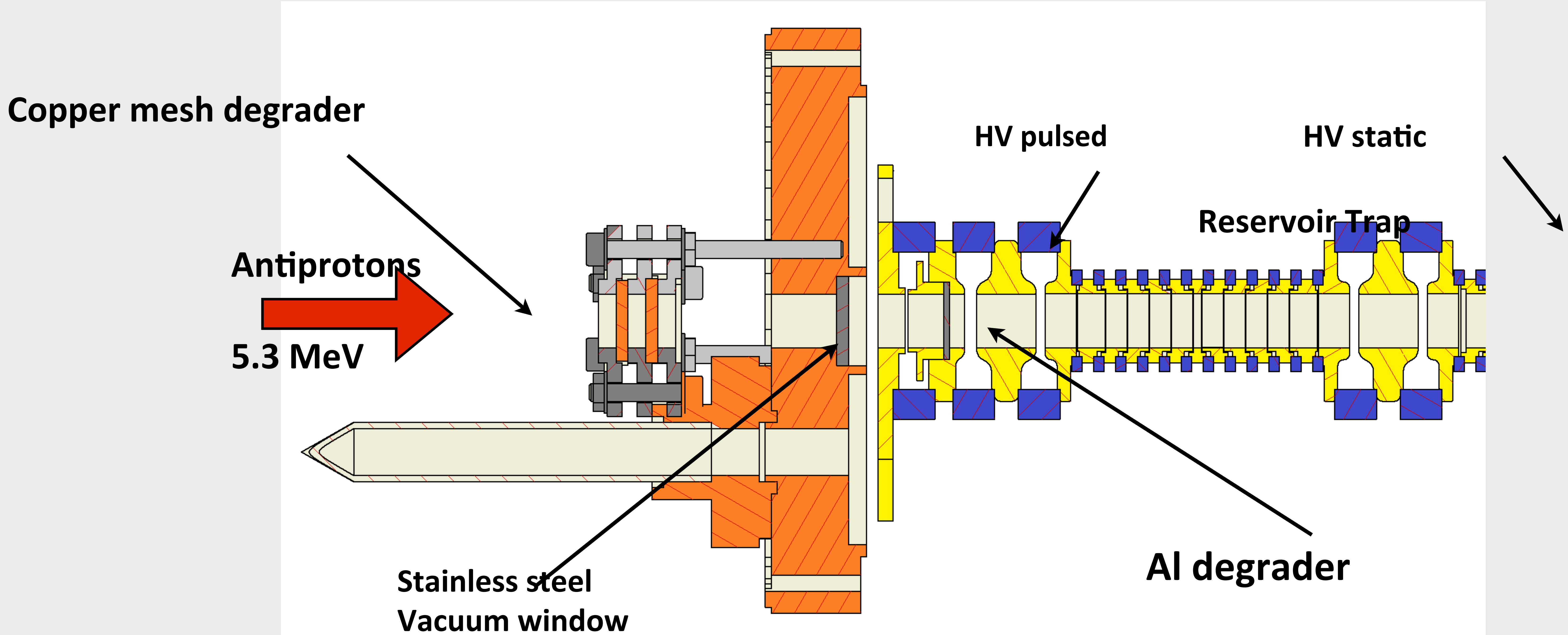

- Ultra high vacuum was achieved by an indium shielded trap chamber (1.2 / volume). Pumped to < 1E-6 mbar, pinched-off, cooled down.
- Storage time : stored ~ 50 antiprotons for three months. No particle was observed. -> $t_{1/2}$ > 1.08 yrs (-> estimated vacuum :5E-18 mbar)
- Enables operation of the experiment during accelerator shut-down.

C. Smorra *et al.*, *International Journal of Mass Spectrometry* **389**, 10 (2015)

Photos

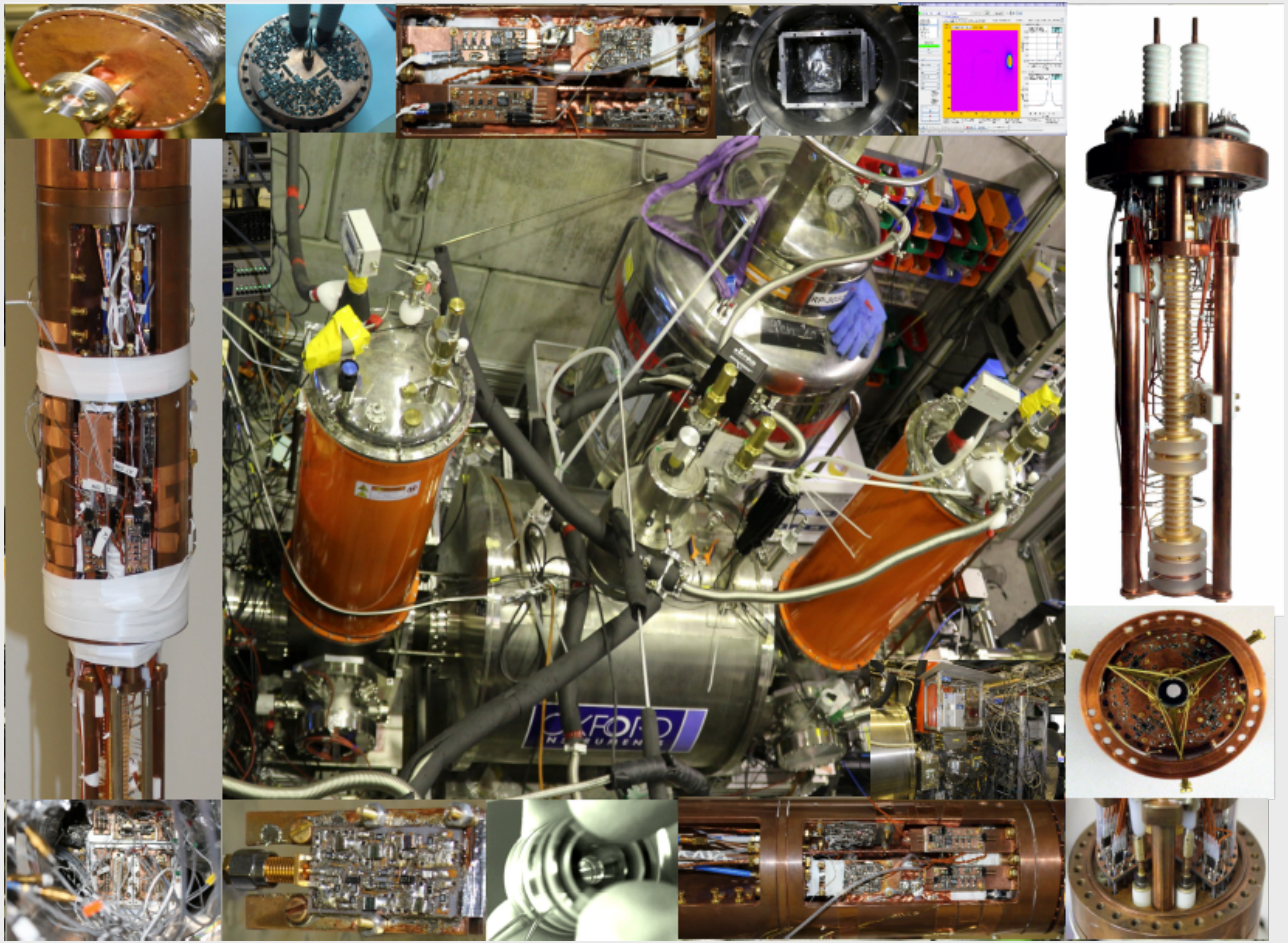

Cleaning methods

Cleaning methods

	Axial frequency ν_z	Modified cyclotron frequency ν_+	Magnetron frequency ν_-
e^-	27.65 MHz	54.47 GHz	7.017 kHz
$\bar{p}$	645.3 kHz	29.66 MHz	7.019 kHz
H^-	644.9 kHz	29.62 MHz	7.019 kHz
C^-	186.9 kHz	2.481 MHz	7.037 kHz
O^-	161.9 kHz	1.861 MHz	7.043 kHz

- Contaminants particles are removed by selective excitations of their eigenfrequencies and subsequent potential ramps.
- SWIFT (Stored Waveform Inverse Fourier Transform) excitation effectively removes heavy ions.

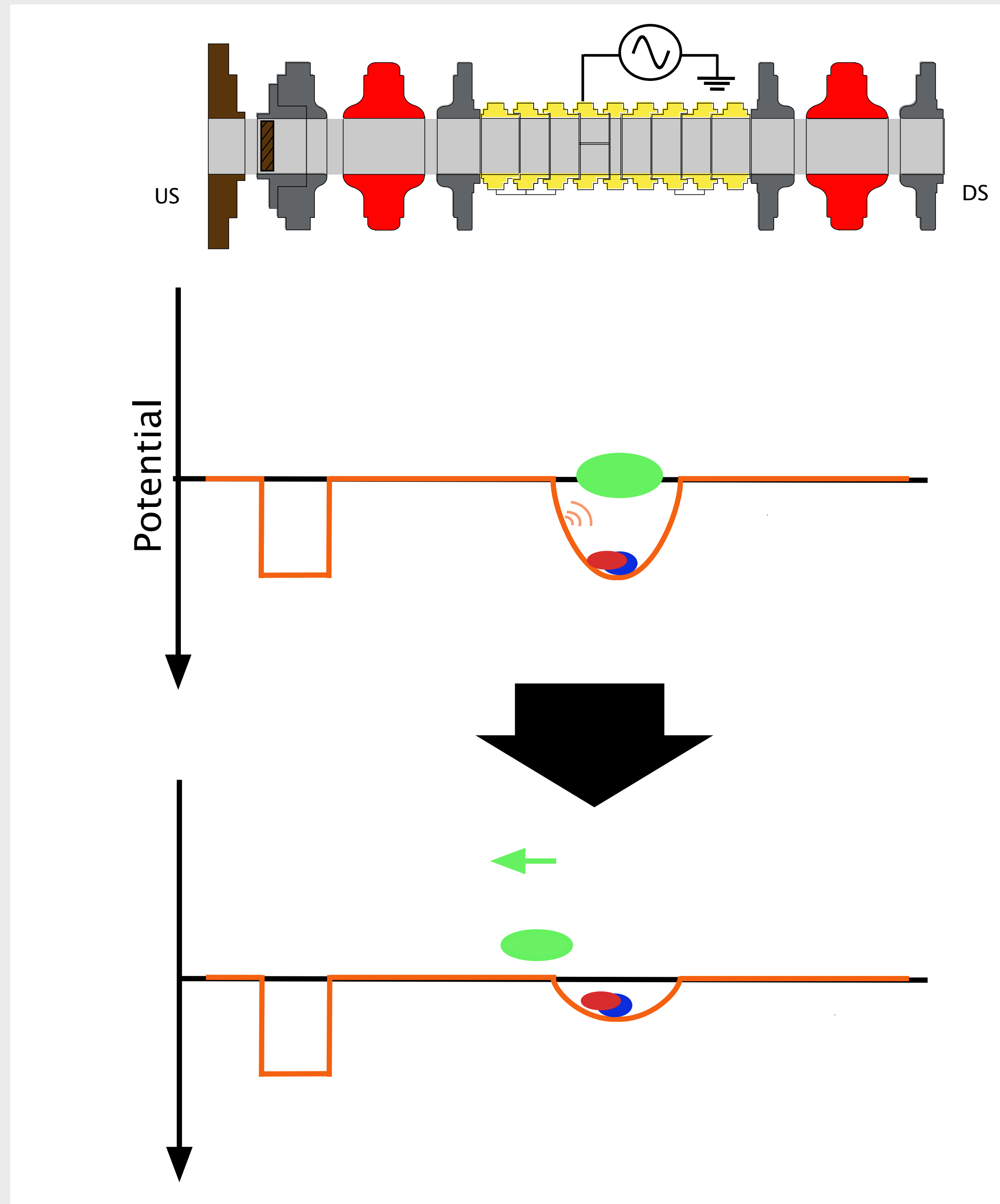

Electron kick-out

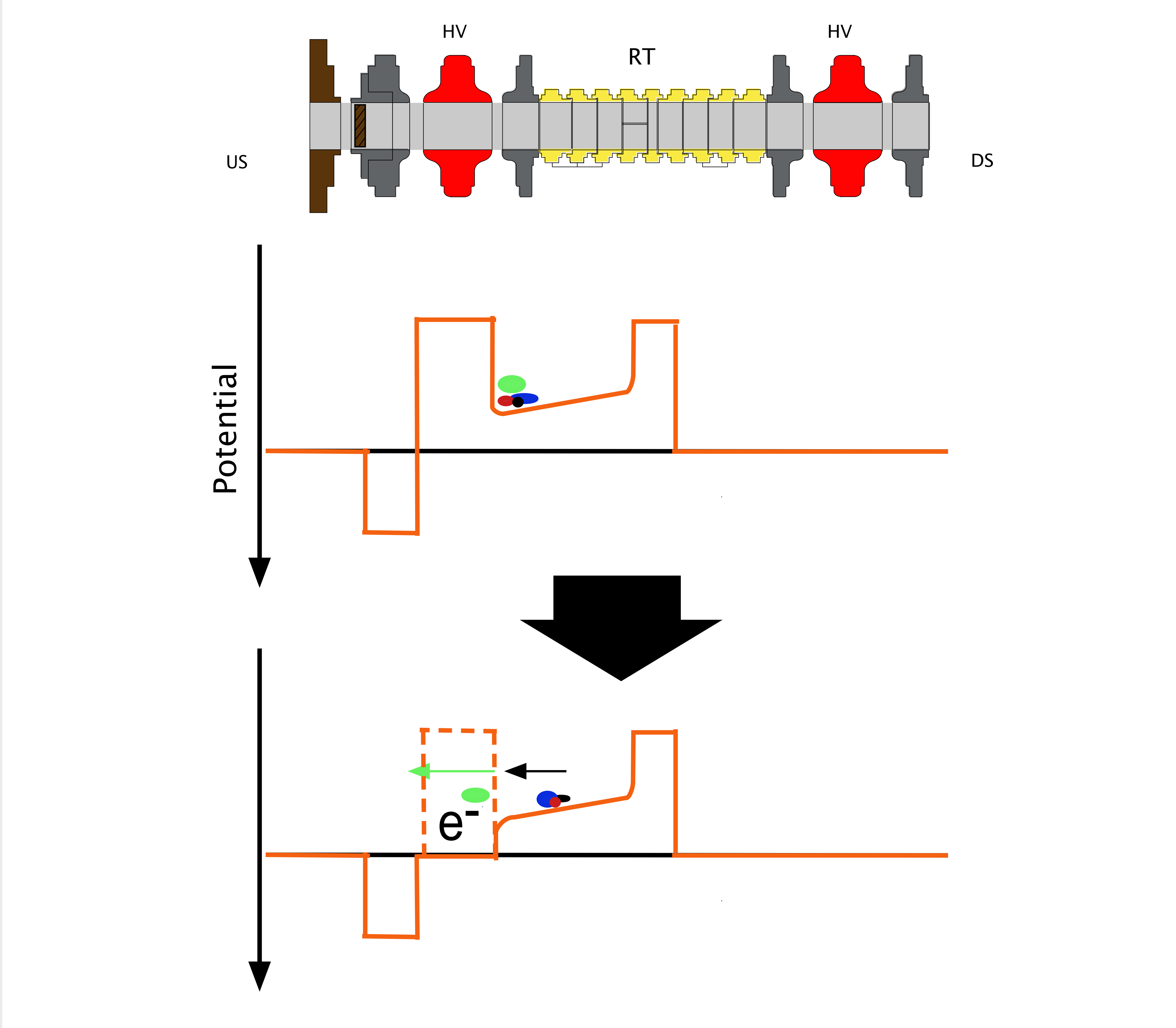

- Effective removal of electrons by a pulsed potential ramp.
- The timing is optimized so that e^- escape the trap, but p / H^- stay in a trap

Stability comparison

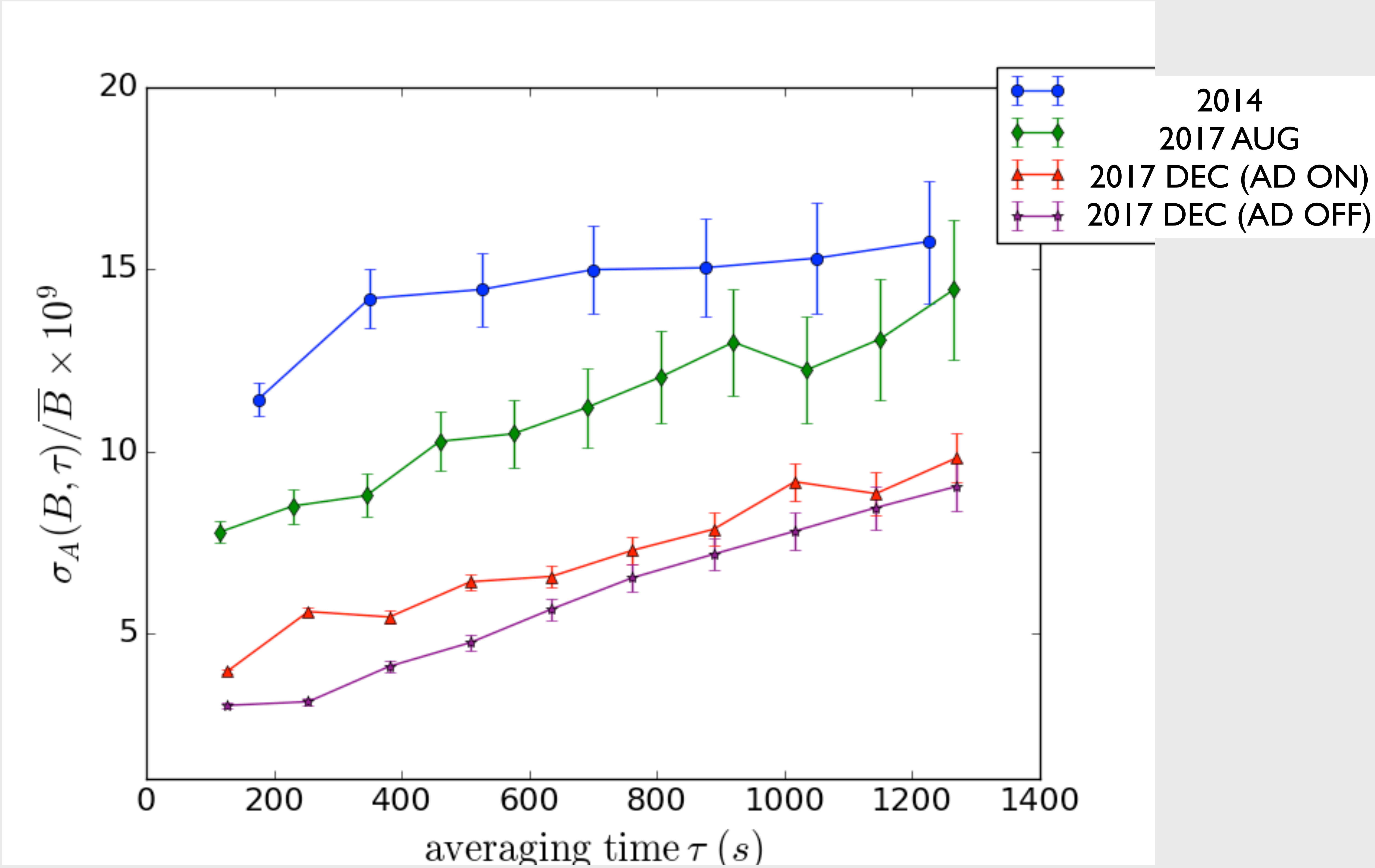

Self shielding coil

Self shielding coil - concept

- A shorted superconductor surrounded over the apparatus which compensate external magnetic field fluctuations by induced currents according to the Lenz's law.
- A solenoid of an infinite length can perfectly compensate the axial magnetic field fluctuations; in reality the shielding performance is position dependent.

- By designing a coil in a right way, theoretically perfect shielding is attained in the center of the coil.

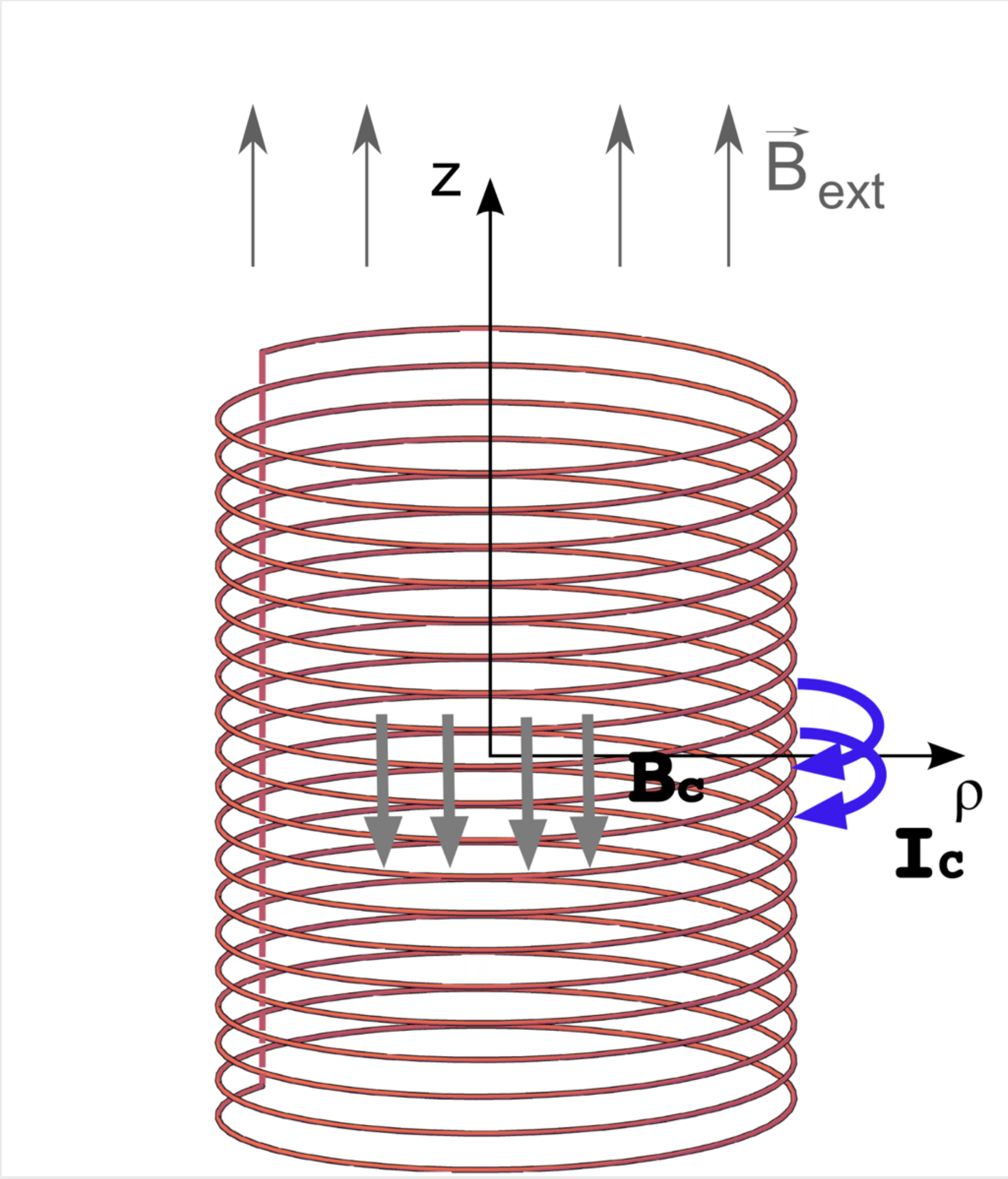

Self shielding coil - principle

- Shielding factor: **S := B_{ext} / B_{in}**

$S^{-1} = 0 \leftrightarrow$ Perfect shielding

$$S^{-1} := \frac{B_{\rm in}(0,0)}{B_{\rm ext}(0,0)} = 1 + \frac{B_{\rm coil}(0,0)}{B_{\rm ext}(0,0)}$$

$$\int_{A_i} (B_{\rm ext} + B_{\rm coil}) \cdot dA = \text{const.}(=0)\;(A_i : \sum_i S_i)$$

Lenz's law

$$\Rightarrow S^{-1} = 1 - \frac{\int_{A_i} B_{\rm ext} dA / B_{\rm ext}(0,0)}{\int_{A_i} B_{\rm coil} dA / B_{\rm coil}(0,0)} = 1 - \frac{b_e}{b_c}$$

b_e, b_c : spatial properties of B_{ext}, B_{coil}

$$b_e := \frac{\int_{A_i} B_{\rm ext} dA}{B_{\rm ext}(0,0) \int_{A_i} dA} = 1$$

(if uniform fluctuations are assumed)

$$b_c := \frac{\int_{A_i} B_{\rm coil} dA}{B_{\rm coil}(0,0) \int_{A_i} dA}$$

$$b_c = 1 \iff B_{\rm coil}(0,0) = \overline{B_{\rm coil}} : \text{perfect shielding}$$

Self shielding coil - principle

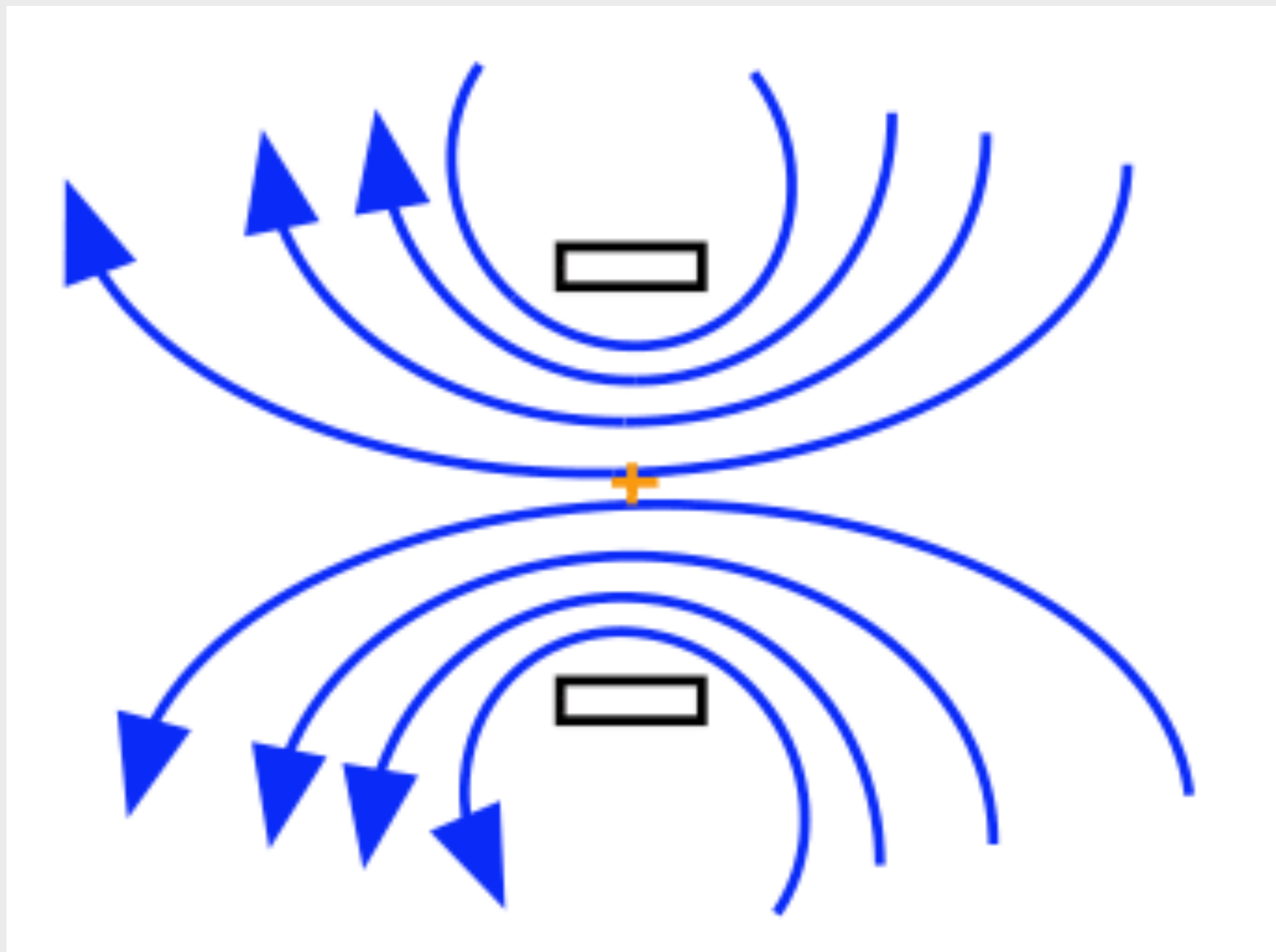

$$B_{\mathrm{coil}}(0,0) < \overline{B_{\mathrm{coil}}} \iff b_c > 1 \iff S^{-1} < 0$$

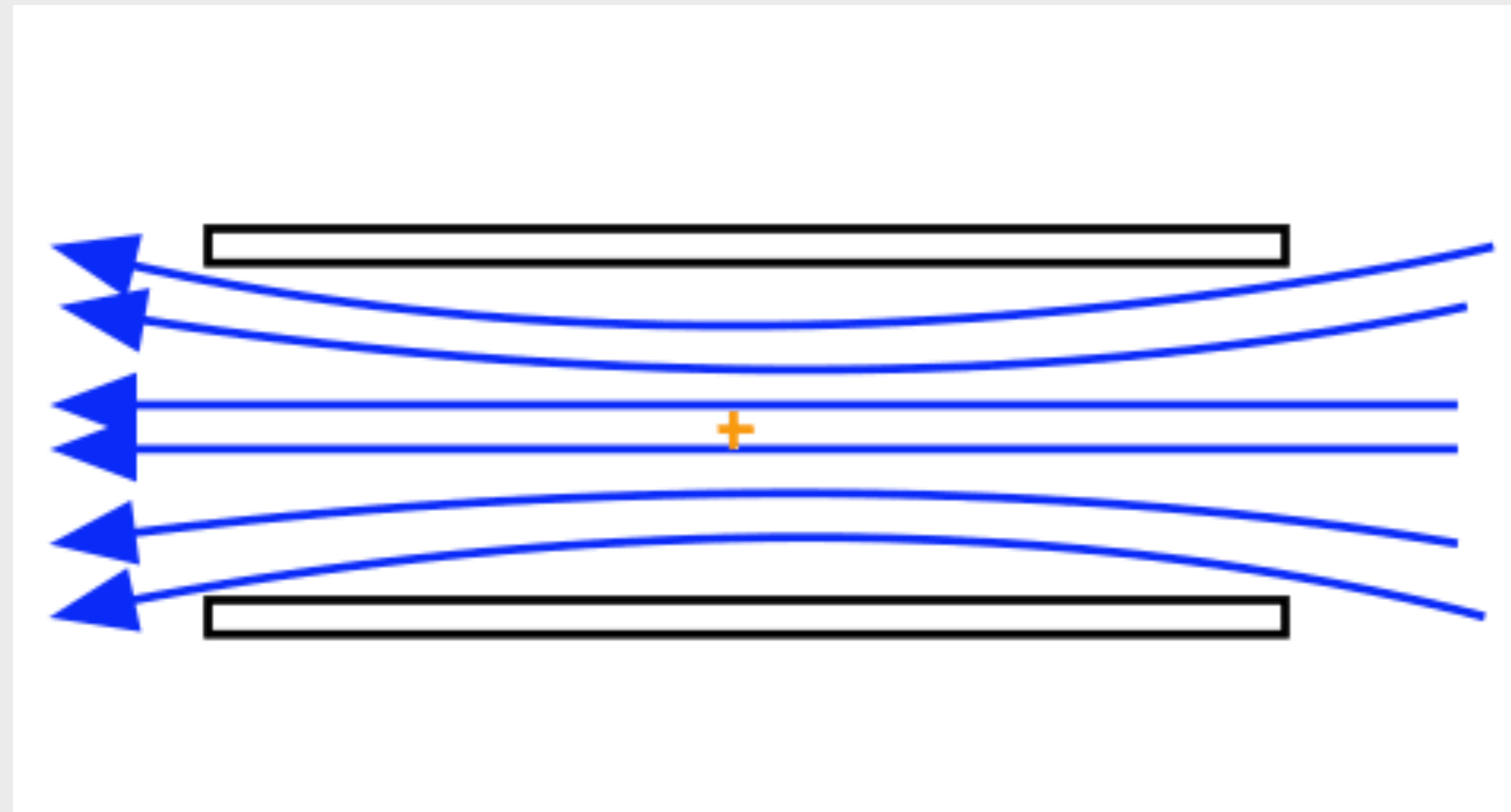

$$B_{\mathrm{coil}}(0,0) > \overline{B_{\mathrm{coil}}} \iff b_c < 1 \iff S^{-1} > 0$$

Self shielding coil - principle

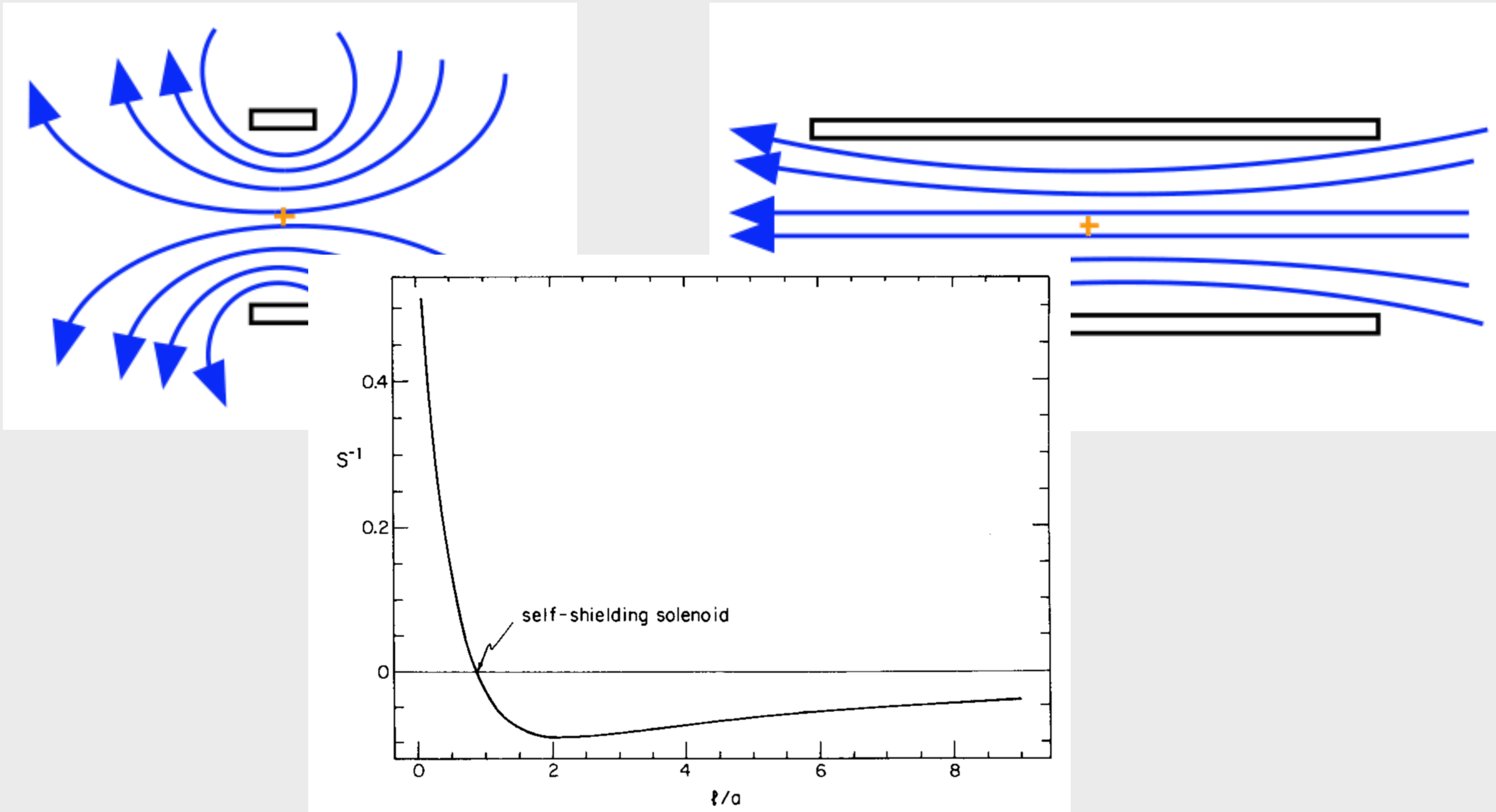

G.Gabrielse and J.Tan, *Jour.Appl.Phys.* **63**, 5143

TRAP measurement 1990

Co-trapped pbar / H^-

- one particle parked on higher orbit while the other is being measured

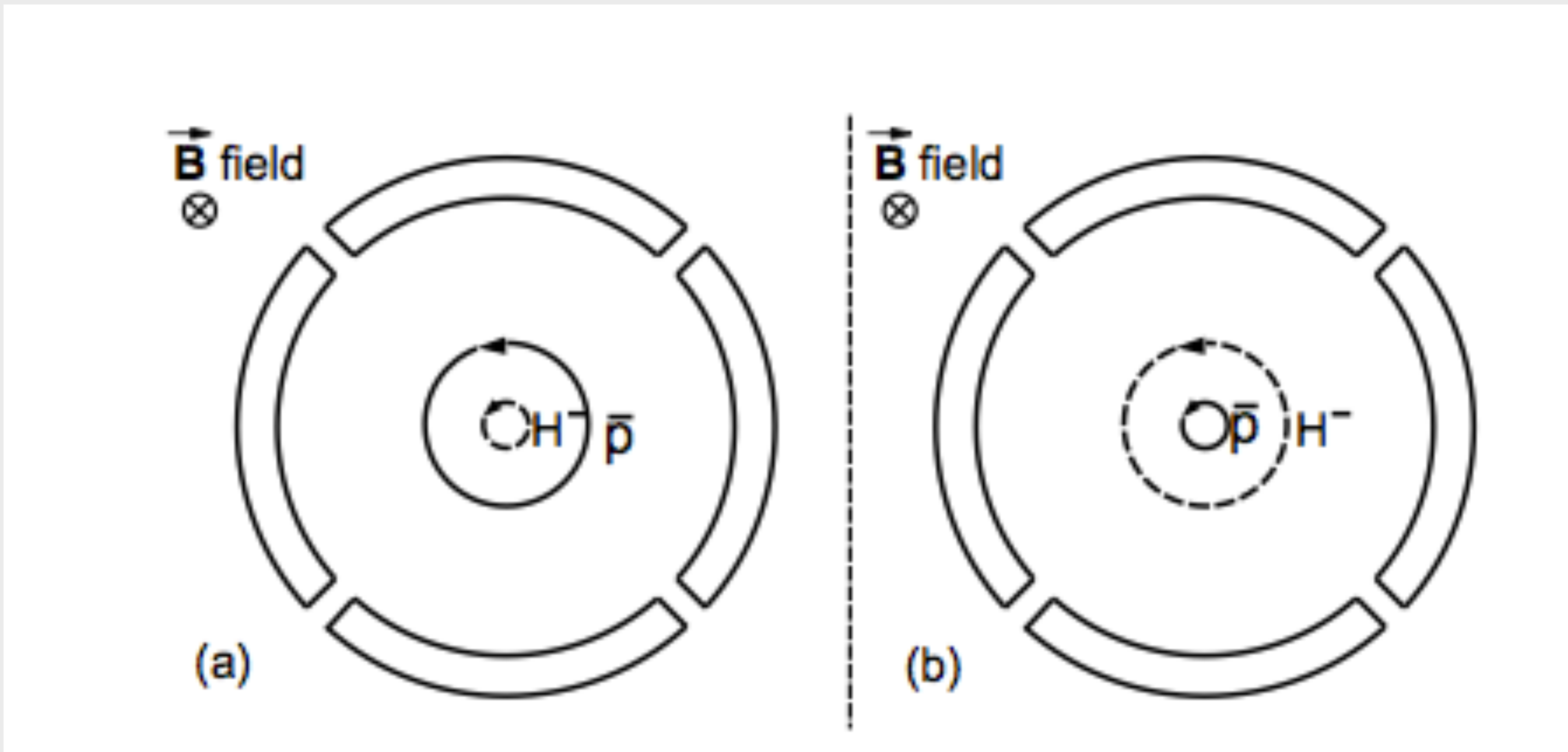

Particle exchange and measurement

- The measurement took long time, limited by the cooling time constant of the detector
- a pair of the cyclotron frequencies in ~ 4 hours

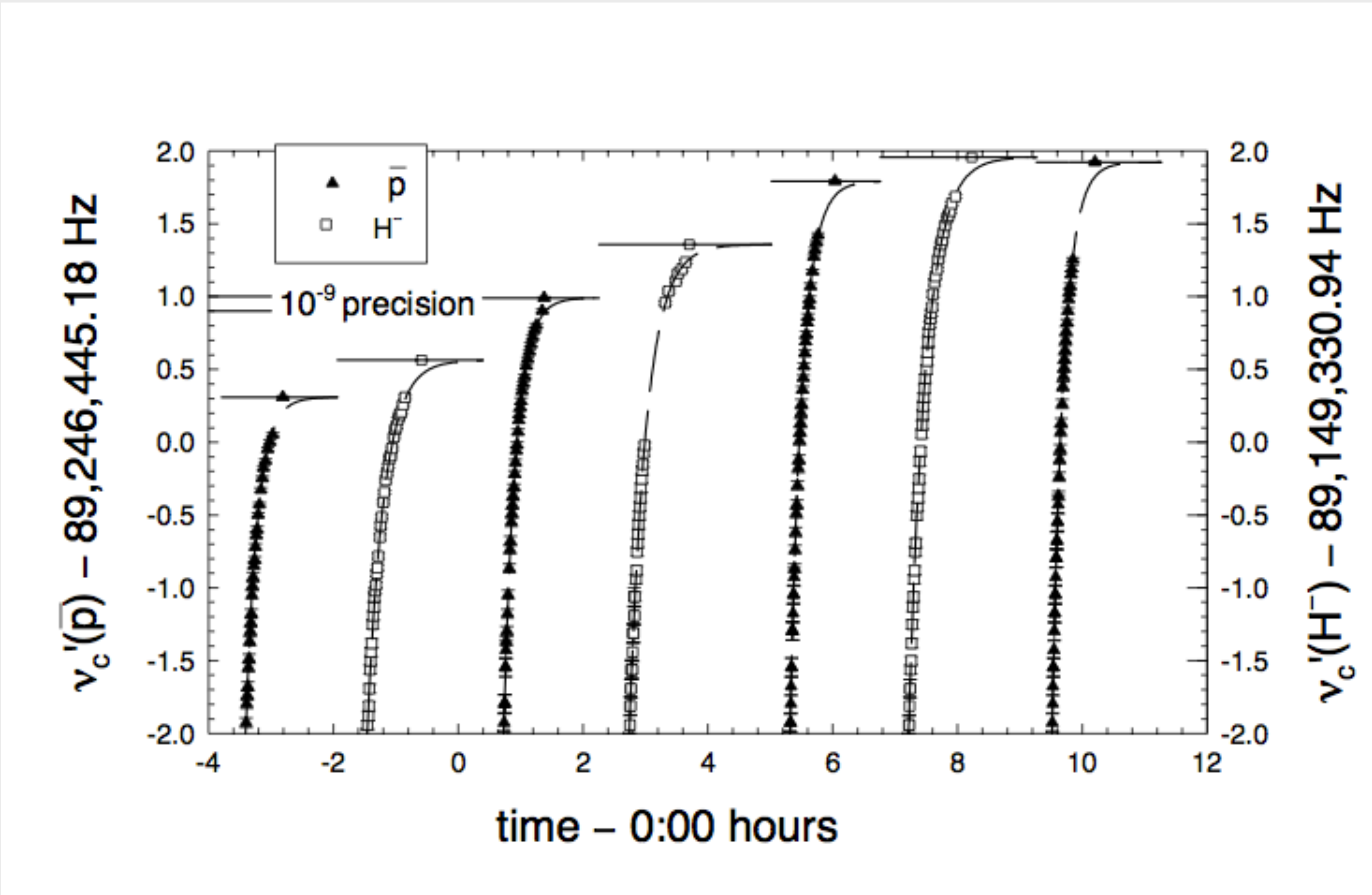

Comparison of different CPT tests

Absolute energy resolution is used to evaluate sensitivities of different CPT tests. The measured physical properties are converted to absolute energy, which limit possible CPT-violating terms in the Hamiltonian.

- Charge-to-mass comparison using H^- ion :

$$\delta E^{q/m} = (1 - R_{exp,c}) h\nu_{c,\mathrm{H}^-} < 8.5 \times 10^{-18}$$

- g-factor: $\delta E^g = h\Delta\nu_{a,p-\bar{p}}$ (anomalous frequency $\nu_a := \nu_L - \nu_c$)

	Relative Precision	Energy resolution
$\Delta m_{K_0,\bar{K_0}}$	10^{-18}	10^{-9} eV
$\Delta(q/m)_{p,\bar{p}}$	10^{-11}	10^{-18} eV
$\Delta g_{p,\bar{p}}$	10^{-6}	10^{-12} eV